Northwest Biomechanics Symposium
May 17-18th, 2024
University of Oregon
Eugene, OR

UNIVERSITY OF
OREGON

An American Society of Biomechanics

Regional Meeting

ASB American Society of Biomechanics

FOUNDED IN 1977

Symposium Schedule

Friday, May 17, 2024: Knight Campus

1:00 – 1:30 pm	Registration
1:30 – 1:45 pm	Welcoming Remarks
1:45 – 2:45 pm	Podium Session: Neuromuscular Control
3:00 – 3:30 pm	Student Networking Event (hosted by Society of Biomechanics Students – Northwest)
	Non-Student Networking & Coffee Break
3:30 – 4:30 pm	Podium Session: Assistive Technology & Machine Learning
4:45 – 6:00 pm	Poster Session A
6:15 – 9:00 pm	Dinner & Games

Saturday, May 18, 2024: Knight Campus

8:00 – 8:30 am	Breakfast
8:30 – 9:30 am	Keynote Address: Jill McNitt-Gray
9:30 – 10:45 am	Poster Session B
11:00 – 12:00 pm	Podium Session: Gait & Locomotion
12:00 – 1:15 pm	Lunch
1:15 – 2:30 pm	Podium Session: Sport Biomechanics
2:30 – 3:00 pm	Thematic Research Interest Discussions
	Coffee Break
3:00 – 4:00 pm	Podium Session: Injury & Rehabilitation
4:00 – 4:15 pm	Awards & Closing Remarks

NWBS Keynote Address

Jill L McNitt-Gray PhD FASB FISB FNAK

Departments of Biological Sciences and Biomedical Engineering

Director, USC Biomechanics Research Lab

University of Southern California

"Let's Get Real: Investigation of Control and Dynamics of Movement in Ecologically Relevant Contexts"

Jill L. McNitt-Gray, Ph.D. is a Gabilan Distinguished Professor of Science and Engineering, Professor in the Departments of Biological Sciences and Biomedical Engineering and Chair of the Dornsife Women in Science and Engineering Committee at USC. She is Director of the USC Biomechanics Research Laboratory and is a Fellow of the ASB, ISB, and NAK. She has received numerous prestigious awards, such as the Jim Hay, Harmon Brown, Joe Vigil, Jean Landa Pytel, and Geoffery Dyson Awards. She helped found National Biomechanics Day, served as President of ASB and has been on the Executive Council of ISB. Her research has been funded by the NSF and DoD and recognized by USC Mellon Mentoring Awards, the Center for Excellence in Teaching, and as a 2020 Women in Science and Engineering (WiSE) Architect of Enduring Change. She currently a Co-PI of the NSF BII Integrated Movement Science Institute. Dr. McNitt-Gray's talk with focus on the neuromuscular control and dynamics of human movements associated with improving performance and mitigating risk for individuals with various ability levels (clinical populations as well as Olympic and Paralympic athletes). She uses both experimental and dynamic modeling approaches to test research hypotheses specific to control priorities during well-practiced, goal-directed tasks and provide timely, relevant, understandable, and easy to use feedback to facilitate skill acquisition.

Gold Level Sponsors

UNIVERSITY OF **OREGON**
College of Arts and Sciences

ASB founded 1977
AMERICAN SOCIETY OF BIOMECHANICS

Silver Level Sponsors

Wu Tsai Human Performance Alliance
UNIVERSITY OF OREGON

XSENSOR Intelligent Dynamic Sensing

THEIA Markerless

HAS Motion

AMTI FORCE AND MOTION
slocum

BERTEC

Bronze Level Sponsors

Pacific Sports and Spine

BROOKS LET'S RUN THERE

Podium Session 1: Neuromuscular Control

Friday, May 17

1:45 – 2:45 PM

Moderators: Dave Phillips and Kayla Fewster

FAULTY VISION INFLUENCES SPATIAL REACHING ERROR BUT NOT TIMING ERROR IN VIRTUAL REALITY
Motoki Sakurai, Wilson TJ, Karduna AR

COGNITIVE AND MOTOR PREDICTORS OF DUAL-TASK PERFORMANCE
Alexandra C. Lynch, Aflatounian F, Hutchison KA, Monfort SM

THE EFFECTS OF LUMBAR SPINE CREEP ON BALANCE CONTROL
Isabel D. Evans, McIntosh BA, Carpenter MG, Fewster KM

EFFECT OF SPINAL STIMULATION AND INTERVAL TREADMILL TRAINING ON GAIT MECHANICS IN CHILDREN WITH CEREBRAL PALSY
Charlotte D. Caskey, Shrivastav S, Landrum VM, Bjornson K, Roge D, Moritz C, Steele KM

Podium Session 2: Assistive Technologies & Machine Learning

Friday, May 17

3:30 – 4:30 PM

Moderators: Janet Zhang-Lea and Erin Mannen

RECONSTRUCTING UNMEASURED INERTIAL DATA WITH SPARSE SENSING FOR TREADMILL RUNNING

Mackenzie N. Pitts, Ebers MR, Agresta CE, Steele KM

EVALUATION OF A MULTI-AXIAL SHEAR SENSOR USING A MULTI-LAYER PERCEPTRON MODEL

Austin J. Mohler, McGeehan MA, Ong KG, Hahn ME

HEEL-STRIKE DETECTION ALGORITHM FOR EXOSKELETON WALKING AFTER SPINAL CORD INJURY

Annika Pfister, Henderson R, Moritz C, Ingraham KA

A COMPARISON OF METHODS FOR ASSESSING YOUNG CHILDREN'S MOBILITY DEVICE USE IN REAL-WORLD SETTINGS

Mia E. Hoffman, Sloane B, Fragomeni A, Steele KM, Kenyon LK, Logan SW, Feldner HA

Podium Session 3: Gait & Locomotion

Saturday, May 18

9:30 – 10:45 AM

Moderators: Tyler Brown and Robert Catena

GRADE-DEPENDENT MECHANICAL STRATEGIES FOR INCREASING RUNNING SPEED
Rachel M. Robinson, Donahue SR, Chebbi A, Hahn ME

RUNNING SPEED INFLUENCES PHASE-SPECIFIC CHANGES IN JOINT KINEMATICS DURING FOOT CONTACT
Emily K. Eichenlaub, Saftich M, Day EM, Nyman E, Sumner J

CAN SACRAL OR SHANK ACCELERATION PREDICT PROSTHETIC LEG PROPULSIVE FORCE?
Thomas S. Madden, Pew CA

ACCURACY OF A VIRTUAL GROUND REACTION FORCE CALCULATION IN GAIT
Pegah Jamali, Catena RD

THE EFFECT OF SPEED ON LOWER EXTREMITY JOINT STIFFNESS DURING GRADED RUNNING
Sofia Lee, Robinson RR, Chebbi A, Hahn ME

Podium Session 4: Sports Biomechanics
Sponsored by Lululemon

Saturday, May 18

1:15 – 2:30 PM

Moderators: Grant Kovach, Christopher Lam

USING OPENCAP TO ASSESS SINGLE- AND DUAL-TASK SINGLE LEG VERTICAL JUMP PERFORMANCE

Fatemeh Aflatounian, Wait K, Silva B, Lynch AD, Becker JN, Hutchinson KA, Simon JE, Grooms DR, Monfort SM

SEX-BASED DIFFERENCES IN KNEE MECHANICS AND PLANTAR PRESSURE DURING SOCCER CUTTING

Emily Karolidis, Denton AN, Hahn ME

RELATIONSHIP BETWEEN COM-TO-COP POSITION AND SAGITTAL PLANE ENERGY ABSORPTION DURING THE PENULTIMATE STEP OF SIDE-STEP CUTTING

Stephen Mengoni, Mulligan CMS, Norcross MF

KINEMATIC DIFFERENCES BETWEEN PIN AND FREERIDE BACKCOUNTRY SKI BINDINGS DURING TREADMILL SKINNING

Isaac Burgess, Samuels S, Seifert J, Becker JN

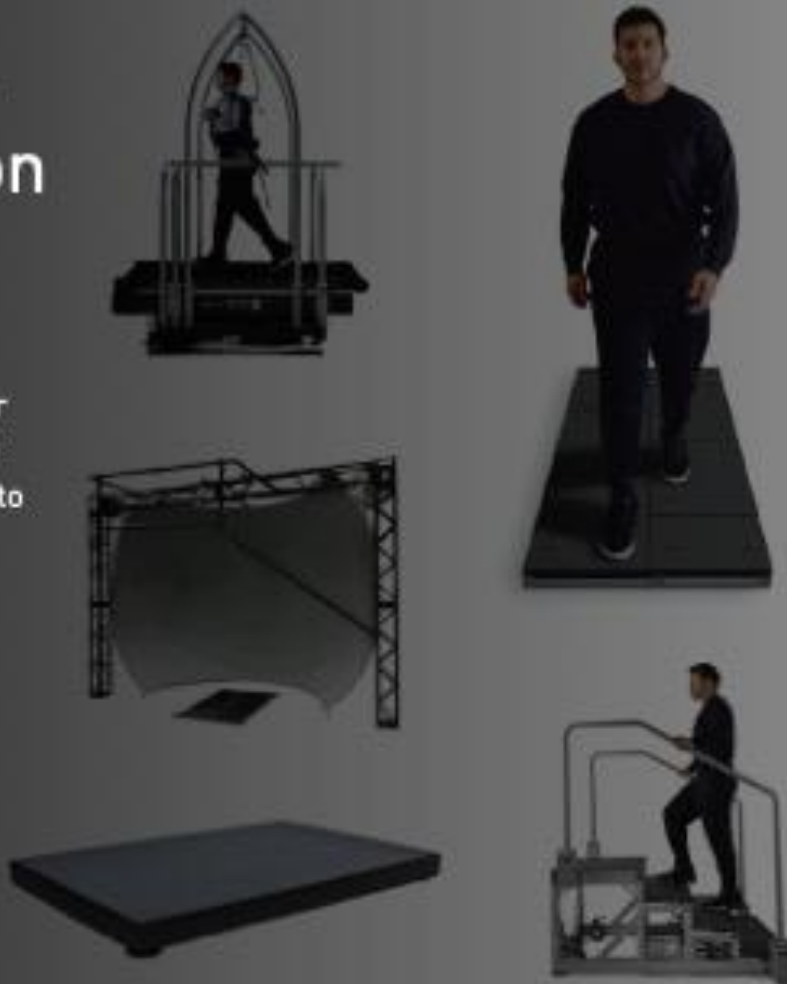**EFFECTS OF FOOTWEAR AND SURFACE ON ANKLE, KNEE, AND HIP KINEMATICS WHILE TRAIL RUNNING**

Kathy Reyes, Dailey M, Lawrence C, Shipman C, Spector Z, Hannigan JJ

Podium Session 5: Injury & Rehabilitation

Saturday, May 18

3:00 – 4:00 PM

Moderators: Damien Callahan and Jim Becker

IMPACT OF A RESISTIVE ANKLE EXOSKELETON ON FATIGUE IN CHILDREN WITH CEREBRAL PALSY
Victoria M Landrum, Caskey CD, Shrivastav SR, Feldner HA, Bjornson KF, Moritz CT, Steele KM

SEX IMPACTS LOWER LIMB STIFFNESS DURING LOADED WALK, JOG AND RUN
Abigail C. Aultz, Francis EB, Brown TN

FUNCTIONAL AND TISSUE DEGENERATION CHANGES AFTER ACL RUPTURE IN A PRECLINICAL MODEL OF POST-TRAUMATIC OSTEOARTHRITIS
Nicholas M. Pancheri, Kyathsandra N, Heinonen J, Sverdrup ES, Lin ASP, Willett NJ, Guldberg RE

QUADRICEPS STRENGTH AND STEADINESS IN INDIVIDUALS WITH KNEE INJURY AND DISEASE
Nicholas L. Hunt, Robinett MV, Brown TN

Discussion & Networking Sessions

Friday, May 17, 3:00 – 3:30 PM

Student Networking Event hosted by Society of Biomechanics Students – Northwest

This student-only event will be held in the Beetham Family Seminar Room. This event is intended to foster meaningful connections with fellow biomechanics students and provide an opportunity for students seeking advice, looking for potential collaborators, or simply looking to expand their network. Trainees of all levels are encouraged to attend. Coffee and snacks will be available in the main lobby. Non-Student Networking & Coffee Break

Non-student attendees are invited to enjoy coffee and snacks during this informal networking period

Saturday, May 18, 2:30 – 3:00 PM

Thematic Research Interest Discussions

Groups will separate based on discussion group assignment cards in nametag pouches. This will be an opportunity to network and ask questions of peers, industry professionals and professors in your interest group.

Friday Night Dinner

A buffet dinner will be held on the 2nd floor terrace of the Knight Campus Building starting at 6pm. Each attendee will be issued 1 drink ticket for beer, wine, or soft drinks. Following dinner, join us for a game of trivia featuring a fun fashion show twist held on the Knight Campus terrace as well.

Poster Session A

Friday, May 17

4:45 – 5:45 PM

Sport Biomechanics

A1. INFLUENCE OF SKI TOURING BINDING DESIGN ON GROUND REACTION FORCES DURING SKINNING
Emma Keating, Burgess I, Samuels S, Seifert J, Becker JN

A2. VALIDATION OF LOADSOL® SENSORS OVER 32 VELOCITY/GRADE RUNNING CONDITIONS
Shannon Hugard, Donahue SR, Chebbi A, Robinson RR, Hahn ME

A3. PHYSIOLOGY & BIOMECHANICS OF A FENCER'S LUNGE
Supriya Nair, Telfer S

A4. EFFECT OF VISUAL AND AUDIO FEEDBACK ON PERCEIVED RUNNING FATIGUE AND RUNNING BIOMECHANICS
Alexis Terterov, Dreher M, Feistner O, Freiermuth L, Schaps P, Yeager H, Zhang-Lea JH

A5. EFFECTS OF CHANGING HIP POSITION ON SCAPULAR KINEMATICS IN AN ATHLETIC POPULATION
Sarah Schlitter, Suprak D, Brilla L, San Juan J

A6. DO STRAPS REDUCE DYNAMIC SOFT TISSUE ARTIFACTS IN INERTIAL MEASUREMENT UNIT MEASUREMENTS?
Josephine Berry, Kuo C

A7. DYNAMICS OF PLAYER MOVEMENTS IN FEMALE SOCCER: IMPLICATIONS FOR ACL INJURY RISK
Jason Fu, Kuo C

Injury & Rehabilitation

A8. **OPPORTUNITIES FOR ULTRASOUND SHEAR WAVE ELASTOGRAPHY USE IN THE DIAGNOSIS AND MANAGEMENT OF ACHILLES TENDON INJURIES**
Nick R. Ozanich, Montiel AM, Agresta CE

A9. **OCCUPANT CHARACTERISTIC RISK FACTORS FOR WHIPLASH IN MOTOR VEHICLE COLLISIONS**
Kjeryn Soetaert, de Lange JE, Gooyers CE, Fewster KM

A10. **INVESTIGATING THE FUNCTIONAL AND PAIN-RELATED THERAPEUTIC EFFECTS OF EXERCISE THERAPY AND VISCOSUPPLEMENTATION IN A PRECLINICAL RODENT MODEL OF POST-TRAUMATIC OSTEOARTHRITIS**
Emily Sverdrup, Pancheri NM, Kyathsandra N, Lin ASP, Willett NJ, Guldberg RE

Orthopedic Biomechanics

A11. **SHOULDER MUSCLE ACTIVITY INCREASES AFTER ACUTE BUT NOT CHRONIC PAIN RELIEF**
Taylor J Wilson, Sakurai M, McClure P, Karduna AR

Neuromuscular Control

A12. **ACUTE FATIGUE MODIFIES ULTRASOUND-BASED PATELLAR TENDON STIFFNESS BY SEX**
Daniel Schlesinger, Ricci AW, Callahan DM

Assistive Technologies

A13. **DESIGN OF A SINGLE-LEG EXOSKELETON WITH AUTOMATIC GAIT CONTROL FOR HEMIPLEGIC PATIENTS**
Tara Zhan, Jovanovic L, Mayerhofer P, Donelan M

A15. INFLUENCING HUMAN GAIT DYNAMICS WITH AN ADAPTIVE SPLIT-BELT TREADMILL

Zijie Jin, Isa JT, Burden SA, Ingraham KA

Gait & Locomotion

A16. KNEE MUSCULATURE CO-ACTIVATION IS ALTERED BY PROLONGED LOAD CARRIAGE

Matthew Robinett, Krammer SM, Drew MD, Brown TN

Infant Biomechanics

A17. SEATED INFANT PRODUCTS ALTER BODY POSITION AND MUSCLE UTILIZATION

Holly Olvera, Siegel DN, Goldrod S, Bossert A, Wilson C, Lujan TJ, Whitaker BN, Carroll CJ, Mannen EM

Modeling & Simulations

A18. COMPARISON OF SEX-BASED BIOMECHANICAL MODELS TO A DEFAULT MODEL

Abby R. Brittain, Brown TN

Poster Session B

Saturday, May 18

9:30 – 10:45 AM

Sport Biomechanics

B19. DEVELOPING A VISUAL-COGNITIVE SINGLE-LEG VERTICAL JUMP TEST
Fatemah Aflatounian, Wait K, Silvia B, Lynch AC, Becker JN, Hutchinson KA, Simon JE, Grooms DR, Monfort SM

B20. A COMPARISON OF MUSCLE RECRUITMENT PATTERNS BETWEEN RECREATIONAL DANCERS AND NON-DANCERS IN DROP JUMP LANDINGS
Bethany Burr, Pollard CD, Hannigan JJ, Phillips D

B21. DIFFERENCES IN MECHANICAL EFFICIENCY BETWEEN PIN AND FREERIDE BINDINGS
Garrett Westling, Burgess I, Samuels S, Seifert J, Becker JN

B22. GROUND REACTION FORCE DIFFERENCES BETWEEN INDOOR AND OUTDOOR SURFACES DURING INCLINE AND DECLINE RUNNING
Anya Anand, Robinson RR, Hahn ME

B23. ASYMMETRY CHANGES DURING DISTANCE RUNNING IN RECREATIONAL RUNNERS
Kayla Smith, Denton AN, Robinson RR, Hahn ME

B24. INVESTIGATE MUSCLE FATIGUE ON LOWER BODY KINEMATICS DURING LAY-UP AND LANDING IN RECREATIONAL BASKETBALL PLAYERS
Brandon Yang, Jin L

Injury & Rehabilitation

B25. VOLUME RECONSTRUCTION ACCURACY OF A 3D FREEHAND ULTRASOUND APPROACH
Hidetaka Hayashi, Hahn ME

B26. FUNCTIONAL RECOVERY TIMECOURSE IN A PRECLINICAL MODEL OF ACHILLES TENDON INJURY
Jarod Forer, Link K, Yannello B, Pacheco YC, Hahn ME, Willett NJ

B27. COMPARING MOTOR VEHICLE COLLISION (MVC) INJURY INCIDENCE BETWEEN PREGNANT AND NON-PREGNANT INDIVIDUALS: A CASE CONTROL STUDY
Jade Levine, Chung V, Lisonkova S, Cripton P

Neuromuscular Control

B28. HIGH-DENSITY SURFACE ELECTROMYOGRAPHIC SIGNAL COMPOSITES FOR LOWER LIMB PROSTHETIC CONTROL
Joseph R. Redmond, Christensen FW, Pew CA

B29. BALANCE PLATFORM AND INVERTED PENDULUM FOR ROBOTIC VESTIBULAR CONTROL
Ben P. Bolen, McNeal JS, Hunt AJ

Assistive Technologies

B31. THE SWITCH KIT: BRIDGING THE GAP IN THERAPEUTIC TOYS FOR CHILDREN WITH MEDICAL COMPLEXITIES
Kate Bokowy, Hoffman ME, Bose A, Li T, Feldner HA, Steele KM

B32. A TELEHEALTH TOOL TO AUTOMATE MOBILITY TESTING FOR LOWER LIMB AMPUTEES
Mojtaba Mohasel, Pew CA

B33. UPPER BODY EXOSKELETON IN ANIMAL CARE TECHNICIANS
Emma J. Conway, Overduin A, Fewster KM

Gait & Locomotion

B34. UNDERSTANDING THE PREGNANT WADDLE: IMPAIRED BALANCE OR PROTECTIVE MECHANISM?
Zahra Abedzadehzavareh, Catena RD

Biomechanics of Respiration

B35. COMMON INFANT PRODUCT MATERIALS NEGATIVELY IMPACT BREATHING PATTERNS IN ADULTS
Holly L. Olvera, Bossert A, Mannen EM

B36. ASSESSING CO2 LEVELS EXHIBITED THROUGHOUT BREATHING DURING NOSE DEFORMATION
Giada Brandes, Olvera HL, Mannen EM

Podium Session 1: Neuromuscular Control

FAULTY VISION INFLUENCES SPATIAL REACHING ERROR BUT NOT TIMING ERROR IN VIRTUAL REALITY

Sakurai, M[1], Wilson TJ[1], and Karduna, AR[1]
[1]University of Oregon, Eugene, OR, USA
email: motokis@uoregon.edu web: http://karduna.uoregon.edu.

INTRODUCTION

Proper visuo-proprioceptive coordination is essential to perform accurate upper limb reaching movements for dynamic targets such as catching or hitting a ball [1]. However, this sensory coordination to reach for dynamic targets in a three-dimensional (3D) space is not well understood as it has been traditionally studied in a two-dimensional paradigm using a computer screen [2]. The current study proposes a novel reaching task in an immersive 3D virtual reality (VR) environment that is closer to real-world hand reaching situations. The purpose of this study is to identify how vision and proprioception are used when subjects are required to move their hand to the correct position at the correct time to intercept a dynamic target while their visual field is manipulated to dissociate vision from proprioception. It was hypothesized that both position (spatial) and timing (temporal) errors would be worse when vision is manipulated compared to when vision and proprioception are congruent.

METHODS

Twenty, physically healthy individuals (Female/Male: 10/10, age: 24.7 ± 7.4yr, height: 1.7 ± 0.1m, weight: 75.3 ± 15.4kg) performed a novel reaching task in a VR environment. They were asked to intercept a baseball-sized target with a smooth shoulder elevation movement. They needed to move their reaching (dominant) arm in the correct plane of shoulder elevation at the correct time to accurately intercept the target moving from five meters in front at three meter per second (Figure 1). The target was first projected at shoulder height in all reaching trials, then it moved straight to one of five different end points that varied horizontally. The five target end points corresponded to ± 0, 8, or 16º around shoulder flexion with 0º defined as the shoulder flexion plane. The target end points were randomized between the trials within a block. Each block consisted of 30 "adaptation" trials, immediately followed by 10 "testing" trials. In the adaptation trials, a visual representation of the subject's reaching hand in VR was either visible and congruent with their actual hand position (accurate vision block; AB), not visible at all (no vision block; NB), or visible but with an 8º offset in the transverse plane (offset vision block, OB). In the testing trials, the reaching hand was not visible regardless of the block performed earlier. With the 8º visual offset, subjects saw their hands medially shifted 8º in the transverse plane from their actual hand position. Subjects were not informed about the offset.

Spatial reaching error was calculated as the angle difference between the target end point and reaching hand position in horizontal plane when reaching arm reached 90º of shoulder elevation. Temporal reaching error was the time difference between the two time points that target reached the end point and hand reached the end point. Two-way repeated measured ANOVAs and post-hoc pairwise t-tests with Bonferroni correction were performed to examine whether endpoint angles and trial blocks had the effect and interaction on spatial and temporal reaching errors.

RESULTS AND DISCUSSION

Two-way ANOVAs found the main effects of target endpoints and blocks on spatial error ($p < .001$; Figure 2), but not on temporal error ($p > .05$) with no interaction on both spatial and temporal errors. Post-hoc testing found that spatial error was larger in trials with ±16º endpoints than ones with 0º endpoint ($p < .05$). It was also found that spatial error was larger in OB than AB and NB ($p < .001$). During subsequent testing trials, the spatial reaching error increased in OB, while no change was observed in NB. Humans may be able to perform accurate reaching movements without seeing their reaching hands by relying on proprioception. However, vision is used to adjust the hand position for reaching when present and caused a larger reaching error in offset vision trials.
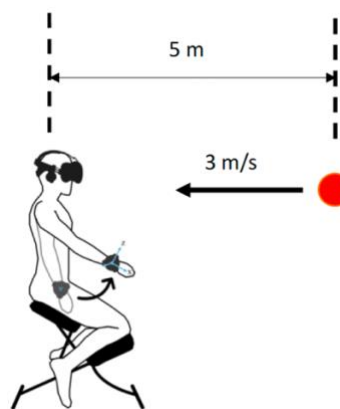
Figure 1: Lateral view of reaching test setting using VR system.
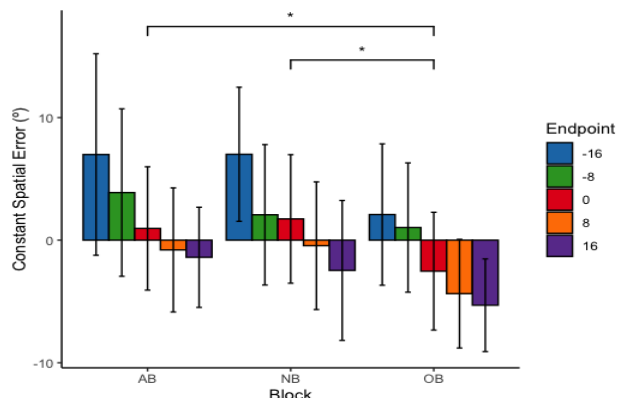
Figure 2: Mean spatial error in testing trials between each block and target endpoint. * denotes $p < 0.001$.

CONCLUSIONS

This is the first study that tested reaching accuracy with dynamic targets in 3D space. The reaching protocol used in this study will be useful for not only assessing individuals' motor control skill, but also has the potential to train people in need of increasing neuromuscular control function such as patients and athletes.

REFERENCES

1. Chen et al. (2021), *J Vis* 21(3).
2. Brouwer et al. (2005), *Exp Brain Res*.165(1)

COGNITIVE AND MOTOR PREDICTORS OF DUAL-TASK PERFORMANCE

Alexandra C. Lynch, Fatemeh Aflatounian, Keith A. Hutchison, Scott M. Monfort
Montana State University, Bozeman, MT, USA
Email: alexandralynch@montana.edu

INTRODUCTION

In sport, athletes are subject to scenarios that challenge both motor and cognitive function. Concurrent cognitive and motor demands (i.e., a dual-task (DT) scenario) require that the athlete distributes finite amounts of cognitive resources between these two tasks, often resulting in detriments to one or both facets of the DT. Identifying correlates of DT (dys)function may enhance risk assessment efforts for preventative and rehabilitation efforts. Previous research suggests that baseline cognitive function influences DT function[1]; however, prior literature has not systematically assessed the relevance of attention control (AC) to physically-demanding cognitive-motor function. The prominent role that AC has in relation to other cognitive processes and cognitive multitasking motivates the need to evaluate its potential as a correlate for cognitive-motor function[2]. Baseline testing of cognitive and motor correlates of DT performance provides a potential pathway to predict individuals who may have deficits in DT performance. The purpose of this study was to determine the extent that isolated cognitive and motor tasks could predict performance during a cognitively challenging single-leg squatting task. We hypothesized that increased performance on cognitive and motor single-tasks (ST) would result in less DT deficits.

METHODS

Twelve healthy controls (20.3±1.4 years, 6 females, 1.77±0.08 m, 77.8±13.8 kg, Tegner: 7.5±1.6, Marx: 13.3±2.0) participated in the study, which included assessments of attentional control and motor tasks both as single- and DTs. The cognitive assessment consisted of a battery of computerized tests (Stroop Squared, Flanker Squared, Simon Squared) that assessed baseline AC [4]. The scores [# correct - # incorrect] of each test in the AC battery was then weighted into a composite score based on previous weightings to define an AC latent variable from these tests (0.58*Stroop, 0.64*Flanker, 0.82*Simon)[3].

Isolated and combined cognitive and motor tasks were used to evaluate DT deficits. Motor performance was evaluated with repeated single-leg squats (45° knee flexion at 0.5 Hz, auditory metronome to maintain frequency). 95% confidence ellipse area of the center of pressure (10 Hz lowpass filtered) was the metric used to assess gross motor performance during the task, with increased ellipse area corresponding to more sway[4]. The isolated cognitive task was the Antisaccade test of attention control[5], with the performance metric being participants' accuracy in identifying briefly-presented stimuli on the opposite side of a screen from a distractor cue. The DT condition consisted of the repeated squatting and Antisaccade tests performed concurrently. Each condition was repeated for 5 blocks of 54 seconds and the average over the five blocks was used in analyses. The order of the conditions was randomized. Cognitive (DTC_c) and motor DT (DTC_m) deficits were characterized as percent change relative to ST conditions, with positive values indicating worse DT performance, and lower magnitude DTC indicating less change between ST and DT. Correlations were used to assess correlations between ST and DTC measures.

RESULTS AND DISCUSSION

A significant negative correlation was found between AC and DTC_m (r = -0.783, p = 0.002) with a similar, albeit nonsignificant, negative correlation between AC and DTC_c (r = -0.542, p = 0.069) **(Figure 1)**. Other correlations were also negative but did not reach statistical significance.
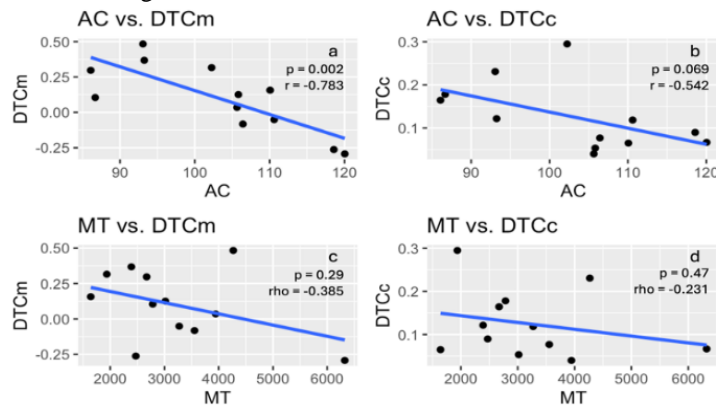

Figure 1: Correlations between cognitive ST (AC) and motor ST (MT) variables and DT change measured with motor (DTC_m) or cognitive (DTC_c) variables.

The purpose of this study was to determine how well ST cognitive or motor performance could predict DT deficits. Our hypothesis was partially supported, as the results show negative correlations between AC and DTC_m. Low magnitude DTC scores reflect little difference between the ST and DT conditions. The significant negative relationship between AC and DTC_m suggests that high performers in AC tasks mitigated differences in postural sway between ST and DT conditions. These findings illustrate how AC may provide a protective role in DT scenarios. Although not all significant, these correlations show trends indicating that this healthy control group was likely to have less DT change either from a cognitive or motor variable when they performed better on a cognitive ST. This study is ongoing and additional data are currently being collected, which will help further elucidate the relationships that are present.

CONCLUSIONS

These preliminary results show that AC may be a salient correlate of DT performance deficits. This has the potential to augment efforts to identify those who are likely to be most adversely affected by real-world DT demands, which has injury risk assessment applications.

REFERENCES

1. Monfort et al (2019). *American J. Sports Med.* **47**, 1488-1495.
2. Draheim et al (2021). *J Exp Psychol Gen.* **150**, 242-275.
3. Burgoyne et al (2023). *J Exp Psychol Gen.* **152**, 2369-2402.
4. Prieto et al (1996). *IEEE Transactions on BME.* **43**, 956-966.
5. Hutchison (2007). *J Exp Psychol. L.M.C.* **33**, 645-662.

ACKNOWLEDGEMENTS

THE EFFECTS OF LUMBAR SPINE CREEP ON BALANCE CONTROL

Evans, I.D.*, McIntosh, B.A., Carpenter, M.G., and Fewster, K.M.
School of Kinesiology, University of British Columbia, Vancouver, BC, Canada
email: isabel.evans@ubc.ca*

INTRODUCTION
Low back pain (LBP) plagues 84% of today's society [1]. Previous research has identified multiple risk factors for LBP including prolonged sitting [2]. When in a seated position, the intervertebral joints flex forward, resulting in deformation to the passive structures [3]. Such deformation within the passive tissues of the spine can result in creep, which has been shown to result in joint laxity, decreasing spinal stability [4]. This decrease in stability could place individuals at greater risks for low back injury, particularly during sudden perturbations, when the lumbar spine is particularly reliant on the passive structures. Therefore, the objective of this investigation is to evaluate the influence of creep on lumbar spine kinematics during a sudden perturbation. We hypothesize that flexion-induced creep will lengthen the passive tissues of the spine and result in increased motion of the lumbar spine in response to sudden trunk perturbations.

METHODS
Four participants visited the lab on two separate occasions, one which exposed participants to sudden perturbations following a creep protocol (creep day) and one where participants were exclusively exposed to sudden perturbations (control day) [5]. On both days, rigid bodies placed at L1 and S1 were used to track digitized anatomical landmarks on the torso and pelvis (Optotrak Certus, Northern Digital, Waterloo, ON, Canada). On creep day, two Vicon (Oxford, UK) Blue Trident IMUs were placed on the same anatomical landmarks to measure flexion angle during the creep protocol.

Participants underwent five perturbations which consisted of an initial 300ms acceleration phase, a 2-second constant velocity period and a 200ms deceleration phase, with a total sled displacement of 46cm [6]. The identical perturbation was applied in either the forward (forward) or reverse (backward) direction with respect to the participant. The order of the perturbations was kept constant for the purpose of comparison between subjects and experimental days – backward, backward, forward, forward, backward – however, participants were naïve to perturbation order. Maximum flexion angle, maximum extension angle and anterior-posterior center of pressure (COP) excursion (mm) were analyzed over the initial 700ms of the first two backwards perturbations [6], using V3D Software (C-Motion Inc., Kingston, Ontario, Canada) and force and moment data were obtained from an AMTI BP400600 force plate (Watertown, Massachusetts, USA) embedded in the moving platform.

Prior to perturbations on creep days, participants underwent a five-minute creep protocol in which they passively hung over a bar adjusted to the height of their ASIS. The IMUs' were utilized as tiltmeters and were used to measure changes in lumbar spine flexion throughout the creep protocol. Immediately following the creep protocol, participants underwent the same perturbation procedure to control days.

RESULTS AND DISCUSSION
Perturbation responses were separated into kinematic responses during the first 700ms and the full perturbation, allowing for analysis of during the constant velocity period, before any deceleration, and the full perturbation [6]. The first two backwards perturbations were averaged across subjects. Preliminary findings demonstrate no apparent differences in total lumbar spine range of motion (ROM) between control and creep conditions, $9.84 \pm 5.73°$ and $8.98 \pm 4.95°$ respectively. However, on creep days, participants did not enter lumbar spine extension throughout a perturbation response and instead remained in flexion throughout the perturbation – resulting in a greater peak flexion angle (Table 1). The average displacement of COP during the initial 700ms of the perturbation was smaller during creep days, 29.11 ± 4.95 mm compared to 37.86 ± 61.14 mm during control days (Table 1).

Table 1: Average kinematics during initial 700ms of perturbation.

Collection	Max Angle	Min Angle	Trunk ROM	COP Excursion
Control	$3.14 \pm 6.79°$	$-6.70 \pm 7.70°$	$9.84 \pm 5.73°$	37.86 ± 61.14 mm
Creep	$-8.37 \pm 7.50°$	$-17.35 \pm 6.43°$	$8.98 \pm 4.95°$	29.11 ± 4.95 mm

Note: Positive angle values indicate extension with respect to upright standing whereas negative values indicate flexion.

CONCLUSIONS
The findings of this study, provide insight into the influence of creep in the lumbar spine on responses to a sudden perturbation. Preliminary findings suggest changes in lumbar spine kinematics during perturbations following creep.

REFERENCES
[1] Gross et al., 2006. *Spine*, *31*(18), 2142-2145.
[2] Bombardier et al., 2002. *Best Practice & Research Clinical Rheumatology,* 16(5), 761–775.
[3] De Carvalho, 2015. *University of Waterloo.*
[4] McGill & Brown, 1992. *Clinical Biomechanics,* 7(1), 43-46.
[5] Abboud et al., 2018. *Journal of Neurophysiology, 120(4), 1591-1601.*
[6] Carpenter et al., 2010. *Clinical Neurophysiology, 121(1), 109-117.*

ACKNOWLEDGEMENTS

EFFECT OF SPINAL STIMULATION AND INTERVAL TREADMILL TRAINING ON GAIT MECHANICS IN CHILDREN WITH CEREBRAL PALSY

Charlotte D. Caskey[1]*, Siddhi Shrivastav[1], Victoria M. Landrum[1], Kristie Bjornson[1,2], Desiree Roge[2], Chet Moritz[1], Katherine Steele[1]
[1]University of Washington, Seattle, WA, USA
[2]Seattle Children's Hospital, Seattle, WA, USA
email: cdcaskey@uw.edu

INTRODUCTION

Children with cerebral palsy (CP) have a brain injury around the time of birth that affects the development of neuromuscular motor control and integration of sensory information. Many children with CP have spasticity, an exaggerated stretch reflex, which is thought to contribute to altered gait mechanics [1]. Transcutaneous spinal cord stimulation (tSCS) is a novel, non-invasive neuromodulation technique that activates sensory pathways to amplify communication in the nervous system [2]. Our prior work has shown that pairing tSCS with short-burst interval locomotor treadmill training (SBLTT) reduced spasticity more than SBLTT alone and may lead to increases in peak hip and knee extension and total joint excursion during overground walking [3]. This study evaluated the effects tSCS + SBLTT on the coordination of hip and knee extension and subsequent muscle-tendon lengths (MTLs) throughout the gait cycle. Due to the reductions in spasticity from tSCS and SBLTT, we hypothesized that hip and knee kinematic trajectories will be more extended throughout the gait cycle with an increase in peak operating MTLs during gait.

METHODS

Four children ages 4-13 years old with spastic CP received 24 sessions each of each intervention, first SBLTT only followed by tSCS + SBLTT. Spasticity and biomechanical walking assessments were collected the week before and after each intervention and at 8-weeks follow-up. Spasticity was evaluated using the Modified Ashworth Scale for the quadriceps, hamstrings, gastrocnemius, and soleus muscles bilaterally. Optical motion capture data were collected during barefoot, overground, self-selected walking on a 10-meter walkway. Data were processed using custom MATLAB scripts (MathWorks, Natick, MA, USA) and OpenSim v4.3 (Stanford, USA). Statistical parametric mapping was used to compare joint kinematics during each phase and at follow-up timepoints with respect to the timepoint corresponding to the start of that phase. A Bayesian Additive Regression Trees (BART) model was built to isolate the direct effect of spasticity on MTLs, while controlling for participant, muscle, side of the body, study timepoint, and walking speed.

RESULTS AND DISCUSSION

All four participants exhibited the greatest improvements in hip and knee extension after tSCS + SBLTT or at 8-weeks follow-up after tSCS + SBLTT (Figure 1A and B; example from one participant). For the example participant, both the hip and knee were more extended throughout the entire gait cycle after tSCS + SBLTT. This increased extension was maintained into the 8-week follow-up period (Figure 1A and 1B). The BART model using all participants' spasticity data and peak operating MTL had high model fit (R^2 = 0.99) with reductions in spasticity corresponding to a 7.7 mm/m increase in MTL, after controlling for participant,

muscle, side of the body, study timepoint, and walking speed (Figure 1C). Current spasticity treatments reduce spasticity but do not consistently translate to improved walking function without extensive additional rehabilitation [4]. These results suggest that tSCS + SBLTT may be able to reduce spasticity while maintaining walking mechanics.
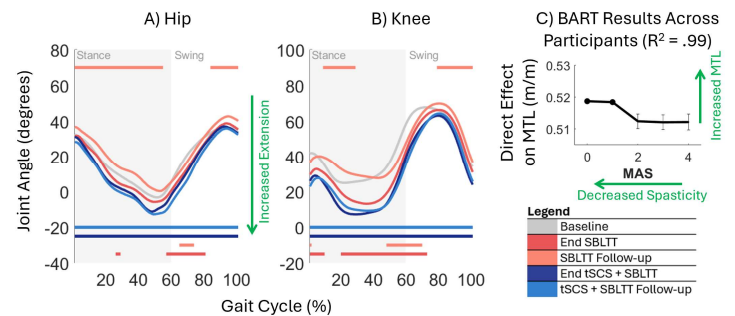

Figure 1: A) Hip and B) knee kinematics during the gait cycle from an example participant. Horizontal colored lines indicate where there were significant changes in kinematics over each phase of the study based on statistical parametric mapping (p<0.05). Lines on top indicate locations of significant increases, while lines on the bottom indicate points of significant decreases. C) Bayesian Additive Regression Trees (BART) results quantify direct effects of spasticity as measured by the Modified Ashworth Scale on muscle-tendon lengths (MTL) across muscles. Results are visualized using Accumulated Local Effects Plots.

CONCLUSIONS

This pilot study provides foundational work for developing our understanding of the mechanisms behind which tSCS affects movement for children with CP and how the observed reductions in spasticity with tSCS may affect gait. We highlight the importance of quantifying clinical assessments, such as those for spasticity, with biomechanical outcomes to better understand how novel treatment options translate to changes in function that impact daily life.

REFERENCES

1. van der Krogt et al. (2009) Gait Posture (29)2009
2. Edgerton et al. (2021) Front. Hum. Neurosci. (15)643463
3. Shrivastav, Caskey, et al. (2023) Preprint: medRxiv
4. MacWilliams et al. (2022) DMCN (64)5

ACKNOWLEDGEMENTS

Abstracts

Podium Session 2: Assistive Technology & Machine Learning

RECONSTRUCTING UNMEASURED INERTIAL DATA WITH SPARSE SENSING FOR TREADMILL RUNNING

Pitts, MN[1], Ebers, MR[2], Agresta, CE[3], Steele, KM[1]
[1]Department of Mechanical Engineering, University of Washington, Seattle, WA USA
[2]Department of Applied Mathematics, University of Washington, Seattle, WA USA
[3]Department of Rehabilitation Medicine, University of Washington, Seattle, WA USA
email: mnp0020@uw.edu

INTRODUCTION

Running is a popular and accessible form of exercise, and measuring a runner's biomechanics can provide insight for performance and injury evaluation. Wearable sensors, such as inertial measurement units (IMUs) offer a way to capture running data in diverse environments. Multiple sensors enable access to more information for tracking digital biomarkers and monitoring full-body movement. However, many running studies that use IMUs only include one sensor, often at the lower leg [1], suggesting that sparsity is favored or necessary when evaluating running. Our team has developed a method that utilizes shallow recurrent decoder networks (SHRED) to leverage time-series data from a small or sparse set of mobile sensors to reconstruct a full or dense set of unmeasured data [2]. The purpose of this study was to quantify the accuracy of individualized SHRED models for expanding to a dense set of unmeasured IMU signals from a single IMU during treadmill running.

METHODS

We used an open-source dataset with nine adults who completed three 6-minute treadmill runs at speeds of 1.8, 2.2, and 2.7 m/s [3]. IMUs (Opal APDM, 128Hz) were placed at the center of the chest, left hip, and lateral side of each ankle. Because a triaxial accelerometer at the lower leg is commonly leveraged for running studies, we used triaxial acceleration at the right ankle as sparse input to train individualized SHRED models for estimating the full set of IMU signals. We first quantified accuracy for models trained and tested on a single speed of 2.2 m/s. Each subject's data was split into 60% training, 20% validation, and 20% test and used to train individual-specific SHRED models. We also trained models for each subject on the 1.8 m/s and 2.7 m/s speeds to quantify interpolation accuracy of reconstructing signals from the held-out 2.2 m/s running speed. Reconstruction error was calculated as the mean squared error (MSE) between the measured and predicted values of the output signals for linear acceleration and angular velocity triaxially at each sensor location.

RESULTS AND DISCUSSION

Individualized SHRED models had low reconstruction error for all IMU signals based on only right ankle accelerometry input. For single speed models, the reconstruction error (mean ± SD) across subjects for all acceleration signals was 0.28 ± 0.17 m/s^2 with the lowest error occurring at the ankles (Fig.1). An accelerometer at the lower leg is commonly used in running studies to estimate loading with a minimum detectable change of 5.2 m/s^2 for tibial accelerometers [4]. With SHRED, we estimated unmeasured accelerations of the left ankle below this threshold with an error of 0.27 ± 0.09 m/s^2. For interpolation models, reconstruction error of acceleration signals increased to 1.14 ±

0.30 m/s^2, with left ankle error being 1.14 ± 0.32 m/s^2. These comparisons indicate that unmeasured signals reconstructed from individualized SHRED models perform within the range of the variance inherent in the sensor system.
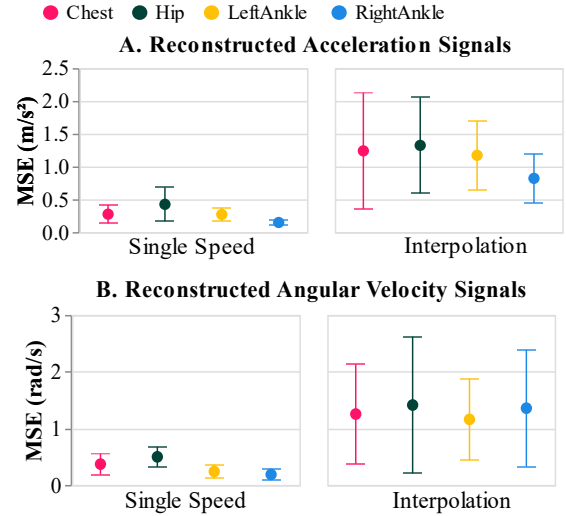
Figure 1: Reconstruction error of accelerations (A) and angular velocities (B) at each sensor location from right ankle triaxial acceleration input.

Angular velocity reconstruction error for single speed and interpolation models was 0.32 ± 0.15 rad/s and 1.53 ± 0.46 rad/s, respectively. This corresponds to 9.2% and 44.1% of the mean angular velocity magnitude at the ankle in the sagittal plane.

CONCLUSIONS

Data expansion with individualized SHRED models can be useful to quantify unmeasured sensors, potentially reducing the number of sensors required for measuring inertial data across sessions and estimating full-body movement in remote environments. Further work is needed to establish accuracy thresholds for acceleration and angular velocity signals at multiple sensor locations and various running speeds to fully validate this method. These models may enable better estimates for remotely monitoring digital biomarkers during running and increased accuracy of movement classification algorithms with sparse sensing.

REFERENCES

1. Benson LC et al., *Sensors*, 2022; **22**(5), p.1722.
2. Ebers MR et al., arXiv:2307.11793 [cs, math].
3. Ingraham K et al., 2018, Dataset.
4. Hughes T et al., *J. Electromyogr. Kinesiol.*, 2019; **44**, p.156-164.

Evaluation of a Multi-Axial Shear Sensor Using a Multi-Layer Perceptron Model

Mohler, AJ[1], McGeehan, MA[2], Ong, KG[2] and Hahn, ME[1]

[1]Neuromechanics Lab, Department of Human Physiology, University of Oregon, Eugene, OR USA
[2]Ong Lab, Phil and Penny Knight Campus for Accelerating Scientific Impact, University of Oregon, Eugene, OR USA
Website: https://bssc.uoregon.edu/neuromechlabs/ Email: amohler@uoregon.edu

INTRODUCTION
The use of tactile shear sensors has recently increased, particularly in limb protheses [1]. McGeehan et al. (2021 [2] developed an optoelectronic-based sensor for measuring shear force and displacement. Previously used regression models [2] were unable to predict X and Y coordinates simultaneously, therefore we opted to design a multilayer perceptron (MLP) model to achieve our primary objective of developing a dual-output machine learning algorithm and characterize its accuracy for transducing four inputs from the sensor (RGBC light intensity) into two-axis shear displacement data.

METHODS
Sensor data were collected using a modified computerized numerical control (CNC) router positioning stage with 3D printed housing designed to secure the sensor. The displacement data gathered from the CNC router were used as a gold standard reference to model and compare the MLP-ANN's performance. To map the full surface of the sensor, the CNC displaced the sensor pattern in 1 mm increments along the X and Y directions for a total test range of ± 10 mm. Ten RGBC sensor measurements were collected at each increment for a total of 1100 measurements.

Our methodology is constructed around the scikit-learn sk.learn.neural_network.MLPRegressor API. Using our hyperparameter tuning algorithm, the following parameters were set: *hidden_layer_sizes: (512, 256, 128, 64, 32, 16), activation: ('logistic'), alpha: (0.001), learning_rate_init: (0.001)*. The remaining parameters were not changed from default.

To characterize model performance, the X and Y coordinate data derived from the MLP-ANN model were compared to displacement data from the CNC testbench. Residuals were calculated for each data point across the test range by subtracting the MLP-ANN predicted coordinate from the known CNC displacement. Overall model performance was quantified using root-mean-squared error (RMSE) and coefficient of determination (R^2) between the MLP-ANN X and Y outputs and gold standard CNC (i.e., predicted vs actual) displacement data.

RESULTS AND DISCUSSION
The MLP-ANN algorithm resulted in R^2 values of 0.99 for both X and Y coordinates, and average RMSE of 0.23 mm ± 0.26 mm and 0.36 mm ± 0.38 mm for X and Y, respectively (Figure 1, Table 1). The averaged RMSE results show most predicted X coordinates having RMSE < 0.25 mm, with certain areas exhibiting RMSE > 0.40 mm. The Y coordinate RMSE values were more consistent at < 0.15 mm, with certain areas of > 0.25 mm. For both the X and Y coordinates, error was generally higher near the limits of the testing range. Overall, the spatial results of the MLP-ANN gathered show good agreement and consistency with the gold standard displacement data from the CNC testbench. These data support the use of the MLP-ANN as a valid model for the shear sensor in question up to 0.23 mm resolution for the X coordinate, and 0.36 mm resolution for the Y coordinate.
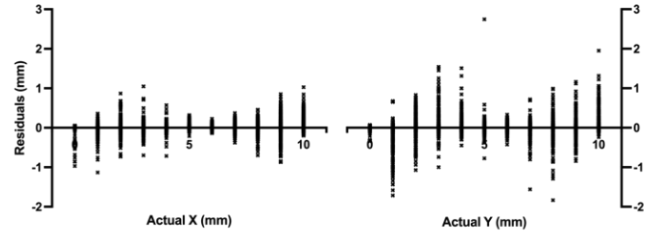
Figure 1: Actual Residuals; X on the left, Y on the right.

CONCLUSIONS
The goal of this work was to design a dual-output machine learning algorithm that could transduce optical shear sensor outputs into displacement data. Our MLP-ANN model achieved benchmark results of 99.18% accuracy in the X (medial-lateral) direction, and 97.87% accuracy in the Y (anterior-posterior) direction.

REFERENCES
[1] Tiwana, M.I, et al. *Sensors and Actuators A: Physical,* **165**, 164-172, 2011.
[2] McGeehan M.A, et al. *IEEE Sensors Journal,* **21**, 25641-25648, 2021.

ACKNOWLEDGEMENTS

Table 1: MLP-ANN post-training results.

Coordinate	Accuracy (%)	RSME + STD (mm)	R^2
X	99.18	0.23 ± 0.26	0.99
Y	98.17	0.36 ± 0.39	0.99

HEEL-STRIKE DETECTION ALGORITHM FOR EXOSKELETON WALKING AFTER SPINAL CORD INJURY

Annika Pfister[1*], Rich Henderson[2], Chet Moritz[1,2], and Kimberly A. Ingraham[1]
[1]Department of Electrical and Computer Engineering, University of Washington, Seattle, WA USA
[2]Department of Rehabilitation Medicine, University of Washington, Seattle, WA USA
email: apfist8@uw.edu, web: kim-ingraham.com

INTRODUCTION

Exoskeletons are increasingly used for gait rehabilitation following spinal cord injury (SCI) in research and clinical settings. Gait biomechanics are a key indicator of whether a rehabilitative technique is successful. To evaluate the effects of using exoskeletons for rehabilitation settings, muscle activity (EMG), inertial measurement units (IMUs), and other gait data must be segmented by stride for analysis, often using heel-strike as a marker for segmentation. Without automation, heel-strike detection must be done manually, relying on visual evaluation of considerable amounts of data. This requires a deep understanding of gait patterns in adults with SCI, is incredibly time-consuming, and can introduce inherent bias in stride segmentation. Previous methods for automated heel-strike detection have been proposed using data from both nondisabled and SCI participants [1,2,3]. However, these works do not account for the added influence of wearing a robotic exoskeleton, particularly with high levels of swing assistance, which may influence the characteristics of heel strike during the gait cycle. This study demonstrates the utility and accuracy of automated heel-strike detection for gait analysis of exoskeleton walking in adults with SCI.

METHODS

We collected 3-D acceleration and shank angular velocity, as well as force-sensitive resistor (FSR) data (Delsys Trigno Avanti, sampled at 148 Hz) from a representative participant with SCI (male, age 49, injury level C6, AIS C). The participant walked overground in an Ekso Bionics exoskeleton using the ProStep+ mode. The algorithm defined a heel-strike as the first "zero-crossing" following a mid-swing peak in the sagittal plane gyroscope data (filtered using a 5 Hz-lowpass 5th order Butterworth). Peaks were detected using the SciPy 'findpeaks' function, with a minimum peak height defined as 80% of the mean of all data points greater than the average (a user-adaptive threshold [1]), and a prominence of 50. We defined mid-swing peaks as being separated by at least a 200-sample window length. Between each mid-swing peak, heel-strike was detected as the first index where the angular velocity was less than or equal to zero. We validated the algorithm by comparing detected heel-strike time indices to the ground truth, determined via FSR data collected from the center of the heel. FSR heel-strike was determined as a local minimum prior to the characteristic peak during stance phase.

RESULTS AND DISCUSSION

We compared the performance of our IMU-based heel-strike detection algorithm to the FSR-defined ground truth for the representative participant (Fig. 1A). Over 2 minutes of continuous overground walking data, we found that our IMU-based method had an overall mean error of 10-150 milliseconds (ms). Compared to the participant's average step duration of 5.5 seconds, this is a relatively small error – less than 2.7% of the gait cycle. Similar work has reported errors on the order of 10 ms for automated heel-strike detection, validated by force plate data [1].

We applied the same algorithm to data from three different participants with SCI. The algorithm yielded consistent stride segmentation of sagittal-plane gyroscope data (Fig. 1B), indicating that this method is robust to individual variation in gaits in adults with SCI using an exoskeleton.
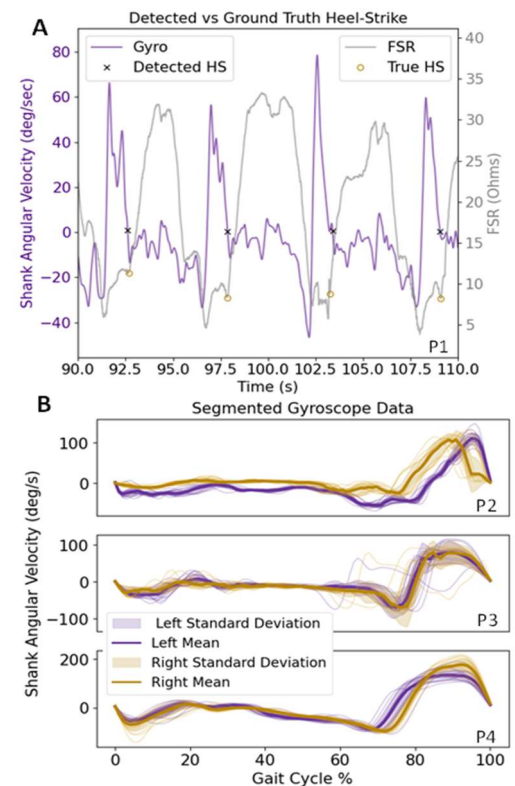
Figure 1: A) Validation of IMU-based heel-strike detection algorithm using FSR data for the representative participant (P1). **B)** Stride-segmented angular velocity data for novel participants (P2-P4) when our heel-strike detection algorithm is applied.

CONCLUSIONS

Accurate heel-strike detection is crucial for biomechanical analysis of data including EMG signals and gait kinematics, especially in participants with SCI who have variable gait speed and kinematics. Our algorithm for automating heel-strike detection demonstrated relatively low error while successfully implementing a consistent and objective method for determining heel-strike time indices. Future work will address algorithm robustness to periods of standing or pivoting in an exoskeleton, as well as detecting toe-off for more refined gait segmentation. Ultimately, this work holds promise for creating streamlined data processing pipelines to analyze exoskeleton gait training in the field of SCI rehabilitation.

REFERENCES

1. Greene BR, et al. *Med Biol Eng Comput* **48**, 1251-1260, 2010.
2. Han et al. *IEEE Sens J* **19**, 3439-3448, 2019.
3. Jasiwicz et al. *Gait Post* **24**, 502-509, 2006.

ACKNOWLEDGEMENTS

A Comparison of Methods for Assessing Young Children's Mobility Device Use in Real-world Settings

Mia E. Hoffman[1,2], Bethany Sloane[3], Anna Fragomeni[4], Kat M. Steele[1,2], Lisa K. Kenyon[5], Sam W. Logan[3], Heather A Feldner[2,4]

[1]Department of Mechanical Engineering, University of Washington; [2]Center for Research and Education on Accessible Technology and Experiences, University of Washington; [3]Oregon State University College of Public Health and Human Sciences; [4]Department of Rehabilitation Medicine, University of Washington; [5]Department of Physical Therapy and Athletic Training, Grand Valley State University

email: miahoff@uw.edu, web: miahoffmannd.github.io

INTRODUCTION

Mobility aids, such as powered mobility devices, can support the exploration and play of young children with disabilities at the same rate as their nondisabled peers. Assessing a child's use of powered mobility through data-driven approaches can not only aid caregivers and therapy teams, but also substantiates insurance claims for device coverage. A recent review paper showed that the use of the modified ride-on car (MROC), a common type of mobility device for young children, has been tracked by 39% of studies using caregiver-reported activity logs and 4% of studies using electronic tracking[1]. One additional study published since the review has used electronic tracking combined with geospatial positioning (GPS) to measure MROC use[2]. However, the optimal method to quantify a child's exploration and use of mobility aids in home and community environments remains unknown. The aim of this work was to compare three methods of device tracking: activity logs, loggers integrated into the electronics of the device, and GPS trackers.

METHODS

Twelve children with cerebral palsy (age: 15-32 mo, GMFCS: II-V) were provided with two powered mobility devices, the Permobil Explorer Mini (EM) and a MROC, to use for 8 weeks each as part of a larger randomized, crossover clinical trial[2]. The participants' device usage was tracked using all three methods simultaneously. Caregivers wrote the start and end activity time, location of use, and general notes in the activity logs. Arduino-based loggers integrated into modified ride-on cars only measured the time and duration of switch activation. The GPS trackers measured time and geospatial position. Play sessions were identified by either switch activation or by a period of change in geospatial position. Play sessions were defined as being at least two minutes in duration and were distinguished by a period of at least 10 minutes from the end of the last play session. For the GPS tracker data, device use was differentiated from device transport in a vehicle by a velocity threshold of 2 m/s. Using custom Python scripts, we calculated the duration and date of each play session, as well as total number of sessions.

RESULTS AND DISCUSSION

Caregiver-reported activity logs are the current standard for tracking powered mobility device use for young children, as they are most widely utilized. Correlation was the highest between the integrated logger and GPS tracker for the three main outcome measures: total session minutes, unique days, and number of sessions. The outcome measures were not consistent for each participant between all three logging methods (Figure 1). The
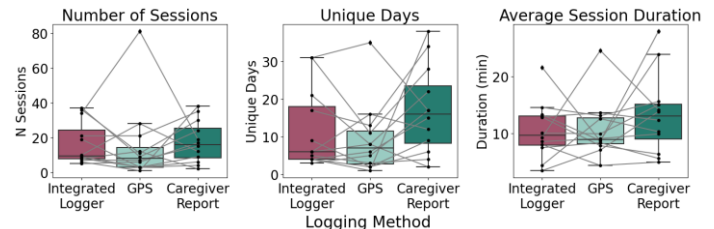

Figure 1: The number of sessions, unique days, and average session duration for all 12 participants using the MROC as measured by the integrated logger, GPS tracker, and caregiver-reported activity logs.

GPS trackers under identified sessions. The caregiver-reported activity logs over-estimated session duration.

The high correlation between the quantitative measurement methods, indicates that both may be more reliable than caregiver-reported data. Quantitative loggers offer objectivity and are likely less-time consuming for families to manage. However, while the caregiver-reported activity logs provide qualitative insights of a child's interaction with the device, they may lack the precision of quantitative measures. Both quantitative loggers present technical challenges. The integrated loggers required altering the device's electronics, risking device malfunction. Meanwhile the GPS tracker's performance is hindered by signal strength issues, particularly indoors, limiting its usability in certain locations.

CONCLUSIONS

Each tracking method exhibits strengths and weaknesses, suggesting potential of combining multiple systems, such as inertial measuring units with GPS, to develop a comprehensive tracking system. A successful logging device shouldoffer quantitative guidance for clinicians and caregivers while accommodating diverse environmental settings to support young children's self-exploration effectively.

REFERENCES

1. Hospodar, CM, et al., *Assistive Technology* **18**, 974-988, 2023.
2. Hoffman et al., *Dis & Rehab: AT*, 2023.
3. Feldner, et al., *Physical Therapy*, **102**, 2022.

ACKNOWLEDGEMENTS

Abstracts

Podium Session 3: Gait & Locomotion

GRADE-DEPENDENT MECHANICAL STRATEGIES FOR INCREASING RUNNING SPEED

Robinson, RR[1], Donahue, SR[2], Chebbi, A[1], and Hahn, ME[1]
[1]Neuromechanics Lab, Department of Human Physiology, University of Oregon, Eugene, OR USA
[2]Northwestern University Prosthetics-Orthotics Center, Northwestern University, Chicago, IL, USA
email: rrobins3@uoregon.edu

INTRODUCTION

When running on level ground (LG), faster submaximal speeds are achieved by increasing stride length, stance phase positive hip and ankle work, and swing phase positive hip work [1,2]. Fewer studies have evaluated the mechanisms for increasing speed when running uphill (UH) and downhill (DH) [3]. By evaluating spatiotemporal variables and joint kinetics during stance and swing phases of running, the purpose of this study was to determine whether the mechanical strategies to increase speed are different between LG, UH and DH running. Due to greater changes in step frequency when increasing UH speed, it was hypothesized that increasing UH speed would elicit greater increases in swing phase positive hip flexor work and smaller changes in stance phase work than LG [4]. Due to similar spatiotemporal changes with speed for LG and DH running, no differences were expected between LG and DH strategies.

METHODS

Twelve recreational runners (7 female, age: 24.4 ± 7.7 yr., mass: 63.2 ± 10.0 kg, height: 171.0 ± 9.65 cm) completed 30s running trials at 5 speeds on LG, 7.5° UH, and 7.5° DH. Kinematic data were collected at 200 Hz using an 8-camera motion capture system (Motion Analysis Corp.) and kinetic data were collected at 1000 Hz using a force-instrumented treadmill (Bertec). Running speed was based on each participant's self-reported 5k pace. Speed categories were defined as Speed 1 (1:30 min/mile slower than 5k pace), Speed 2 (1:00 min/mile slower than 5k pace), Speed 3 (:30 min/mile slower than 5k pace), Speed 4 (5k pace), and Speed 5 (:30 min/mile faster than 5k pace). Since not all subjects were able to complete the UH trial at 5k pace, only Speeds 1-3 were analyzed. Step length, step frequency, contact time, swing time, and flight time were averaged across the middle 10s of each trial. Sagittal plane hip, knee, and ankle power were calculated using inverse dynamics in Visual 3D (C-Motion, Inc.). Joint work was calculated as the time integral of the of the power-time curves. Positive and negative work for stance and swing phase were calculated separately. Two-way repeated measures ANOVAs (3 grades x 3 speeds) were performed in SPSS (IBM Corp.) to test for within-subject differences in spatiotemporal and joint work variables.

RESULTS AND DISCUSSION

The average running velocity for speed categories 1, 2, and 3 were 3.23 ± 0.38, 3.44 ± 0.43, and 3.68 ± 0.49 m/s, respectively. The only spatiotemporal variable with a significant interaction effect ($p < 0.05$) was swing time. While swing time was not significantly different between speeds during LG running, swing time was shorter for faster speeds during UH and DH running. While no significant interaction effects were observed for stance phase joint work, significant interaction effects ($p < 0.05$) were observed for all swing phase joint work variables except for positive knee work. For all grades, increasing speed required greater swing phase positive hip, negative hip, and negative knee

work (Figure 1). While swing phase positive and negative ankle work increased with speed, their magnitude was near zero.
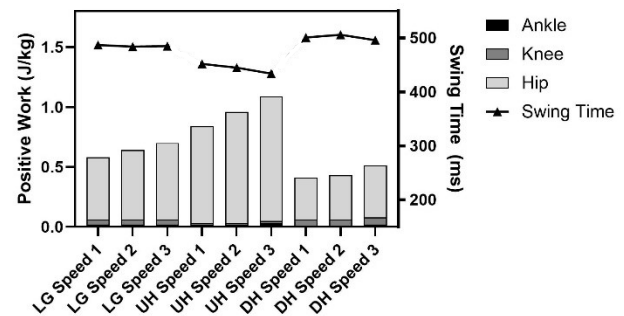

Figure 1: Swing phase positive joint work and swing time

Positive hip work, which accounted for the majority of swing phase positive work, increased by 25% on LG, 29% on UH, and 24% on DH from Speed 1 to 3. This greater increase in positive hip work with faster UH running speed supports our hypothesis. Contrary to our hypothesis, no significant interaction effects were observed for stance phase kinetics [3]. This may be due to the previous study's greater difference between test speeds compared to the current study. The reduction in swing time while running UH during faster speeds may be a strategy to minimize stance phase energy generation. Rather than generating more energy per step to increase speed, the leg swings forward more quickly. Despite the increased hip work required to swing the leg during faster UH running, body weight support is more costly than leg swing, and this may be a worthwhile trade-off [5]. Reduced swing time while running DH at faster speeds may reflect participant comfort levels running DH on a treadmill. If uncomfortable with steep DH running, participants may contact the ground earlier, thus limiting swing time.

CONCLUSIONS

This study expands on previous investigations into the combined effects of speed and grade on running mechanics by including swing phase joint kinetics. Understanding the mechanical demands of UH and DH running at common training speeds may guide selection of rehabilitation and training techniques for runners who train or compete on hilly terrain.

REFERENCES

1. Weyand PG, et al. *J Appl Physiol* **89**, 1991-1999, 2000
2. Jin L, et al. *Hum Mov Sci* **58**, 1-9, 2018
3. Khassetarash A, et al. *Scand J Med Sci Sports* **30**, 2020
4. Vernillo G, et al. *Scand J Med Sci Sports* **30**, 1642-1654, 2020
5. Arellano CJ, et al. *ICB* **54**, 1084-1098, 2014

ACKNOWLEDGEMENTS

RUNNING SPEED INFLUENCES PHASE-SPECIFIC CHANGES IN JOINT KINEMATICS DURING FOOT CONTACT

Emily K. Eichenlaub[1], Megan Saftich[1], Evan M. Day[1], Ed Nyman[1], Jennifer Sumner[1]
[1]Brooks Sports, Seattle, WA, USA
Email: emily.eichenlaub@brooksrunning.com

INTRODUCTION

Quantifying the ability of footwear to help keep a runner close to their habitual motion path (HMP) is the principal basis upon which footwear performance is evaluated at Brooks [1]. Recent HMP methodological advancements utilize joint range of motion (ROM), in addition to other kinematic variables derived from the entire stance phase, to understand a runner's unique kinematics. Running speed affects sagittal plane joint angles [2], but there is a relative void in understanding how speed affects frontal and transverse plane joint angles, which are used to inform footwear construction [1]. The purpose of this study was to investigate temporal changes in joint and foot angles and ROM during stance as a result of changing running speed.

METHODS

Data from human-participant product testing rounds were aggregated (n=96). Participants ran on an instrumented treadmill (Bertec, Columbus, OH, USA) at two speeds: (1) 3.35 m/s, and (2) self-selected preferred running speed. Footwear was controlled across participants (Brooks Launch 4). Three-dimensional kinematics of the rearfoot, shank, and thigh segments were acquired using an optical motion capture system (Motion Analysis Corporation, Rohnert Park, CA, USA). Ankle and knee joint and global foot angles were calculated using a Cardan-Euler approach. Knee internal rotation (TIR), ankle eversion, and foot eversion ROM were calculated for each speed. As most participants slowed down (79/96), this analysis focused the comparison of slowing down from 3.35 m/s by 1-10% (speed range: 3.04-3.25 m/s, average speed 3.14 m/s, n=32) and 10-20% (speed range: 2.68-3.00 m/s, average speed 2.90 m/s, n=45). Dependent t-tests were used to determine statistical significance (α=.05) for ROM magnitudes and dependent t-test statistical parametric mapping (SPM) was used to compare time normalized joint angles during stance between the preferred speed bins and 3.35 m/s.

RESULTS AND DISCUSSION

Our results only focus on runners with a preferred speed decrease of 10-20% below 3.35 m/s, as this aligns with speed changes in the literature showing joint angle differences [2]. On average, runners exhibited 4% greater TIR ROM (p=0.01), 5% greater ankle eversion ROM (p=0.01), and 8% greater foot eversion ROM (p<0.001) at 3.35 m/s compared to their slower preferred speed. Runners exhibited greater foot inversion during early and late stance when running at 3.35 m/s (**Fig. 1A**), compared to ankle eversion and TIR exhibiting differences at ~30-40% and 60-70% of stance, corresponding to foot-flat and heel-off gait events, suggesting joint coupling during these phases [3] (**Fig. 1B-C**).
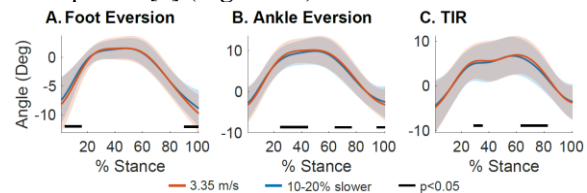
Figure 1. Group average and standard deviation for (A) foot eversion, (B) ankle eversion, and (C) knee internal rotation (TIR) across stance at 3.35 m/s and 10-20% slower. SPM paired t-test p-values<0.05 are denoted using a black bar.

CONCLUSION

Our results suggest that increased speed modulates knee, ankle, and foot kinematics at different phases of stance. Interestingly, foot position changes happened out of phase with ankle and knee changes; suggesting a need to further investigate factors affecting proximal joint angle orientations. These phase-specific changes in joint motion can inform design of specific areas of a shoe (i.e., heel, midfoot, and forefoot), as increased joint motion may be associated with joint pain [4]. While these results provide an understanding of how small changes in speed (~0.5 m/s) influence running kinematics, future work should aim to include a wider range of speeds to fully elucidate the effects of speed. When designing footwear products as a biomechanical support system, it is important to consider population average changes in joint motion across a range of speeds.

ACKNOWLEDGEMENTS

REFERENCES [1] Sumner et al. (2024), *Footwear Science;* [2] Orendurff et al. (2018), *J Biomech*; [3] Hintermann & Nigg, (1998), *Sports Medicine;* [4] Rodrigues et al. (2013), *J Appl. Bmech*

CAN SACRAL OR SHANK ACCELERATION PREDICT PROSTHETIC LEG PROPULSIVE FORCE?

Madden, TS and Pew, CA
Department of Mechanical Engineering, Montana State University, Bozeman, MT
email: thomasmadden4@montana.edu

INTRODUCTION

Prostheses aim to restore walking ability after lower limb amputation (LLA), yet individuals walking with passive prostheses show deficits in propulsive force (F_P; anterior ground reaction force) and walking speed relative to nonamputees [1,2]. F_P is directly related to walking speed [3], a significant predictor of function [4] and mortality [5], and therefore, represents an important target for rehabilitative outcomes and interventions. Wearable accelerometers may provide a more accessible alternative to force plate measurements of F_P. Because F_P contributes center of mass and trailing limb acceleration during late stance, acceleration at the sacrum or shank may be able to predict F_P. However, these relationships have not been investigated for individuals with LLA. The purpose of this study was to evaluate the associations between peak sacral and shank accelerations near toe-off and peak F_P while walking in healthy adults and individuals with LLA. Based on correlations between shank acceleration and F_P in healthy young adults [6], we hypothesized that peak resultant accelerations at the sacrum and shank near toe-off would correlate with peak F_P in healthy adults and individuals with LLA.

METHODS

Lower limb amputee participants included two females (19-26y, 164-180cm, 56.3-86.6kg), one transtibial amputee and one nonamputee prosthesis user. Four healthy nonamputee adult females (21 ± 1y, 174 ± 9cm, 60.0 ± 5.7kg) served as controls. Participants walked overground at three speeds (self-selected, 15% slower, 15% faster) while inertial measurement units placed on the sacrum and distal shank (prosthetic leg or bilaterally for controls) recorded acceleration (148Hz) with synchronous force plate data (1000Hz). Correlations between peak F_P and resultant accelerations at 0-250ms from the time of peak F_P (Fig. 1) were tested using Spearman correlation coefficients with a 0.05 overall significance level, adjusted for multiple tests (0.0125 for controls and 0.025 for amputee participants).
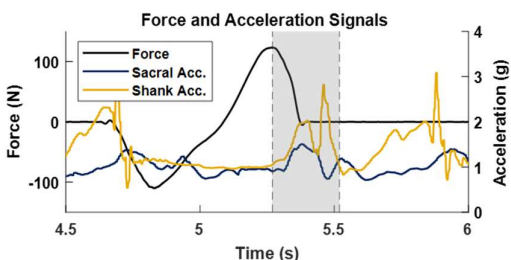

Figure 1: Data from one amputee trial showing peak sacral and shank accelerations near toe-off captured within 0-250ms from the time of peak F_P (shaded area).

RESULTS AND DISCUSSION

In control participants, peak F_P correlated significantly with peak resultant sacral ($p < 0.001$ both legs) and left shank acceleration ($p = 0.004$), while right shank acceleration showed a similar albeit nonsignificant ($p = 0.019$) correlation with F_P (Fig. 2A). These results are overall consistent with our hypothesis and previous work showing a significant association between F_P and shank acceleration [6]. Our results suggest sacral acceleration may be a better predictor of F_P than shank acceleration in healthy young adults.
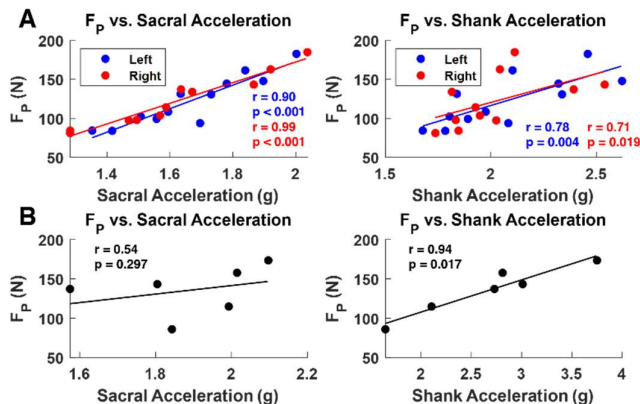

Figure 2: (A) Peak F_P correlated with left and right peak sacral acceleration and left peak shank acceleration in control participants. **(B)** Peak prosthetic leg F_P correlated with peak shank but not sacral acceleration.

Peak prosthetic leg F_P correlated significantly with peak resultant shank ($p = 0.017$) but not sacral ($p = 0.297$) acceleration (Fig. 2B). In partial support of our hypothesis, these results identify shank acceleration as a potential predictor of peak prosthetic leg F_P. The lack of a significant correlation between sacral acceleration and prosthetic leg F_P was inconsistent with our hypothesis, potentially due to the small sample size or sensor placement relative to the sacrum and greater frontal plane trunk motion in individuals with LLA [7]. Interestingly, shank acceleration showed a stronger correlation with F_P than sacral acceleration – opposite our results in healthy young adults – underscoring the need to investigate amputee-specific relationships.

CONCLUSIONS

Results suggest peak shank acceleration near toe-off can predict peak prosthetic leg F_P during walking. This will allow clinicians to assess changes in F_P using small inexpensive sensors, enhancing their abilities to implement and evaluate rehabilitative interventions for individuals with LLA. Future work is needed to examine the clinical utility of this approach.

REFERENCES

1. Carse B, et al.. *Gait Posture* **75**, 98-104, 2020.
2. Silverman AK, et al.. *Gait Posture* **28**, 602-609, 2008.
3. Campanini I, et al.. *Gait Posture* **30**, 127-131, 2009.
4. Batten HR, et al.. *Prosthet Orthot Int* **43**, 196-203, 2019.
5. Studenski S, et al.. *JAMA* **305**, 50-58, 2011.
6. Pieper NL, et al.. *J Biomech* **98**, 109449, 2020.
7. Rueda FM, et al.. *Gait Posture* **37**, 436-439, 2013.

ACKNOWLEDGEMENTS

ACCURACY OF A VIRTUAL GROUND REACTION FORCE CALCULATION IN GAIT

Jamali, P and Catena, RD
Gait and Posture Biomechanics Lab, Washington State University, Pullman, WA USA
email: pegah.jamali@wsu.edu, web: https://labs.wsu.edu/biomechanics/

INTRODUCTION

Force plates are commonly used to measure ground reaction forces (GRFs) but can be inconvenient because they tether the subject to walk a predefined path with a confined step length, and certain populations struggle to consistently hit force plates with their entire foot. Alternatively, a virtual ground reaction force (vGRF) can be calculated through inverse dynamics using measured kinematics of the whole body and assumed inertial parameters, ideally replicating the actual GRF. [1] The purpose of this study was to evaluate the accuracy of triaxial vGRFs during gait calculated in Cortex (MotionAnalysis Corp.)[2]. The outcomes of this project will inform future use of this beneficial method to avoid prolonged lab testing waiting for clean natural foot strikes onto force plates or artificial gait patterns from instructing participants to make clean foot strikes onto force plates.

METHODS

Twenty-three healthy young adults performed 5-10 minutes of natural self-selected pace over-ground walking with constant start location adjustments until a clean (one entire foot on each force plate) level-walking trial was performed naturally. Participants walked across two in-series force plates that were adjusted in separation distance prior to testing based on an approximation of the participant's natural step length (another reason vGRF is preferable). Full body marker set data and de Leva [3] segment inertial parameters were used to derive inputs into vGRF calculations. We also wanted to determine if the prescribed motion of the center of pressure (vCOP) accurately mimics true COP motion along the foot. To assess the validity of the triaxial vGRF and biaxial vCOP, the residual error between the calculated (virtual) and measured (real) data were determined using root mean square error (RMSE), mean absolute error (MAE), and coefficient of determination (R^2). Additionally, we used statistical parametric mapping (SPM) to determine specific times in stance phase of the gait cycle when errors are occurring.

RESULTS AND DISCUSSION

The calculated triaxial vGRF magnitude showed good agreement with the true GRF magnitude (Figure 1a). The vGRFs were most accurate in the Anterio-Posterior (AP) direction (R^2=0.95, RMSE=18.27). The vertical vGRFs also illustrate excellent agreement with GRFs (R^2=0.88, RMSE=50.24). However, the small medio-lateral (ML) vGRF values with similar error to the AP direction result in reduced accuracy (R^2=0.59, RMSE=19.76) in the ML direction. SPM could not differentiate significant differences at certain time points between vGRFs and GRFs in ML direction. SPM clearly indicates many of the errors in vGRF magnitudes show up at early and late stance.

We also found great agreement between actual COP and the vCOP (Figure 1b) in AP and ML directions (R^2=0.98, RMSE=37.36 and R^2=0.97, RMSE=10.38 respectively). SPM again indicated differences primarily in early and late stance

(p<0.001) because the AP vCOP is modeled to follow a linear trajectory over time. Our results may indicate we should change to using quadratic estimation for calculating AP vCOP trajectory.
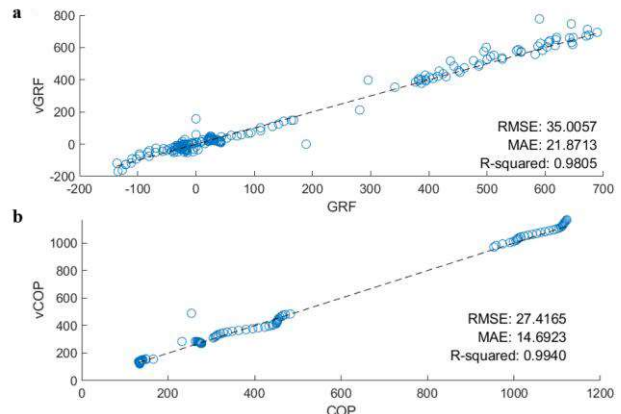
Figure 1: Single person sample comparison of (a) calculated triaxial vGRF against measured triaxial GRF and (b) of calculated biaxial vCOP against measured COP for both feet. The dotted line represents the identify line (y=x).

Possible sources of error in virtual calculations are: (1) how the foot is modeled, with changes in marker positions of the ankle and toe affecting calculations inaccurate inertial parameters. In our next analysis, we will be analyzing the sensitivity of vGRFs to errors in segment inertial parameters. Third, variations in gait patterns and sudden changes in movement may create non-smooth transitions between consecutive gait events. Fourth, the manual inspection of gait events and slight errors in event timing; (5) skin motion artifact. Additionally, having to down-sample the GRF to the frequency of motion capture data may not be ideal for some labs, especially when dealing with faster gaits.

CONCLUSIONS

A virtual ground reaction force would allow research of gait without using force plates with minimal error. The popularity of technologies like markerless motion capture demonstrates desire among biomechanists to untether research from controlled lab settings. This study sets the stage for conducting kinetic research outside laboratories in real environments without force plates. Even in the lab, not having to rely on participants cleanly striking force plates will allow for more natural gait variations, allow kinetic analyses using standard non-instrumented treadmills, and eliminate significant time from setup and testing.

REFERENCES

1. Ren, L., et al. *J Biomech* **41**, 2750–2759 (2008).
2. Hatfield, D. et al. *Med Sci Sports Exer* **41**, 29 (2009).
3. de Leva, P. *J Biomech* **29**, 1223–1230 (1996).

ACKNOWLEDGEMENTS

THE EFFECT OF SPEED ON LOWER EXTREMITY JOINT STIFFNESS DURING GRADED RUNNING

Lee, S[1], Robinson, R[1], Chebbi, A[1] and Hahn, M[1]
[1]Department of Human Physiology, University of Oregon
Eugene, OR USA
email: slee20@uoregon.edu

INTRODUCTION

Joint stiffness can be defined as a given joint's resistance to angular displacement under mechanical loading expressed as a moment of force [1]. Increased joint stiffness is associated with a decrease in range of motion, as well as the inability to adequately attenuate shock throughout the body; all of which are associated with running related injuries [2]. Understanding the factors that influence stiffness has potential application in injury prevention and rehabilitation with respect to running related overuse injuries [2]. Increases in running speed have been correlated with increased measures of joint stiffness [4]. However, this relationship has only been examined during level ground running; the effect of speed on joint stiffness during uphill and downhill running is relatively unexplored [1]. The purpose of this study is to examine the effect of speed on joint stiffness and quantify differences in stiffness between the hip, knee, and ankle during graded running. It was hypothesized that as speed increases, stiffness of all joint types and across all grades will also increase.

METHODS

Approval from the Institutional Review Board was obtained, and all participants provided informed consent prior to data collection. Twelve healthy participants (7 female, age: 24 years, height: 162 cm, mass: 72 kg) performed three 30s running trials at speeds based on each participant's self-reported 5k pace: 1:30 min/mile slower (Speed 1), 1:00 min/mile slower (Speed 2), and 0:30 min/mile slower (Speed 3) than 5k pace. Trials were conducted on an instrumented treadmill on level ground (LG), 7.5° incline (INC), and 7.5° decline (DEC). Kinetic data were collected at 1000 Hz (Bertec, Columbus, OH) and kinematic data were collected at 200 Hz (Motion Analysis, Santa Rosa CA). Sagittal plane joint angles and internal moments of the hip, knee, and ankle were calculated using a custom pipeline in Visual 3D software (C-motion, Inc., Germantown, MD). Joint stiffness was quantified by the equation:

$$K_{joint} = \frac{\Delta M_{joint}}{\Delta \theta_{joint}},$$

where ΔM_{joint} is the change in sagittal joint moment, and $\Delta \Theta_{joint}$ is the change in sagittal angular displacement over the first half of stance phase [3]. A two-way repeated measures ANOVA was performed for each grade condition using Excel (Microsoft, Redmond, WA) to determine the effect of speed and joint type on joint stiffness. Post hoc pairwise t-tests were run in the case of a significant main effect ($\alpha = 0.05$).

RESULTS AND DISCUSSION

The average velocity for speed categories 1, 2 and 3 were 3.23, 3.44, and 3.68 m/s, respectively. For all grades, a significant main effect was detected for joint type ($p < 0.001$), but not speed. No significant interaction effects were detected. On LG, ankle stiffness was significantly greater than hip and knee stiffness across all speeds. On DEC, ankle stiffness was significantly greater than hip and knee stiffness across all speeds, and hip stiffness was greater than knee stiffness for the first two speeds. On INC, ankle and knee stiffness were significantly greater than hip stiffness across all speeds. During LG and DEC running, stiffness was greatest at the ankle, but during INC running stiffness was greatest at the knee. This increase in knee stiffness during INC running suggests that when running uphill, the role of the knee shifts from a more deformable shock absorber, to a stiffer and more stable joint. This may allow for improved transmission of propulsive energy generated by the hip and ankle. While previous studies have reported increases in hip, knee and ankle joint stiffness with faster running speeds, a significant speed effect was not observed in the current study [1]. This may be attributed to the smaller margins between speed categories in the current study compared to previous studies. To characterize the role of each joint more thoroughly during uphill and downhill running, future studies should analyze the interaction effects of speed and grade on joint stiffness, with a greater variety of grades.

CONCLUSIONS

While joint stiffness differs between the hip, knee, and ankle when running on graded surfaces, stiffness does not appear to change in response to speed. This study highlights how the role of each lower extremity joint changes to adapt to sloped terrain.

REFERENCES

1. Davis JJ and Gruber AH. *OJSM*, **9(5)** 2021
2. Brughelli M and Cronin J. *Sports Med*, **38**, 647-657 2008
3. Jin L and Hahn M. *J Biomech*, **2**, 441-452, 2022
4. Jin L and Hahn M. *Hum Mov Sci,* **58**, 2018

ACKNOWLEDGEMENTS

Table 1: Joint stiffness across grades and speeds. Significant difference ($p < 0.05$) between hip/knee denoted as *, knee/ankle°, ankle/hip•

	LG1	LG2	LG3	INC1	INC2	INC3	DEC1	DEC2	DEC3
Hip	0.08±0.04	0.08±0.05	0.09±0.05	0.02±0.01*	0.04±0.05*	0.03±0.05*	0.11±0.05*	0.12±0.06*	0.10±0.06
Knee	0.08±0.02°	0.10±0.07°	0.09±0.02°	0.30±0.21	0.28±0.26	0.27±0.20	0.06±0.02°	0.06±0.02°	0.06±0.02°
Ankle	0.17±0.0•	0.17±0.0•	0.19±0.0•	0.16±0.0•	0.16±0.0•	0.19±0.1•	0.24±0.1•	0.24±0.0•	0.22±0.12•

Podium Session 4: Sport Biomechanics

USING OPENCAP TO ASSESS SINGLE- AND DUAL-TASK SINGLE LEG VERTICAL JUMP PERFORMANCE

Fatemeh Aflatounian[1], Kaylan Wait[1], Brendan Silvia[1], Alexandra C. Lynch[1], James N. Becker[1], Keith A. Hutchison[1], Janet E. Simon[2], Dustin R. Grooms[2], and Scott M. Monfort[1]
[1]Montana State University, Bozeman, Montana, USA, [2]Ohio University, Athens, Ohio, USA
email: fatemehaflatounian@montana.edu, web: https://www.montana.edu/biomechanics/index.html

INTRODUCTION

Single-leg vertical jump (SLVJ) assesses upward jumping ability, emphasizing knee extensor power, particularly relevant to identifying altered function following an anterior cruciate ligament (ACL) reconstruction [1]. ACL injuries often happen during sports when visual attention is externally focused; however, common clinical assessments often neglect cognitive-motor deficits that lead to riskier movements [2]. Dual-task screening simultaneously tests cognitive and motor skills, aiding in identifying such deficits [3]. However, traditional motion analysis is costly and time consuming for data collection and processing [4]. OpenCap enhances clinical accessibility to full-body kinematics by using iOS devices and automated cloud processing, reducing both cost and time burden [4]. The purpose of this study was to demonstrate the ability of a clinically-feasible approach (i.e., OpenCap) to reflect similar kinematics obtained by standard marker-based motion capture during single- and dual-task SLVJ. Given OpenCap's success in capturing sagittal plane kinematics in other jumping movements, we hypothesized strong correlations between OpenCap and marker-based outcomes.
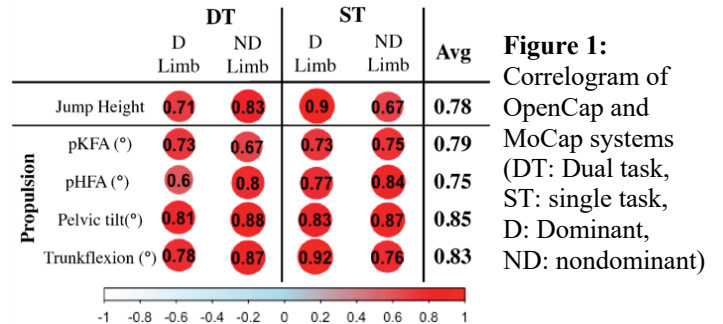
METHODS

10 healthy athletes (5F/5M, 19.8±2.3 yrs; 1.66±0.18 m; 67.8±11.0 kg; Tegner: 7.5±1.3; Marx: 10.6±3.6) completed the SLVJ task. Participants performed the SLVJ under both single-task (ST) and dual-task (DT) conditions on both limbs, with three trials each. DT involved two peripheral lights (FITLIGHT Sports Corp) for Go/No-Go cues and one overhead light for a memory task, adapted from a visual-cognitive triple hop [5]. Participants awaited a pre-defined 'Go' color on one of the peripheral lights before performing the SLVJ, focusing on the overhead light to recall three rapidly displayed colors. Full-body kinematics were simultaneously captured using both a marker-based motion capture system (MoCap) (10 cameras, Motion Analysis Corp; 5 AMTI force plates) and OpenCap with two iOS devices. MoCap data were processed in Visual3D using an inverse kinematics model [6], while OpenCap data were processed using the automated cloud processing within the OpenCap workflow. Kinematic trajectories from both methods were analysed in MATLAB to extract jump height and peak trunk, hip (pHFA), and knee flexion angle (pKFA), and pelvis tilt during the propulsive phase (from 0.4 sec before leaving the force plate until toe off) [1]. Toe-off was defined using force plate data for MoCap and when the pelvis vertical position exceeded a 5% increase from the standing position for the OpenCap data. Pearson correlations (or Spearman if data were not normally distributed) were used to compare outcomes between two approaches, with $p < 0.05$ indicating statistical significance.

RESULTS AND DISCUSSION

There were strong correlations between MoCap and OpenCap values for both ST and DT variables jump height and joint kinematics during the propulsion phase of SLVJ (r = 0.6 to 0.92,

p = 0.05 to <0.001, Figure 1). These results demonstrate a strong ability for OpenCap to capture trends in SLVJ outcomes (e.g., the individuals with higher jump height or joint flexion measured via MoCap were also identified with OpenCap). It is worth noting that these strong correlations were obtained after omitting OpenCap trials with unrealistic pose estimation from the automated OpenCap cloud processing. Out of the 120 good (i.e., hands remained on hips, clean landing, reacting to correct color for DT) trials collected, 10 were later omitted due to unrealistic OpenCap pose estimations. Opportunities to further enhance the ability to leverage OpenCap to assess SLVJ performance and minimize dropped trials include optimizing the number and position of the cameras for this movement as well as improving the color contrast between participants and their environment. Additional opportunities to refine the analyses pipeline to more robustly extract the variables with minimal manual effort also exists. In general, OpenCap captured essential variables related to ACL injuries during SLVJ, which has potential as a useful tool for clinicians. However, there is a still need for future studies with larger cohorts, including individuals with ACL reconstruction, and to streamline the workflow to optimize clinical feasibility.

	DT		ST			
Propulsion	D Limb	ND Limb	D Limb	ND Limb	**Avg**	
Jump Height	0.71	0.83	0.9	0.67	0.78	
pKFA (°)	0.73	0.67	0.73	0.75	0.79	
pHFA (°)	0.6	0.8	0.77	0.84	0.75	
Pelvic tilt(°)	0.81	0.88	0.83	0.87	0.85	
Trunkflexion (°)	0.78	0.87	0.92	0.76	0.83	

-1 -0.8 -0.6 -0.4 -0.2   0   0.2 0.4 0.6 0.8   1

Figure 1: Correlogram of OpenCap and MoCap systems (DT: Dual task, ST: single task, D: Dominant, ND: nondominant)

CONCLUSIONS

Improving clinicians' access to high resolution, joint-level kinematics during return-to-sport tasks may provide a more comprehensive approach for clinicians to evaluate the readiness of their patients to return to sport. In this study, OpenCap strongly correlated with key kinematic outcomes across multiple joints during single- and dual-task SLVJ. Future efforts using this clinically-feasible approach to collect these data and relate to patient outcomes are needed to demonstrate the clinical relevance of these data.

REFERENCES

1. Kotsifaki et. al. (2022) *Br J Sports Med* 56(9): 490-498
2. Vargas et. al. (2023) *IJSPT* 18(1): 122-131
3. Monfort et. al. (2019) *Am J Sports Med* 47(6):1488–1495
4. Uhlrich et. al. (2023) *PLoS Comput Biol* 19(10): e1011462
5. Farraye et. al. (2023) *J Sport Rehabil* 32(7): 802-809
6. Fischer et al. (2021) *J Applied Biomech* 37(4)

ACKNOWLEDGEMENTS

SEX-BASED DIFFERENCES IN KNEE MECHANICS AND PLANTAR PRESSURE DURING SOCCER CUTTING

Karolidis, EC[1], Denton, AN[1,2] and Hahn, ME[1]
[1]Bowerman Sports Science Center, Department of Human Physiology, University of Oregon, Eugene, OR USA
[2]Knight Campus for Accelerating Scientific Impact, University of Oregon, Eugene, OR USA
email: ekarolid@uoregon.edu

INTRODUCTION

Anterior cruciate ligament (ACL) tears occur at a three-time higher rate in female soccer athletes than males [1]. This sex-based disparity is associated with differences in neuromuscular control, joint laxity, and anatomical alignment, altering kinetic and kinematic performance profiles [2]. These differences widen with fatigue, furthering the risk of injury in females [3].

Despite mechanical differences between sex, soccer footwear is designed for male users. With known sex differences in movement patterns and joint loading, it should not be assumed that females can withstand the same amount of traction as males. High traction footwear may exacerbate female susceptibility to torsional injury mechanisms, such as those of ACL injury, if rotational resistance exceeds ligament loading capacity [4]. Cleat outsole properties, such as stud shape, are direct moderators of rotational resistance at the shoe-surface interface [4]. With ACL injuries typically occurring within the first 0.05 seconds of ground contact, cleat-foot interactions, and therefore plantar loading, are of keen interest during initial stance [5]. However, the effect of stud shape on female cutting mechanics remains unknown. This study investigates the influence of soccer cleat stud shape, elliptical and bladed, on the knee kinetics, kinematics & plantar pressure of athletes pre- and post-fatigue.

METHODS

College-aged soccer athletes (10 male, 8 female) performed two data collections. Each visit, cleated footwear of different stud shapes was worn- bladed (adidas Predator .2), or elliptical (adidas Copa Sense .3). Cleat order was randomized for each subject.

Athletes performed cutting tasks in a turfed facility before and after a fatigue protocol. A 19-camera system (Vicon, 100 Hz) collected the trajectories of 28 retroreflective markers, while 4 force platforms (AMTI, 1000 Hz) recorded ground reaction force data. Athletes performed 6 cuts (80% maximum speed to unanticipated 120° cut, 3 trials each direction), representing the pre-fatigue state. A field-based fatigue protocol was then administered; athletes completed five running stages in the least amount of cumulative time- 1600, 800, 400, 200 and 100 m, each separated by one minute of rest. Pedar insoles (Novel, 100 Hz) recorded plantar pressure as athletes performed intermittent cuts down the length and width of the field. Immediately following, the athlete repeated the unanticipated cutting tasks, representing the post-fatigue state. Knee flexion angle at initial contact (KFA), peak valgus angle (KVA) and peak knee extensor moment (KEM) were calculated using inverse dynamics and compared across fatigue state, cleat and sex. Peak pressure within the first 0.05 seconds of cutting step initial contact were calculated across 11 forefoot and heel masks during the 1600 m (pre-fatigue) and 400 m (fatigued) stages, and then compared across cleat and sex. A series of mixed effects ANOVAs (sex X fatigue X cleat) were conducted to determine significance ($\alpha = 0.05$).

RESULTS AND DISCUSSION

There were no significant three-way interactions on the knee kinetic or kinematic variables (Figure 1). There was a significant two-way interaction between sex and fatigue state on KEM ($p = 0.04$), with fatigue detrimentally increasing KEM in females, while protectively decreasing KEM in males. Main effects were observed for sex on KVA ($p = 0.02$), with females effecting greater KVA, and for fatigue state on KFA ($p = 0.01$), with fatigue decreasing KFA for both sexes and cleats.
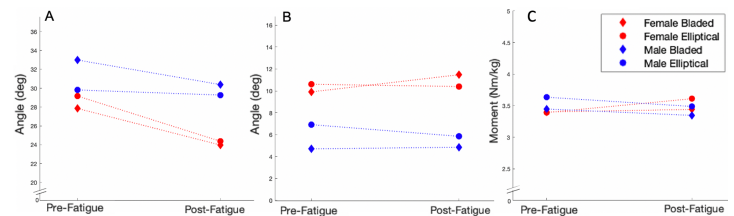

Figure 1: Interaction plots of knee mechanical parameters averaged across sex, cleated condition, and fatigue state: (A) knee flexion angle at initial contact, (B) peak knee valgus angle (C) peak knee extensor moment.

Significant three-way interactions in plantar pressure were observed in both upper heel masks ($p < 0.03$), and two forefoot masks ($p < 0.05$), seen in Figure 2. Main effects ($p < 0.05$) were also observed throughout. Localized interactions across the heel and forefoot masks suggest pressure distribution patterns are moderated by fatigue and cleat, uniquely, between males and females.
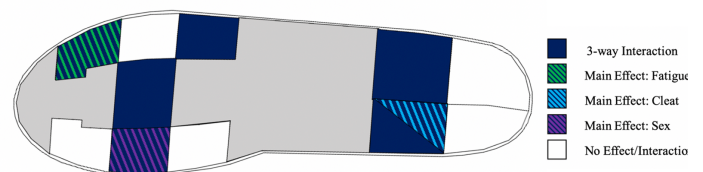
Figure 2: Significant main and interaction effects of sex, cleat condition and fatigue state on peak regional plantar pressure.

CONCLUSIONS

Results demonstrate the importance of female-centric cleat design, likely moderating traction according to mechanics observed during the more mechanically susceptible, fatigued state.

REFERENCES

1. Waldén et al., *Knee Surg Sport Tr A*, 2011
2. Decker et al., *Clin Biomech*, 2003
3. Kernozek et al. *Am J Sports Med*, 2008
4. Butler et al., *Scan J Med Sci Sport*, 2012
5. Krosshaug et al., *Am J Sports Med,* 2007

ACKNOWLEDGEMENTS

RELATIONSHIP BETWEEN COM-TO-COP POSITION AND SAGITTAL PLANE ENERGY ABSORPTION DURING THE PENULTIMATE STEP OF SIDE-STEP CUTTING

Mengoni, SA, Mulligan, CMS, and Norcross MF
College of Health, Oregon State University, Corvallis, OR USA
Email: mengonis@oregonstate.edu

INTRODUCTION

A majority of non-contact anterior cruciate ligament (ACL) injuries occur during cutting maneuvers that require rapid deceleration and redirection of the center of mass (COM) [1]. Previous work has highlighted that athletes can utilize the penultimate step to decelerate their center of mass and reduce ACL-injury related biomechanics during the final step of side-step cutting maneuvers [2,3]. It has been suggested that athletes can increase the distance between their COM and their center of pressure (COP) at initial contact to facilitate deceleration during the penultimate step [4]. However, it is unknown whether increasing the COM-to-COP distance at initial contact of the penultimate step is associated with more effective deceleration during the penultimate step of side-step cutting. Therefore, the purpose of this study was to determine the relationship between COM-to-COP distance at initial contact of the penultimate step and sagittal plane energy absorption at the ankle, knee, and hip during planned and reactive side-step cuts.

METHODS

Thirty-six females (20.9±1.7 years 1.66±0.07 m, 62.4±8.7 kg) completed five reactive (*i.e.,* in response to a light stimulus) and five pre-planned 90-degree side-step cuts using their dominant limb. Kinematics and kinetics were recorded during the penultimate step using an optical motion capture system interfaced with a single force plate. COM and COP position were defined as the anterior-forward coordinate position of the COM and COP in the x-axis at initial contact of the penultimate step, respectively. COM-to-COP distance was defined as the COM position subtracted from the COP and normalized to body height. Sagittal plane energy absorption at the ankle, knee, and hip were quantified by integrating the negative area under the joint power curve during the deceleration phase (i.e., initial contact through peak knee flexion). Relationships between COM-to-COP distance and energy absorption at the ankle, knee, and hip were assessed via Spearman rank correlation coefficients (ρ) due to the non-normal distribution of outcome variables ($\alpha \leq 0.05$).

RESULTS

There was a very strong relationship between COM-to-COP distance and energy absorption at the ankle during pre-planned (ρ=0.71, p<.001) and reactive cuts (ρ=0.76, p<.001) (Figure 1). No significant relationships between COM-to-COP distance and energy absorption at the knee, or hip during pre-planned and reactive cutting were identified (p>0.05) (Figure 1).

DISCUSSION

Increasing COM-to-COP distance is associated with greater energy absorption at the ankle during the penultimate step of pre-planned and reactive side-step cuts. This suggests that with a greater anterior foot placement at initial contact, athletes can absorb more kinetic energy through the ankle to arrest their COM velocity during the penultimate step. Greater energy absorption through the penultimate step may facilitate more favorable cutting mechanics due to a decrease in the COM velocity to be arrested during the final step of both pre-planned and reactive side-step cuts.

REFERENCES

1. Olsen OE, Myklebust G, Engebretsen L, Bahr R. Injury mechanisms for anterior cruciate ligament injuries in team handball: a systematic video analysis. *Am J Sports Med*. 2004;32(4):1002-1012.
2. Jones PA, Herrington L, Graham-Smith P. Braking characteristics during cutting and pivoting in female soccer players. *J Electromyogr Kinesiol*. 2016;30:46-54.
3. Havens KL, Sigward SM. Whole body mechanics differ among running and cutting maneuvers in skilled athletes. *Gait Posture.* 2015;42(3):240-245.
4. Dos'Santos T, McBurnie A, Donelon T, Thomas C, Comfort P, Jones PA. A qualitative screening tool to identify athletes with 'high-risk' movement mechanics during cutting: The cutting movement assessment score (CMAS). *Phys Ther Sport*. 2019;38:152-161.
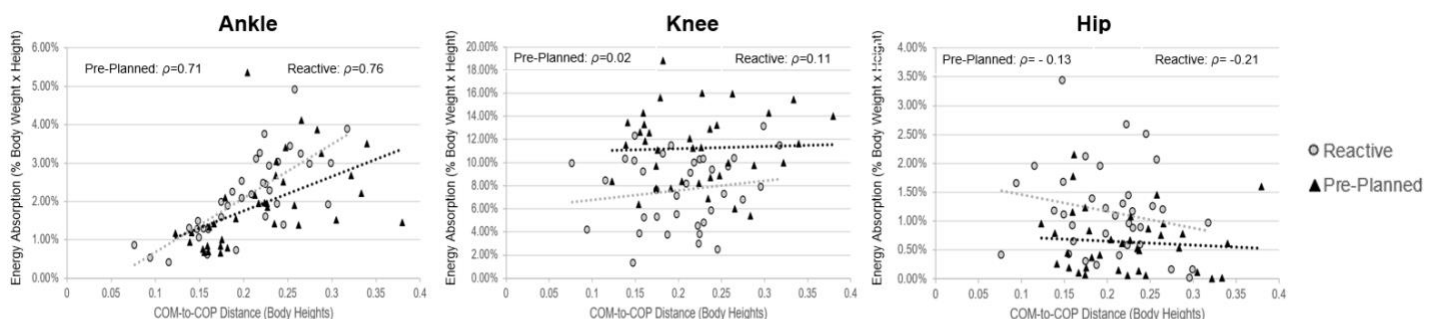
ACKNOWLEDGEMENTS

Figure 1. Scatter plots for the COM-to-COP distance at initial contact and sagittal plane energy absorption at the ankle, knee, and hip during the penultimate step of pre-planned and reactive side-step cuts.

Kinematic Differences Between Pin and Freeride Backcountry Ski Bindings During Treadmill Skinning

Burgess I, Samuels S, Seifert J, Becker J

Department of Food Systems, Nutrition, and Kinesiology, Montana State University, Bozeman, MT USA

email: isaacburgess@montana.edu , web: https://www.montana.edu/biomechanics/

INTRODUCTION

In backcountry ski touring, the ski binding is the critical connection between skier and the skis, allowing free heel movement during uphill travel and secure fixation of the boot during descents. Individuals may choose to use either lightweight pin bindings (P) or heavier free ride (FR) bindings which have safety features such as adjustable DIN settings. Previous research on backcountry skiing shows that increasing weight at the foot negatively impacts the energetic cost of skinning uphill [1]. However, this research only examined the effect on metabolic cost, and artificially added weight, not comparing between bindings. Additionally, it is unknown whether the relatively small additional mass of FR binding influences kinematics of the motion. Therefore, the purpose of this study was to compare ankle, knee, and hip kinematics, as well as stride length and frequency during uphill skinning between the P bindings, and heavier FR bindings.

METHODS

Ten healthy participants with at least two years of backcountry ski experience were recruited for this study (M:8,F:2, Age: 21 ± 1.48 yrs, height:1.81 ± 0.06 m, mass: 78.1 ± 7.25 kg). Whole body kinematics were recorded using a 6-camera motion capture system while participants skinned uphill on a skiing treadmill. Following a 5-minute warm-up, participants skinned on P or FR bindings, mounted on matching skis, for 3-minute stages at 1.1 m/s at grades of 8% or 15%. Order of binding and grade were randomized, and the last 30 seconds of each stage were recorded.

Visual 3D was used to calculate cycle time, step length and frequency, ankle, knee, hip, and trunk range of motion (ROM) and peak flexion across 10 gait cycles. Kinematic data was averaged for each trial and differences between bindings and grades were compared using a 2x2 repeated measures ANOVA.

RESULTS AND DISCUSSION

Ankle, knee, hip, and trunk kinematics were all not significantly different between bindings, but all showed main effects of grade (Figure 1). There were main effects of binding for both step length (p = .019) and step rate (p = .018), with length being longer and rate being slower with the FR binding. Step time also had a main effect of grade (p = .019), being longer with the FR binding. There were no differences in cycle time, however swing time showed main effects of both binding (p = .018) and grade (p = .007), with swing time being longer with the FR binding and at 8%.
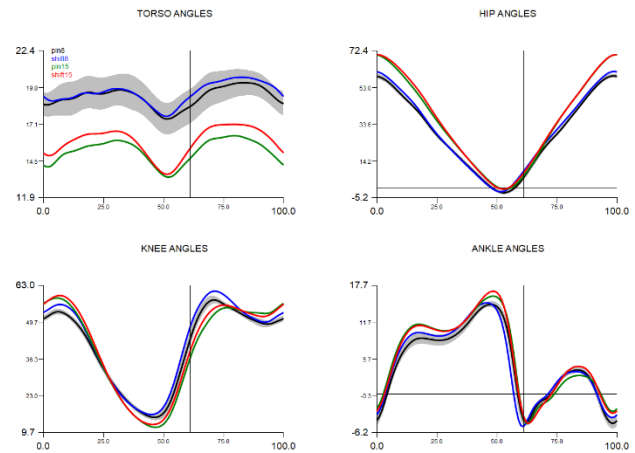

Figure 1. Normalized joint angles across 10 gait cycles. Note the offset in curves due to grade.

These differences may be attributed to the increased weight of the FR binding. With the heavier binding the skier keeps the ski closer to the ground, resulting in more glide of the ski, and Therefore, more horizontal momentum. Increased momentum causes a longer step length, and when at a controlled speed, a slower step rate. Swing time is longer in lower grades and the FR binding, which is similar to previous studies examining cycle characteristics with increasing grade [2].

These results provide insight regarding the effects of increased binding weight on kinematics and cycle characteristics while skinning. This study should be replicated on snow over longer distances, in order to examine how these results change in real touring conditions.

CONCLUSIONS

In laboratory settings, binding type influences cycle characteristics but not kinematics while skinning.

REFERENCES

1. Tosi, P. et al., *J. Sports Med. Phys. Fitness*, *49*, 25-29 (2009).
2. Lasshofer, M. et al. *Frontiers in Sports and Active Living*, *4*, 886025. (2022).

ACKNOWLEDGEMENTS

Table 1. Cycle metrics mean and standard deviations, averaged across 10 gait cycles

	Pin 8%	Pin 15%	Freeride 8%	Freeride 15%
Step Length (m)	1.42 ± 0.02	1.39 ± 0.019	1.45 ± 0.01	1.43 ± 0.015
Cycle Time (S)	1.267 ± 0.01	1.248 ± 0.017	1.297 ± 0.01	1.283 ± 0.013
Step Rate (Step/Min)	76.00 ± 2.40	74.84 ± 2.86	77.80 ± 1.74	76.94 ± 2.23
Swing Time (S)	0.490 ± 0.008	0.467 ± 0.006	0.505 ± 0.005	0.488 ± 0.004

EFFECTS OF FOOTWEAR AND SURFACE ON ANKLE, KNEE, AND HIP KINEMATICS WHILE TRAIL RUNNING

Reyes, K[1], Dailey, M[2], Lawrence, C[2], Shipman, C[2], Spector, Z[2] and Hannigan, JJ[2]
[1]Program in Kinesiology, Oregon State University, Corvallis, OR USA
[2]Program in Physical Therapy, Oregon State University-Cascades, Bend, OR USA
email: reyeskat@oregonstate.edu

INTRODUCTION
With the growing popularity of trail running, footwear companies have made an effort to develop and modify shoes to accommodate various running conditions and reduce the risk of running-related injuries. However, whether on paved surfaces or trails, trail runners continue to face high rates of running-related injuries with runners reporting 61.2 injuries per 1000 hours [1], representing an increased risk of acute and chronic injuries [2].

Maximal footwear was introduced with the aim of decreasing the risk of injury. Despite the growing popularity of the maximal shoe, limited research has analyzed the effects of maximal shoes on ankle, knee, and hip kinematics associated with injury risk [3]. Currently, limited research has investigated the effects of footwear on road and trail surfaces. Therefore, the purpose of this study was to determine, in experienced trail runners, the effects of footwear (maximal vs. traditional shoes) and surface (road vs. trail) on ankle, knee, and hip kinematics.

METHODS
Seven experienced trail runners between the ages of 18 and 45 who ran a minimum of 15 miles per week and at least 1 day per week or 5 miles on a trail participated in this study. Participants warmed up for 10 minutes outdoors (5 minutes on the paved trail and 5 minutes on a flat, single-track trail) at an easy pace. Participants then completed 5 successful running trials outdoors at their comfortable pace wearing a traditional shoe (New Balance 880 v11: heel height, 33.3mm; forefoot height, 23.2mm) and a maximal shoe (Hoka One Bondi v7: heel height, 41.6 mm; forefoot height, 34.7) on both surfaces in random order.

Ten Sony RX0 II Cameras (Sony Corporation, Minato, Japan) were positioned around parallel paved and single-track trail surfaces and connected and synchronized using the Sony Camera Control Box, collecting at 120Hz. Video data for each trial was processed using Theia3D (Theia Markerless Inc., Kingston, ON, Canada). Visual3D (HAS-Motion, Kingston, ON, Canada) was used to calculate ankle, knee, and hip kinematics of the dominant limb in the frontal and sagittal plane. The effect of footwear condition (maximal vs. traditional shoes) and running surface (trail vs. road) were assessed using 2-way repeated measures ANOVAs, with an alpha level set at 0.05. Follow-up pairwise comparisons were used to examine specific differences between footwear conditions and surfaces ($\alpha = .05$).

RESULTS AND DISCUSSION
Hip flexion at initial contact (road: $33.5 \pm 2.7°$, trail: $36.1 \pm 2.4°$, $p < 0.001$) and hip extension excursion (road: $46.0 \pm 5.4°$, trail: $48.10 \pm 4.5°$, $p = 0.004$) were significantly lower on road surface, while hip adduction excursion (road: $5.2 \pm 1.8°$, trail: $3.8 \pm 2.4°$, $p = 0.011$) was significantly lower on the trail surface.

Knee flexion at initial contact (road: $17.6 \pm 3.5°$, trail: $19.7 \pm 5.3°$, $p = .039$) was significantly lower while running on road surface. An interaction effect was seen in knee flexion excursion, with the greater excursion noted on the road surface in the maximal shoe compared to the traditional shoe (road max: $27.2 \pm 4.3°$, road trad: $24.9 \pm 3.9°$, $p = 0.022$).

Ankle inversion at initial contact (road: $6.6 \pm 2.9°$, trail: $10.3 \pm 2.6°$, $p = 0.023$), peak eversion (road: $0.5 \pm 2.8°$, trail: $4.7 \pm 2.3°$, $p = 0.002$), and eversion at toe-off (road: $3.2 \pm 2.9°$, trail: $6.5 \pm 2.8.1°$, $p = 0.007$) were significantly lower on the road surface. No other interactions or significant differences were found between shoe conditions and surfaces for joint angles at the ankle, knee, and hip, $p > .05$.
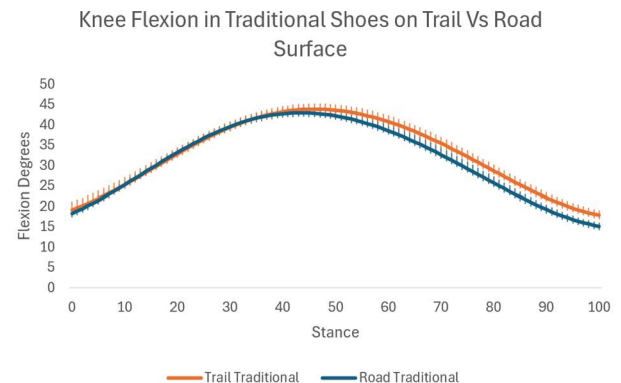
Figure 1: Ensemble curve for knee flexion kinematics in each shoe condition.

CONCLUSIONS
There were significant differences between surfaces when analyzing ankle, knee, and hip kinematics. These differences may imply that trail surface could influence limb stiffness, indicating differences in loading strategies in the sagittal plane at the hip and knee. Additionally, trail surfaces appear to influence ankle kinematics in the frontal plane as the ankle attempts to stabilize, which may relate to the increased risk of ankle injury during trail running.

REFERENCES
1. Viljoen CT, et al. *Int J of Environ Res and Pub Health* **18**, 1-13, 2021.
2. Hamill J, et al. *Foot Sci* **14**, 113–121, 2022.
3. Hannigan & Pollard, *J Sci Med Sport* **23**, 15–19, 2020.

ACKNOWLEDGEMENTS

Podium Session 5: Injury & Rehabilitation

IMPACT OF A RESISTIVE ANKLE EXOSKELETON ON FATIGUE IN CHILDREN WITH CEREBRAL PALSY

Landrum, VM[1], Caskey, CD[1], Shrivastav, SR[1], Feldner, HA[1], Bjornson, KF[1], Moritz, CT[1], Steele, KM[1]
[1]University of Washington, Seattle, WA USA
Email: vlandrum@uw.edu

INTRODUCTION

Cerebral palsy (CP) is a group of neurological disorders caused by a brain injury around the time of birth that adversely impacts muscle tone and motor function. Children with CP exhibit muscle weakness, co-contraction, stiffness, and involuntary muscle contractions that contribute to challenges in coordinating movements, such as walking [1]. Consequently, individuals with CP report increased fatigue in daily life compared to typically developing peers [2].

Interventions that emphasize walking function for children with CP include a resistive ankle exoskeleton (Exo) that targets increased plantarflexor activity, which is crucial for stability and locomotion [3]. Ensuring that these rehabilitation strategies avoid excessive fatigue is important for effective rehabilitation, as previous studies have shown that fatigue can reduce intervention effectiveness [4]. Consequently, strategies aimed at improving locomotion, such as increasing soleus activity, should account for fatigue onset and timing to maximize potential benefits.

The aim of this research was to quantify the impact of using a resistive Exo on fatigue in the soleus among children with CP. We hypothesized that utilizing a resistive Exo during treadmill walking would lead to decreases in muscle firing rate and increases in peak activation, indicating more muscle fatigue compared to normal treadmill walking (Non-Exo).

METHODS

Soleus firing rate and peak activation were quantified during walking with and without the Biomotum SPARK [2] Exo for nine children with CP (10.9 ± 4.1, GMFCS I-II, 6 Male). Walking was performed on a treadmill (Bertec, Columbus OH) and electromyography (EMG) data were recorded on the more-affected limb (2000 Hz; Delsys, Inc., Natick MA) for the soleus during the first 5-minutes. Walking tasks were performed at consistent speeds on separate days at least five days apart in a pseudo-randomized order. The ankle resistance force of the Exo was set at 12% of participant body weight. A custom MATLAB (MathWorks, Natick MA) was used to calculate soleus firing rate by segmenting high-pass filtered (20 Hz) EMG data into approximately 30-second intervals and calculating the median frequency [5]. EMG data were then rectified and low-pass filtered (10 Hz) to generate a linear envelope and normalized to the 95th percentile of the first 30 seconds of walking. Peak activation was defined as the max amplitude in each 30 second time window. The nonparametric Wilcoxon signed rank test was used to test for significant changes in firing rate and peak activation, where significance is defined as $p < 0.05$.

RESULTS AND DISCUSSION

During the initial 5-minutes of Exo walking, soleus firing rate decreased by 17.9 ± 34.6 Hz and activation amplitude increased by 0.29 ± 0.65 mV/mV (Fig. 1). These changes were greater than Non-Exo walking where soleus firing rate decreased by 6.5 ± 17.0
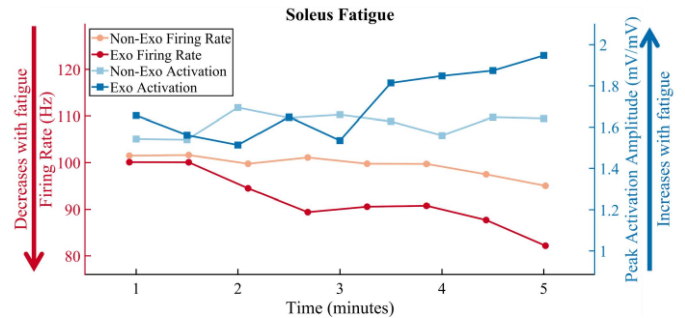

Figure 1: Average peak soleus activation amplitude (blue) and firing rate (red) for nine participants across 5-minutes of walking for walking with and without an Exo.

Hz and activation amplitude increased by 0.10 ± 0.29 mV/mV (Figure 1). Exo walking demonstrated greater, non-significant increases in fatigue ($p = 0.3$ for firing rate, $p = 0.1$ for activation amplitude) compared to Non-Exo walking. Previous studies demonstrated decreased muscle firing rate of approximately 50% and increased muscle activation of about 100% during 5-minutes of overground walking without resistance for a child with CP [5]. We observed similar trends, but to a lesser extent, suggesting fatigue may not occur as quickly with treadmill walking. Prior work also suggests that children with CP may adapt their kinematic patterns in response to muscle fatigue [6]. Given the greater fatigue with Exo walking compared to Non-Exo walking observed in this study, it may be more critical to be aware of alterations to a child's gait kinematics when the rehabilitation goal focuses generating a specific walking pattern for more fatiguing tasks, such as Exo walking.

CONCLUSIONS

Walking with an Exo led to greater increases in fatigue when compared to Non-Exo walking. Understanding the effects of Exo usage on fatigue onset and magnitude during locomotion tasks will be critical to optimize rehabilitation protocols for children with CP and not compromise neuroplasticity. These findings may lead to improved functional outcomes and quality of life for children with CP and other clinical populations by emphasizing fatigue management with dosing of gait training to develop more effective evidence-based rehabilitation strategies.

REFERENCES

1. Graham HK, et al. *Nature Reviews Dis Pri* **2**, 2016.
2. Jahnsen R, et al. *Dev Med & Child Neuro* **45**, 296-303, 2003.
3. Conner BC, et al. *J Biomech* **126**, 2021.
4. Brunton LK and Rice CL *Dev Rehab* **15(1)**, 54-62, 2012.
5. Eken MM, et al. *Dev Med & Child Neuro* **61(2)**, 212-218, 2019.
6. Parent A, et al. *Gait & Posture* **72**, 22-27, 2019.

ACKNOWLEDGEMENTS

SEX IMPACTS LOWER LIMB STIFFNESS DURING LOADED WALK, JOG, AND RUN

Aultz, AC.[1*], Francis, EB., and Brown, TN
[1]Department of Kinesiology, Boise State University, Boise ID USA
email: abbyaultz@u.boisestate.edu

INTRODUCTION
Adequate lower limb stiffness is necessary for locomotor performance; yet, excessive leg and torsional knee joint stiffness reportedly increases musculoskeletal injury risk. Limb stiffness is reported to increase with faster locomotor speeds and addition of body-borne load, which may contribute to the sex dimorphism in lower limb injury [1,2]. However, it is unknown if females exhibit larger increases in lower limb stiffness with faster locomotor speeds during load carriage. We hypothesized that females would exhibit a stiffer leg and knee joint as well as larger stiffness increases than males with each incremental addition of load and locomotor speed.

METHODS
9 male and 9 female recreational runners had lower limb biomechanics quantified during a walk (1.3 m/s), jog (3.0 m/s), and run (4.5 m/s) with (15 kg) and without (0 kg) body-borne load. During each task, synchronous 3D marker trajectories and GRF data were collected using ten high-speed optical cameras (240 Hz, Vantage, Vicon Motion Systems LTD, Oxford, UK) and a single force platform (2400 Hz, OR6, AMTI, Watertown, MA). Marker and GRF data were lowpass filtered (12 Hz, 4th order Butterworth), and processed in Visual3D (C-Motion, Rockville, MD) to obtain knee joint biomechanics.

Custom MATLAB (Mathworks, Natick, MA) code quantified each dependent variable. From filtered GRF data, peak vertical GRF and loading rate, defined as the slope of the vertical GRF between 20% and 80% of the period between heel strike and impact peak, were quantified. Leg stiffness was calculated as GRF component directed from COP to the hip joint center divided by the change in leg length during stance. Knee joint stiffness was calculated as the change in joint flexion moment divided by the corresponding change in joint flexion angle from initial contact to peak knee flexion.

Vertical GRF metrics and stiffness measures were submitted to a linear mixed model with load, speed, and sex as fixed effects and subject identity as the random effect. A Bonferroni correction was used for post-hoc comparisons. Alpha level was $p < 0.05$.

RESULTS AND DISCUSSION
Contrary to our hypothesis, the females did not exhibit larger increases in leg and knee stiffness than males with increased locomotor speed or body borne load. Sex only impacted leg stiffness (p=0.033), and unexpectedly the males exhibited a 12% stiffer leg than females (Fig. 1). The male's stiffer leg may be attributed to smaller changes in leg length during stance [2], which may help them perform locomotor tasks, but may also increase GRF transmission to the musculoskeletal system, elevating their injury risk.

Faster locomotion speeds increased leg and knee joint stiffness, and peak vertical GRF (all: p<0.001). Specifically, with each incremental increase in locomotor speed (walk to jog, and jog to run) participants exhibited a significant increase in peak vertical GRF and knee joint stiffness (all: p<0.001). Leg stiffness, however, was only greater for jog and run compared to walk (p<0.001), as participants exhibited an insignificant, negligible 2% decrease in leg stiffness during the run compared to jog. Further study is needed to determine whether the slight reduction in leg stiffness is necessary during running to aid with elastic energy storage and forward propulsion.
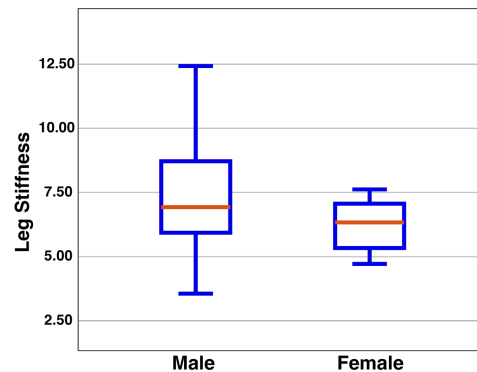

Figure 1: Depicts mean (SD) leg stiffness for male and female participants

In agreement with previous literature, adding body-borne load may elevate musculoskeletal injury risk by producing a stiffer leg and knee, and larger, faster vertical GRFs (all: p<0.038). Specifically, peak and loading rate of the vertical GRF increased 12% and 21% with load, which may elevate injury risk by coinciding with the subsequent 5% and 18% increases in leg and knee joint stiffness currently observed with body borne load. Considering recreational runners with a stiffer knee are 18% more likely to suffer an overuse injury [3], the large knee stiffness increases with load may pose a great musculoskeletal injury risk. Interestingly, however, there was significant load-by-speed interaction for leg stiffness (p=0.021), as participants increased leg stiffness with the addition of load during the walk (p<0.001), but not jog or run tasks (p>0.05). Further study is needed to determine why participants needed a stiffer leg to walk, but not jog or run with load.

CONCLUSIONS
These results provide valuable insight into the sex dimorphism of lower limb stiffness during load carriage, and whether the differences are magnified by locomotor speed. Although males exhibited a stiffer leg, sex differences were not magnified by locomotor speed. Injury prevention programs may need to tailor to participant size, rather sex to facilitate a meaningful reduction in musculoskeletal injury during load carriage.

REFERENCES
1. Brown TN et al. *JAB* **37**(2), 95-101, 2020
2. Slider A et al. *J Biomech* **48**(6), 1003-1008, 2015
3. Messier et al. *AJSM* **46**(9), 2018

ACKNOWLEDGEMENTS

FUNCTIONAL AND TISSUE DEGENERATION CHANGES AFTER ACL RUPTURE IN A PRECLINICAL MODEL OF POST-TRAUMATIC OSTEOARTHRITIS

Pancheri, NM[1], N, Kyathsandra, N, Heinonen, J, Sverdrup, ES, Lin, ASP, Willett, NJ, Guldberg, RE
[1]Department of Bioengineering, Knight Campus for Accelerated Scientific Impact, University of Oregon, Eugene, OR USA
email: npancher@uoregon.edu,

INTRODUCTION
The anterior cruciate ligament (ACL) plays a crucial role in knee joint stability, with ACL rupture causing delitorous changes to knee joint and gait biomechanics. ACL rupture also increases the risk of developing post-traumatic osteoarthritis (PTOA) by 4-10X, which can result in impaired mobility, signifincant pain, and long-term financial burden[1,2]. However, the specific tissue maladaptation that occurs in the knee joint after ACL rupture and resultant PTOA pathogenesis is poorly understood. This study establishes a physiologically relevant preclinical ACL rupture model and provides guidelines for quantitative assessment of cartilage and bone for the study of PTOA etiology and joint injury. *We hypothesized that ACL rupture would induce cartilage and bone degradation by 4-weeks, with more severe phenotypes by 8-weeks, with both time points accompanied by increased pain-relrelated behaviors.*

METHODS
Male Lewis rats received either a non-invasive ACL rupture (ACLr, n=10/timepoint) via a single applied load (55 N +/- SD) or a sham static preload. Spontaneous (limb weight bearing function) and evoked (tactile allodynia) pain behaviors were assessed post-injury (0, 4, 6, 8 weeks). ACLr animals were euthanized at 4- or 8-weeks, and sham at 8-weeks only. Post-mortem, tibia, femur, and patella were imaged using micro-computed tomography (vivaCT 40, Scanco Medical) with or without contrast enhancement (Conray). Morphometric analyses utilized established[3] and custom local VOIs. Computed tissue metrics include cartilage volume, thickness, exposed bone area (a proxy for lesion size), osteophyte volume, and bone volume and density. One-way ANOVA with Tukey's posthoc or Kruskal-Wallis test with Dunn multiple comparison were used when appropriate (reported for $p<0.05$).

RESULTS AND DISCUSSION
Pain-related behaviors: Rear limb weight bearing behavior was significantly reduced at all time points after injury compared to
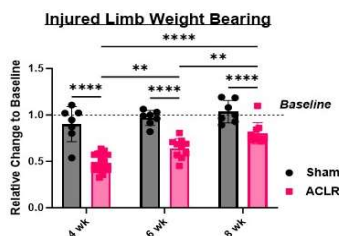

Figure 1: ACL rupture significantly reduced weight bearing on injured hindlimbs at all timepoints compared to sham controls. One-way ANOVA with Tukey's posthoc ($p<0.05$).

sham but recovered to baseline levels by 8-weeks post-injury (Figure 1A). ACL rupture reduced the limb withdrawal threshold response at 4-weeks compared to baseline and sham (not shown). Results describe an increase in pain-related behaviors following injury that partially recover, although limb asymmetry remains.

Joint morphology: Typical PTOA pathologies were observed in 2D CT reconstructions. Cartilage swelling and altered bone structure were observed in the posterior medial tibial plateau. Osteophytes were apparent in the tibial margins, femoral trochlear groove, anterior femoral condyles, and patella margins. Cartilage erosion and subchondral sclerosis were evident along the medial posterior femoral condyles by 4-weeks. Patella phenotype transitioned towards an angular geometry with clear bone remodeling. Observations suggest the medial tibial and femoral compartments accumulate severe pathology, which is consistent with similar preclinical models[3]. Quantitative morphometry: Cartilage thickness significantly increased in the medial 1/3 of the medial tibial plateau 4- and 8-weeks after ACL rupture compared to sham animals. Posterior medial horn bone volume and density (not shown) decreased compared to sham. Cartilage thickness was reduced in the lateral 1/3 of the medial femoral condyle (not shown), and exposed bone area was significantly increased. Patella mineral density was reduced by 8-weeks compared to baseline levels (not shown). Evaluation techniques and VOIs effectively captured observed pathologies and describe rapid degeneration throughout the joint after ACL rupture.
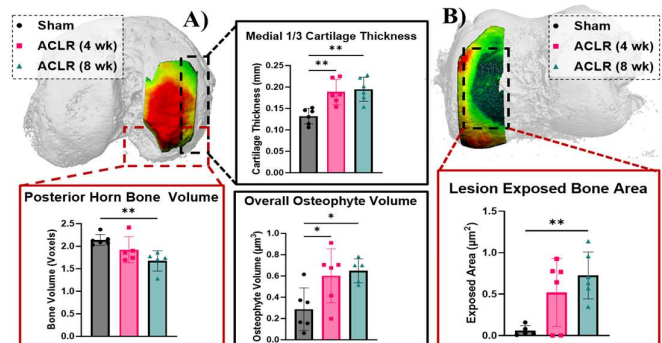

Figure 2: Micro-CT reconstructions of tibia (A) and femur (B) overlaid with medial cartilage thickness maps. (A) ACL rupture increased cartilage thickness and osteophyte volume but decreased bone volume. (B) ACL rupture induced full thickness cartilage lesions. One-way ANOVA with Tukey's posthoc ($p<0.05$).

CONCLUSIONS
This work establishes a suite of quantitative functional and tissue metrics for assessment of joint pathology after a physiologically relevant ACL rupture in rats. Results further identify the posterior medial tibial and femoral compartments as key regions of interest and may suggest a shift in posterior weight bearing and prolonged functional asymmetry after ACL rupture. Ultimately, this work facilitates future studies investigating disease initiation following ACL injury and will support screening of novel therapeutic interventions.

REFERENCES
1. Muthuri SG, et al. *Osteoarth Cartil* **19**, 1286-2193, 2011.
2. Roos EM. *Curr Opin Rheumatol* **17**, 195, 2005.
3. Willett NJ, et al. *Osteoarth Cartil* **24**, 1604-1612, 2016.

ACKNOWLEDGEMENTS

QUADRICEPS STRENGTH AND STEADINESS IN INDIVIDUALS WITH KNEE INJURY AND DISEASE

Nicholas L. Hunt[1]*, Matthew V. Robinett[1], Tyler N. Brown[1]
1Boise State University, Boise, ID, USA
*Corresponding author's email: nichunt@u.boisestate.edu

INTRODUCTION

Following knee musculoskeletal injury, such as ACL reconstruction (ACL-R), quadriceps strength decrements and altered neuromuscular activation may accelerate knee osteoarthritis (OA) development [1]. Previous literature primarily focuses on strength decrements following ACL-R and OA development; despite the fact both quadriceps contraction strength and steadiness may prevent knee instability and provide valuable insight to the underlying neuromuscular function to mitigate injury and disease development [2]. We hypothesize that ACL-R and OA individuals will exhibit less knee extensor strength and steadiness compared to controls, and a positive, linear relationship will exist between extensor strength and steadiness regardless of knee injury or disease.

METHODS

Four adult cohorts (1: 12 ACL-R, 2: 8 radiographic knee OA, 3: 13 young adult controls, and 4: 8 older adult controls) performed three 5 second knee extensor MVICs on an isokinetic dynamometer with the knee fixed to 60 degrees. The MVIC trial with the highest maximal voluntary torque was selected for analysis.

From the raw torque-time curve, peak knee extensor torque and rate of torque development (RTD) were calculated as the largest value and maximum slope of the torque-time curve, respectively. Then, the raw torque-time curve was bandpass filtered (2 to 15 Hz), linearly detrended, and submitted to a fast-Fourier transform to obtain the power spectral density (PSD) of the signal which provides the signal frequency content for fluctuation analysis. Torque fluctuation magnitude was calculated as the coefficient of variance (CV), or the standard deviation of the filtered torque-time curve divided by the mean of the raw torque time curve expressed as a percentage. From the PSD, peak power, mean, and median frequency as well as total power were calculated. Specifically, peak power frequency (PPF) was calculated as the frequency with the highest power, mean frequency is the weighted average frequency of the signal, median frequency splits the area under the PSD curve in two equal parts, and total power is the area under the PSD curve.

Knee extensor strength (peak torque and RTD) and steadiness (PPF, mean and median frequency, and total power) measures were submitted to a Kruskal-Wallis H test to assess cohort (ACL-R, OA, and age-matched controls) differences. Spearman's rho correlation analysis tested the association between muscle strength and steadiness variables.

RESULTS AND DISCUSSION

In partial agreeance with our hypothesis, the ACL-R and young control cohorts were 47% to 63% stronger (p=0.016; p=0.006) and developed torque 45% to 99% faster (p=0.016; p<0.001) than the OA cohort. Yet, neither peak extensor torque or RTD differed between ACL-R and young controls or OA and older controls. The ACL-R cohort, however, exhibited altered quadriceps neuromuscular function that may predispose them to knee OA development. Specifically, ACL-R were as strong,

but less steady (92% increase in PPF, p=0.050) than their healthy counterparts (Fig. 1A). Further, the OA cohort also exhibited poor knee extensor strength and neuromuscular function, which may contribute to the progression of their OA. The OA cohort had 157% less total power than the ACL-R and young control cohorts (p<0.001; p=0.019), indicating lower signal energy and less fluctuation content throughout the knee extensor contraction that signifies weaker muscle contraction.
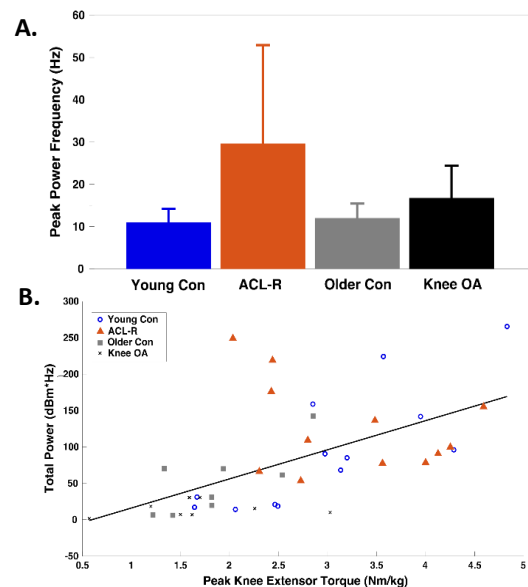

Figure 1: (A) Mean (SD) for peak power frequency by cohort and (B) relation between total power and peak knee extensor torque.

Knee extensor strength may affect joint neuromuscular control, regardless of knee injury or disease. As expected, we observed a significant, positive relationship between knee extensor strength and steadiness. Specifically, peak extensor torque exhibited moderate, positive relation with RTD (ρ=0.668; p<0.001), while mean and median frequency exhibited strong, positive correlation with PPF (ρ=0.656-0.746; both: p<0.001). Total power showed moderate, positive correlation with peak torque (ρ=0.683) (Fig. 1B), RTD (ρ=0.656), and CV (ρ=0.342) (all: p<0.028). More specifically, an individual's strength may affect overall joint neuromuscular control, including rate and fluctuations of torque development.

CONCLUSIONS

Individuals with ACL-R and OA may exhibit harmful biomechanics that affect the quality of knee extensor muscle contractions. Clinicians may need to restore of contraction steadiness to facilitate improved knee neuromuscular control and help prevent the development and progression of knee OA.

REFERENCES

1. Tayfur B, et al., *Sports Medicine* **51**, 321-338; 2021.
2. Satam et al., *Clinical Biomechanics* **99**, 2022.

ACKNOWLEDGEMENTS

Abstracts

Posters

Influence of Ski Touring Binding Design on Ground Reaction Forces During Skinning

Keating, E., Burgess, I., Samuels, S., Seifert, J., Becker, J
Department of Food Systems, Nutrition, and Kinesiology, Montana State University, Bozeman, MT USA

INTRODUCTION

During uphill travel when ski touring, bindings are crucial in determining the angle between the boot and the ski. Previous research has shown that on low-angle slopes changing the foot-ski angle by increasing rear binding riser height increases forces under the forefoot and potentially decreases mechanical efficiency [1]. However, this study was performed with one binding design and manipulated heel height using risers on the rear binding. Even without risers, different binding designs (i.e. pin versus freeride) might have different ramp angles which change the orientation of the boot relative to the ski [2]. However, how different binding designs influence forces under the foot during uphill travel remains unknown. Therefore, the purpose of this study was to compare plantar foot force between pin (P) and freeride (FR) bindings while skinning uphill at different slope angles.

METHODS

Ten healthy participants (M:8 F:2, Age:21±1.49, Height(m); 1.81±0.06, Mass (kg): 78.1±7.25), with at minimum two years of backcountry skiing experience, skinned on a treadmill for two minutes at 0.89 m/s and grades of 8% and 15% using skis mounted with P or FR bindings. Plantar pressures inside the boot were recorded using XSensor Insole System recording at 120 Hz [3]. Plantar pressure maps were segmented into whole foot, rearfoot, and forefoot regions. The following variables were calculated for the right foot for ten consecutive strides: impulse, first peak, and second peak of whole foot force, impulse and peak of rearfoot and forefoot forces. 2x2 repeated measures ANOVAs were used to compare differences in dependent variables between bindings and grades.

RESULTS AND DISCUSSION

There was a significant main effect of grade for whole foot impulse ($p = 0.022$), first force peak ($p = 0.010$), and second force peak ($p = .014$). Whole foot impulses and first force peaks were greater at 8% grade while second force peaks were greater at 15% (Figure 1). For rearfoot impulses, there were significant main effects of both grade ($p = .02$) and binding ($p = .006$), with impulses being less at 8% and in the P binding. There were also significant main effects of both grade ($p = .021$) and binding ($p < .001$) for peak rearfoot force, with forces being lower at 8% and in the P binding. At the forefoot, there was a significant main effect of grade ($p = .006$), with impulses being greater at 8%.
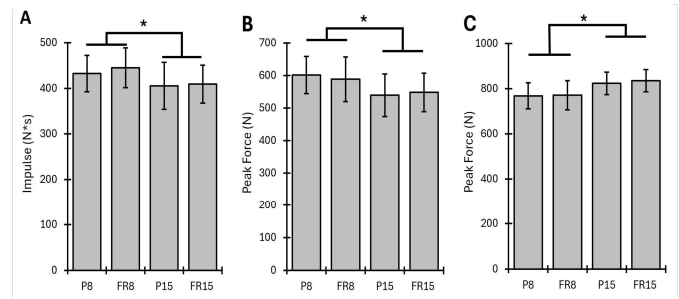

FIGURE 1: Mean ± standard deviation for whole foot impulses (A), first peak forces (B), and second peak forces (C) for all conditions. *Indicates significant main effect of binding.

Forefoot peak forces were not different across grades ($p = 0.253$) or bindings ($p = 0.348$). Whole foot impulses and forefoot forces were not significantly different between bindings.

Whole foot and first peak plantar pressure forces are greater at 8% grade, while rearfoot forces are greater at 15%. This might be due to posterior displacement of the center of mass from a more upright posture at higher slope angles. This may be relevant for injury during long ski tours as higher rearfoot forces directly affect joint loading at the ankle and knee [4]. The higher rearfoot impulses and peak force in freeride bindings may be due to the increased ramp angle between the boot and the ski created by the taller rear binding, which could lead to decreased efficiency.

CONCLUSIONS

Grade appears to be the most important factor in determining force distribution under the foot while skinning. However, pin bindings result in lower forces and impulses under the heel than freeride bindings.

REFERENCES

1. Lasshofer, M., et. al (2022). *Front.Sports and Act Living,* 4, 886025.
2. Dawson, L (2016) *Wild Snow*
3. Parker, D. et. al (2023) *PloS one*, 18(1), e0277971.
4. Haselbacher, et. al (2014). *Wilderness Environ Med* 25(3), 335-339

TABLE 1: Mean and standard deviations of impulse and peak forces for the rearfoot and forefoot regions for each condition.

Condition	Pin 8%		Freeride 8%		Pin 15%		Freeride 15%	
	Rearfoot	Forefoot	Rearfoot	Forefoot	Rearfoot	Forefoot	Rearfoot	Forefoot
Impulse (N)	105.85 ± 52.77	327.90 ± 66.34	135.31 ± 57.89	384.79 ± 67.08	130.92 ± 55.25	274.26 ± 78.61	145.29 ± 61.09	267.46 ± 53.87
Peak (N)	318.49 ± 67.28	703.86 ± 149.63	347.85 ± 68.08	715.83 ± 157.11	347.85 ± 68.66	720.32 ± 104.72	397.02 ± 74.53	773.69 ± 119.64

Validation of loadsol® Sensors Over 32 Velocity/Grade Running Conditions

Shannon Hugard[1*], Seth Donahue[2], Aida Chebbi[1], Rachel Robinson[1], Michael E. Hahn[1]

[1]University of Oregon, Bowerman Sports Science Center; [2]Northwestern University, Prosthetics and Orthotics Rehabilitation Technology Assessment Laboratory (PORTAL)

*Corresponding author's email: hugard@oregon.edu

INTRODUCTION

loadsol® sensors offer a relatively inexpensive and versatile alternative to instrumented treadmills for gait parameter assessment. Previous work has found good to excellent agreement between loadsol® sensors and instrumented treadmills at 1.39m/s, 2.78m/s, 3.0m/s and 3.5 m/s over -10°, 0°, and 10° grades [1, 2]. The purpose of the current post-hoc analysis is to examine whether these findings are consistent across a greater range of velocities and grades. Unlike instrumented treadmills, loadsol® sensors are compatible with most footwear and ground surfaces. Expanded validation of loadsol® sensors could provide options for high-quality ground reaction force data collection in a wider variety of experimental conditions.

METHODS

This study examines data collected as part of a larger study [3]. Fourteen participants completed a series of one-minute running trials based on each participant's self-reported 5k pace. Each participant ran four to five progressively faster trials at -7°, 0°, and 7° grades, for a total of 13 trials. Although all participants did not run at the same set of prescribed velocities, 16 of the 32 velocity/grade conditions had n≥5. Vertical ground reaction forces and foot-shoe normal forces were collected simultaneously using a Bertec instrumented treadmill and loadsol® sensors respectively. Bertec data were collected at 1000 Hz and downsampled to 100 Hz, while loadsol data were collected at 100 Hz. Impulse, peak force, and loading rate were calculated for each step and then averaged for each trial in MATLAB. Bland-Altman plots were generated for all gait parameters in each velocity/grade condition. Bland-Altman plots were also generated to illustrate average gait parameter values for all trials. Two-way mixed effects intraclass correlation coefficients (ICC3,k) with 95% confidence intervals were calculated for all conditions with n≥5. ICC values were categorized as excellent (0.75-1.0), good (0.6-0.74), fair (0.4 - 0.59), or poor (<0.4) [4].

RESULTS AND DISCUSSION

ICC values for impulse indicated high agreement between loadsol® and Bertec measures across most conditions (12/16 excellent, 1/16 good, 3/16 poor). Loading rate ICC values similarly indicated high accuracy across most conditions (12/16 excellent, 1/16 good, 2/16 fair, 1/16 poor). Peak force values displayed greater discrepancies (5/16 excellent, 5/16 good, 3/16 fair, 3/16 poor). However, Bland-Altman plotting for conditions with poor ICC values show that few trials fall outside of the 95% confidence interval boundaries. As ICC3,k measures are the ratio of variance between trials to variance between measurement systems, poor ICC values could be due to low variability between trials. Low variance between trials may be a result of the relatively small sample sizes evaluated in this study; further work

is needed to confirm this possibility. Additional analysis is also required to investigate correlation between condition velocity and
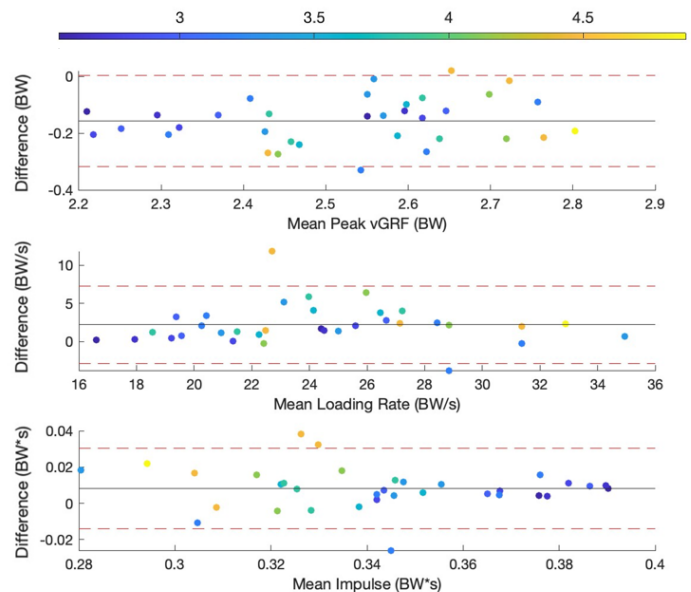

Figure 1: Bland-Altman plots for average peak force, loading rate and impulse at 0° grade. Marker color indicates trial velocity (m/s), as indicated by the colorbar. Difference was calculated by subtracting average loadsol® from average Bertec-generated values.

loadsol® accuracy.

CONCLUSIONS

The relative portability and affordability of loadsol® sensors creates opportunities for athletic and clinical gait parameter testing that cannot be completed on an instrumented treadmill. The current study expands previous validation by evaluating accuracy between loadsol® and Bertec over 32 velocity and grade conditions. ICC values for impulse and loading rate demonstrated high agreement between loadsol and Bertec measures across most conditions. However, ICC values for peak force indicated greater discrepancies between the two measurement methods. Expanded validation of loadsol® has the potential to increase researcher confidence in the sensors as an acceptable alternative to instrumented treadmills for calculating gait parameters.

REFERENCES

1. Burns GT, et al. *J Sports Sci.* **37** (10), 2019.
2. Renner KE et al. *Sensors* **19**, 265, 2019.
3. Donahue et al. *Sci Rep.* **13,** 2023.
4. Cicchetti, et al. *Psychol. Assess*. **6**, 284, 1994.

ACKNOWLEDGEMENTS

PHYSIOLOGY & BIOMECHANICS OF A FENCER'S LUNGE

Supriya Nair[1*], Dr Scott Telfer[2]

[1]Sophomore, Stanford Online High School, Founder - Neurofencing www.neurofencing.com

[2]Department of Orthopaedics and Sports Medicine, University of Washington, Seattle

*Supriya Nair: supriya@neurofencing.com

Introduction: Fencing is one of five sports which have been permanent fixtures at the Olympics. USA Fencing has over 40,000 members and the sport has become popular in the recent years as US athletes have been earning medals at the Olympics and World Cups. Based on sword fighting, fencing demands speed, anticipation, and good reflexes, it requires agile footwork and bladework. Competitive fencing is demanding and injuries of the lower extremities is common. One of the main fencing attack techniques involves the lunge – an explosive extension of the fencer's body propelled by the non-dominant (ND) leg in which the dominant (D) leg is kicked forward. This can be a standard lunge (SL), which involves a single forward step, or an advanced lunge (AL), where 3 rapid steps are taken, ending in the lunge. These lunge techniques provide both power and range to the fencer and helps accelerate the weapon (foil, epee, and saber) for a rapid strike. In this study we analyze the kinematic and kinetic differences between the standard and advanced lunge.

Methods: 30 USA Fencing members from Northwest fencing clubs participated in this IRB approved study (STUDY00019084). These individuals represented all three fencing weapons (Epee, Foil and Saber). A full-body retroreflective motion capture marker set was attached to the fencer to allow 3D kinematics to be captured (Figure 1), and the lunges were performed with the target positioned such that the lead leg during the lunge landed on a floor embedded force plate. After warming up, the fencer performed five SLs and five ALs towards a dummy target. Data were processed and ground reaction forces and joint kinematics were compared between the SL and AL techniques.

Results & Discussion: Significant differences were seen between the vertical and anteroposterior components of the ground reaction force for the leading leg, as well as for sagittal plane knee kinematics. During the extended lunge motion, the dominant (leading) foot lands with more force than the standard lunge, and the peak force is reached in a shorter period of time (Figure 1). Fencers who have a style that involves the use of many extended lunges during a bout could potentially risk injuring or stressing the knee, hip, and ankle joints. The dominant knee was also found to be more extended when the foot is landing during an extended lunge versus the standard lunge. This is because the fencer is trying to kick the front leg in order to propel them forward to hit the target. Both the hamstring and rectus femoris play critical roles in regulating the knee's flexion and extension, as the rectus femoris gets the dominant leg moving forward and the hamstring slows it down preventing over flexion of the knee. Fencers who do many extended lunges risk putting additional stress on the knee joint because they are landing with greater force with the knee extended.
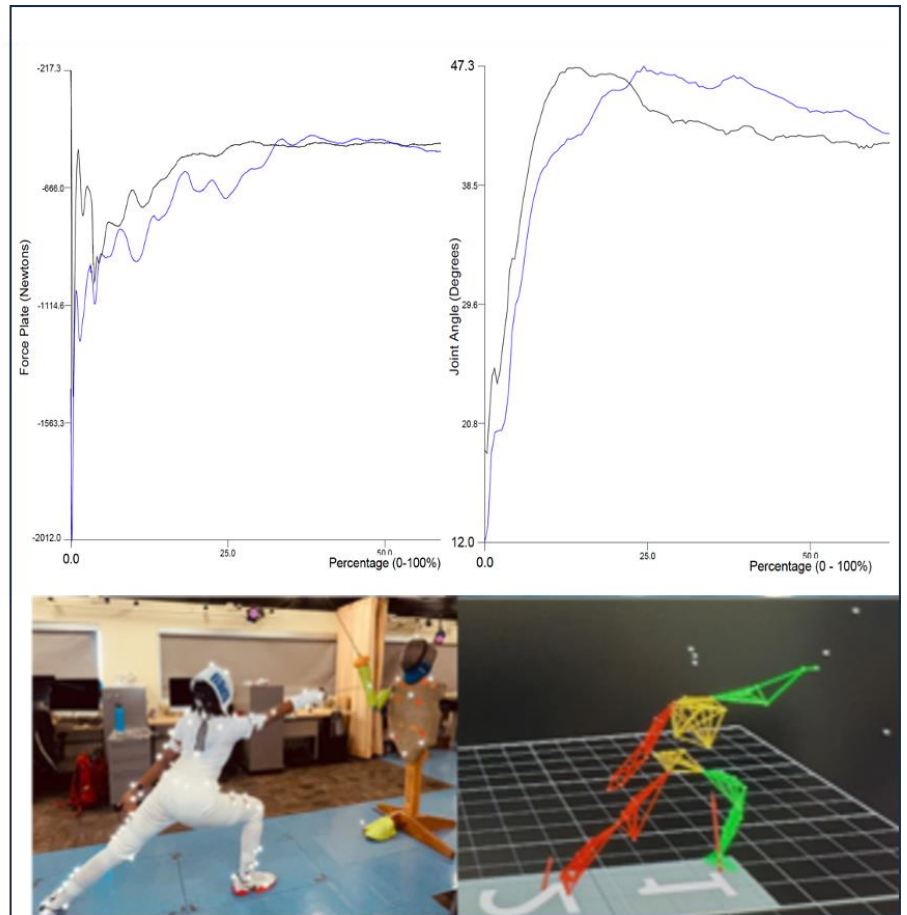

Figure 1: Top left: example vertical ground reaction force data for standard lunge (black) and advanced lunge (blue) from initial contact with the force plate. Top right: sagittal plane knee kinematics for standard and advanced lunges (flexion: positive; extension: negative). Bottom row: fencing lunge and motion capture model.

Significance: Understanding the biomechanics of the fencing lunge and extended lunge may help fencers to optimize their movements, enhance performance and prevent injuries. The rapid and repetitive fencing lunges (as characterized by take-offs and landing) along with rapid extension and flexion of the dominant leg would produce strenuous impact loading on the lower extremities of fencers particularly the knee, hip, and ankle joints. These can be contributing factors for chronic knee injuries and ankle sprains.

References: Engstrom, Ian et al. "The effect of foot-stretcher position and stroke rate on ergometer rowing kinematics." PloS one vol. 18,5 e0285676. 11 May. 2023, doi:10.1371/journal.pone.0285676

EFFECT OF VISUAL AND AUDIO FEEDBACK ON PERCEIVED RUNNING FATIGUE AND RUNNING BIOMECHANICS

A. Terterov, M. Dreher, O. Feistner. L. Freiermuth, P. Schaps, H. Yeager, JH Zhang-Lea
Biomechanics Lab, Department of Human Physiology, Gonzaga University, Spokane, WA
email: aterterov@zagmail.gonzaga.edu

INTRODUCTION

Listening to music while running has been found to delay the time to exercise-induced fatigue (1). However, it remains unclear whether it is the motivational lyrics or beat of the music that affect the delay of fatigue (2). To determine the impacts of different stimuli on perceived fatigue during endurance paced running trials, we utilized a visual metronome to standardize cadence and a non-rhythmic motivational talk to standardize auditory feedback (3). We used self-reported perceived exhaustion (RPE) and center of mass (CoM) dynamic movement to quantify fatigue. We hypothesis that running with visual metronome will reduce RPE and lower CoM dynamic movement compared to running with no stimulus. We also hypothesize the running with visual metronome and motivational talk will further lower RPE and reduce CoM dynamic movement compared to running with visual metronome only.

METHODS

14 subjects ran on treadmill three times at 55% of their maximal sprinting speed for up to 10 minutes each. We varied the stimulus presented to the participants, including no stimulation (Baseline), visual stimulation (VST), and visual and auditory stimulation (VAST). During baseline, we recorded the cadence of the participants, and in VST, participants ran with visual metronome showing a flashing light matching the participant's baseline cadence, with instruction to matching their running cadence to the flashing light. During VAST, we setup the visual metronome same as VST, and we played a non-rhythmic motivational talk to the runners while running as auditory stimulus. For each trial, we recorded participant's RPE for every minute of running, and monitored the heart rate for safety.

We attached one triaxial accelerometer onto the skin at the L1 level, and recorded acceleration at 148 Hz during running. The acceleration data was filtered at 50 Hz, segmented the along each axis into 1-minute intervals. We then calculated root mean square (RMS) along anterior-posterior (RMS_{AP}), medial-lateral (RMS_{ML}), and vertical (RMS_{VT}) axes. We conducted linear mixed models to assess the effect of stimulation on the length the of running trial, RPE, and on center of mass dynamic movement during running.

RESULTS AND DISCUSSION
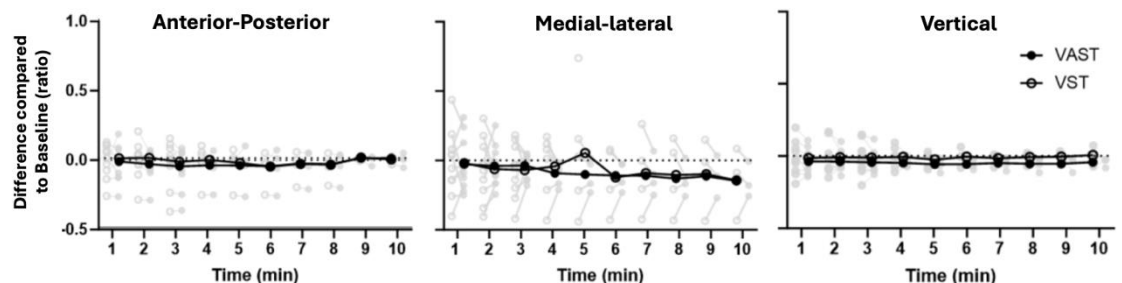
Participants ran at similar cadences (F=0.027, p=0.97) in baseline, VST, and VAST. Trial length did not vary across three stimulus conditions (F=0.038, p=0.96). RPE significantly increased over every minute of running (F=91.131, p <0.001). Stimulus trended towards a significant impact on RPE (F=3.76, p=0.05). Although not reaching statistical significance, linear mixed models showed that compared to baseline, participant's reported RPE values were 0.87 less in VST (p=0.05) and 0.85 less in VAST (p= 0.05).

When controlling for stimulus and interaction effect, time affected acceleration RMS in vertical (p < 0.001), but not in anterior-posterior (p=0.051) or medial-lateral directions (p=0.235). Specifically, RMS_{VT} increased by 0.016 g (p <0.001) for every minute of running. Stimulus condition affected acceleration RMS in anterior-posterior (p=0.014), medial-lateral (p=0.008), but not in vertical direction (p=0.984). Specifically, compared to baseline running, participants showed 0.048 g lower RMS_{AP} (p=0.015), 0.055 g lower RMS_{ML} (p=0.008) when running with visual and auditory feedback (Fig. 1). Compared to baseline running, running with visual feedback only did not reduce acceleration RMS in any directions (p>0.253). Center of mass dynamics movement has been used to indicate fatigue during running, with a greater value associated with fatigue. Our results suggested that combining both visual and auditory feedback managed to reduce center of mass acceleration, potentially delay fatigue in runners compared to running without any stimulus.

CONCLUSIONS

Running with a visual metronome combined with motivational talk reduced CoM dynamic movement compared to running without stimulus, or running with visual metronome only, indicating that the effect of music in delaying fatigue could be a combined result of motivational lyrics and the beats.

ACKNOWLEDGEMENTS

REFERENCES

1. Priest et. al (2012), Int Rev Sport Exer P., 5(1): 44–66
2. Priest et. al (2008), Eur. Phys. Educ. Rev., 14(3): 347-366
3. Vaz et al (2020), Frontiers in Physiology, 11; 1-61

Figure 1: Ratio of difference in acceleration root mean squares in VST and VAST when compared to baseline trial, e.g. (VST-Baseline)/Baseline, across three stimulus conditions.

EFFECTS OF CHANGING HIP POSITION ON SCAPULAR KINEMATICS IN AN ATHLETIC POPULATION

Schlittler, S[1,2], Suprak, D[1], Brilla, L[1], San Juan, J[1]
[1]Department of Health and Human Development, Kinesiology, Western Washington University
[2]email: pines2@wwu.edu, web: https://chss.wwu.edu/health-human-development/pines2

INTRODUCTION

Seated versus standing posture is known to affect scapular kinematics, and activation of the rotator cuff muscles is known to affect the function of the glenohumeral joint [1-3]. However, the effects of these attributes have yet to be directly applied to shoulder function as a result of hip position. Therefore, the purpose of this study is to determine the effect of ipsilateral and contralateral hip position on scapular kinematics during scapular plane elevation.

METHODS

The study population included 20 college-aged males (n=13) and females (n=7) with an average height of 177.66 ± 8.84 cm and an average mass of 73.27 ± 10.65 kg. The subjects were physically active with an average activity level of 2.68 ± 1.70 days per week of strength training and 5.78 ± 1.75 days per week of cardiovascular training. The athletes participated in rowing (n = 10), track (n = 3), soccer (n = 2), and basketball (n= 5). Subjects were recruited via flyer and word of mouth. Following a screening questionnaire and informed consent signing, subjects were included in the study. Exclusion criteria included individuals experiencing pain or who had current or recent shoulder or hip injury and those with tight hip flexors. Tightness of hip flexors was assessed using the modified Thomas test [4].

Scapular kinematics, of the dominant arm were measured using the Polhemus FasTrak electromagnetic tracking system collecting at 40 Hz, in conjunction with a custom LabVIEW script. Polhemus sensors were placed on the thorax, the upper arm (deltoid tuberosity), and the scapular spine of the dominant arm.

Subjects' shoulders were placed in the scapular plane (30-40 degrees from the frontal plane) and a rod was used to ensure the subject maintained this motion within the scapular plane. For each condition, the subject was asked to elevate the arm to approximately 180˚ and back down to neutral (arm at the side) for three repetitions. The four study conditions were pre-randomized: (1) bilateral hip extension (standing) (2) bilateral hip flexion (seated), (3) seated unilateral hip flexion- the subject performed a lunge (such that the ischial tuberosity of the ipsilateral hip was on the chair); and (4) seated unilateral hip flexion- the subject performed a lunge (such that the ischial tuberosity of the contralateral hip was on the chair).

Two-way ANOVAs were used to evaluate effects of shoulder elevation and condition on scapular upward rotation (UR), posterior tilt (PT), and external rotation (ER).

RESULTS AND DISCUSSION

For ER, there was no significant interaction ($F[60,1140] = 1.322$, $p = .054$), no significant effect of condition ($F[3,57] = 0.914$, $p < .001$), but a significant main effect of elevation ($F[20,380] = 15.649$, $p < .001$). For PT (Fig. 1), there was no
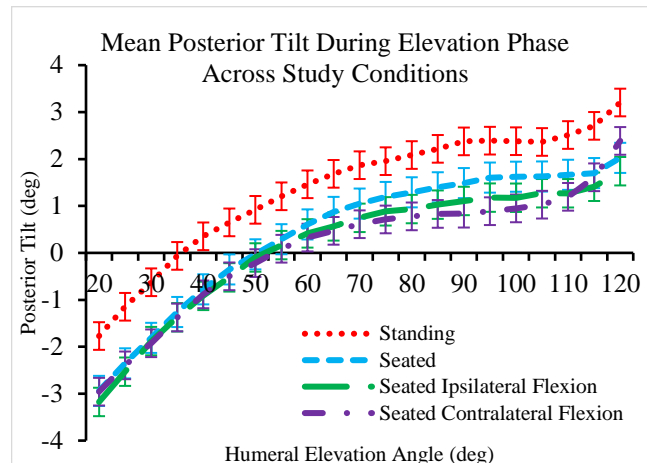

Figure 1: Mean posterior tilt (measured in degrees, deg), during arm elevation (measured in degrees, deg), for all four study conditions.

significant interaction ($F[60,1140] = 0.615$, $p = .991$), no significant effect of condition ($F[2.098,39.862] = 0.950$, $p = .399$), but significant main effects of elevation ($F[20,380] = 15.595$, $p < .001$). For UR, there was no significant interaction ($F[60,1140] = 0.931$, $p = .626$), no significant effect of condition ($F[3,57] = 0.742$, $p = .532$), but a significant main effect of elevation ($F[1.457,27.674] = 532.424$, $p < .001$).

CONCLUSIONS

There was no significant effect of hip position for any scapular rotation. There was significant effect of elevation in all three scapular rotations. As elevation angle increased, PT and UR increased, and ER decreased. The findings of this study suggest that scapular kinematics are affected by arm elevation angle but may not be affected by the position of the hip.

REFERENCES

1. Kanlayanaphotporn, R. Changes in sitting posture affect shoulder range of motion. *Journal of Bodywork and Movement Therapies*, **18**(2), 239-243, 2014. doi:10.1016/j.jbmt.2013.09.008
2. Thigpen, CA, et al. Head and shoulder posture affect scapular mechanics and muscle activity in overhead tasks. *Journal of Electromyography and Kinesiology*, **20**(4), 701-709, 2010.
3. Terry, GC, and Chopp, TM. Functional anatomy of the shoulder. *Journal of athletic training*, **35**(3), 248, 2000.
4. Aslan, H, et al. Acute effects of two hip flexor stretching techniques on knee joint position sense and balance. *Medicine & Science in Sports & Exercise*, **50**(5S), 2018.

Do Straps Reduce Dynamic Soft Tissue Artifacts in Inertial Measurement Unit Measurements?

Berry, J[1] and Kuo, C[2]

Human Motion Biomechanics Lab, School of Biomedical Engineering, University of British Columbia, Vancouver, BC, CA
email: calvin.kuo@ubc.ca , web: https://humbl.bme.ubc.ca/

INTRODUCTION

Inertial measurement unit (IMU) sensors are a common tool for measuring human movement outside of the laboratory. They are prominent in injury monitoring, where wearable devices can measure the accelerations and velocities of impacts to the body that cause real-world acute injuries like ligament sprains. However, while we often want to estimate the accelerations and velocities of the underlying bone, IMUs are almost always attached to soft tissue. Previously, we demonstrated that impacts excite soft tissue, causing it to transiently oscillate as an underdamped second order system and produce dynamic soft tissue artifact errors in the IMU measurements [1]. In this work, we demonstrate pilot data on how a tight strap can mitigate some, but not all of the dynamic soft tissue artifact measurement errors.

METHODS

We consented one female participant with no lower limb injuries in the past year, to participate in our pilot study. Two IMUs were attached to the dominant leg of the participant, one on the posterior of the shank, and one on the anterior of the shank. A third IMU was attached to the ankle on the dominant leg, as shown in Figure 1.A, with the ankle constrained by a brace. To create foot strike impacts such as those in running, we raised the participant's dominant leg to a certain height before dropping it such that the foot impacted a foam pad (to reduce bouncing). The IMU attached to the ankle was used to represent the ground truth measurement (previously cross-validated against a force plate). In our experiment, we adjusted the level of tightness (from 0% to 150% strain in 25% strain increments) of an elastic band that was wrapped around the two IMUs on the posterior and anterior of the shank and performed at least 20 drops at each tightness level (randomized order). We also performed a control without the strap prior to, and following all experiments with the strap, mirroring our previous work.

RESULTS AND DISCUSSION

Over one participant, we observed a trend of decreasing peak vertical acceleration gains as the strap tightness increased (Figure 1.B-D). However, this trend was not continuous over the strap tightness (notable increase at 100% strain) and was most prominent in the posterior IMU location. While the peak vertical acceleration gains decreased as strap tightness increased, we observed that there remained significant post-impact transient oscillations in the IMU measurements due to the dynamic soft tissue artifact. This was most evident in the

angular velocity measurements, where oscillations remained for nearly a second post-impact (Figure 1.E).

CONCLUSIONS

Lower extremity motion testing with IMUs is very common, and thus characterizing how the dynamic soft tissue motion artifacts are affected by strap tightness is important for impulsive load research. If looking to accurately reduce error in the vertical linear accelerations, using a strap tightness of at least 50% appears to be beneficial. Although we are still conducting research on the post impact oscillations, we can show they are still present in the data, regardless of strap tightness. Thus, while tightly strapping the IMU to the body can help improve accuracy of the vertical linear acceleration, which is often used to estimate variables like shank loading, post-impact estimates such as joint angles may still be affected by significant transient oscillations in the IMU.

We want to stress that the results presented here are initial pilot results. There are a number of limitations that we will address in future experiments. First, there appears to be some variability in the application of the strap as evidenced by the difference in the pre- and post- no strap control conditions. Furthermore, these results are currently only from one participant and thus are not generalizable.

One additional limitation we found was in the attachment of the IMU to the skin itself. In the current experiment, we used kinesiology tape to secure the IMU to the body, while in our previous work, we used double-sided tape between the IMU and the body. We noticed in the current data that the overall peak gains are lower than we expected, which we speculate could be related the kinesiology tape providing some additional coupling to the body.

Despite these limitations, our pilot analysis shows promise in furthering our understanding of how strap tightness is correlated to the dynamic soft tissue error and the coupling of hard and soft tissues. This will be critical in understanding when and how IMUs should and can be used in dynamic settings such as injury monitoring.

REFERENCES

1. S. Rong and B. A. Sc, "Quantifications and Characteristics of Dynamic Soft Tissue Artifacts Captured by Wearable Inertial Mea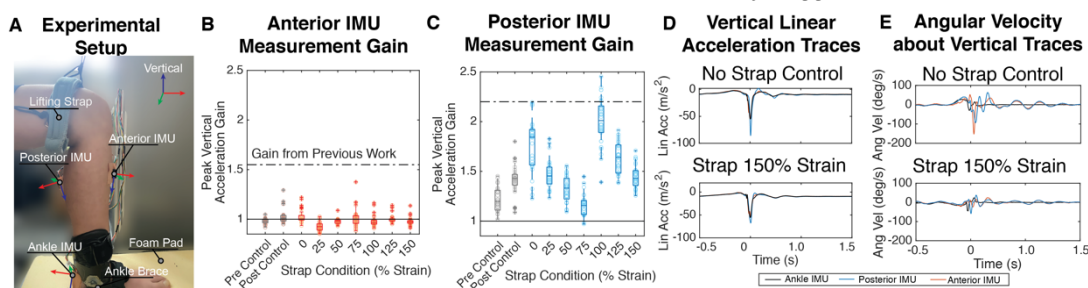surement Unit Sensors," 2022. Available: https://open.library.ubc.ca/soa/cIRcle/collections/ubctheses/24/items/1.0421332

Figure 1: **A)** Experimental setup **B, C)** Overestimation of peak vertical gains **D, E)** Sample impulsive load traces

Dynamics of Player Movements in Female Soccer: Implications for ACL Injury Risk

Fu, Jason and Kuo, Calvin
School of Biomedical Engineering, University of British Columbia, Vancouver, BC Canada
email: jasonf02@mail.ubc.ca

INTRODUCTION

In soccer, injuries are a significant concern due to the sport's dynamic nature and physical demands. Players traverse long distances during matches, which requires a sustained level of physical exertion. Rapid changes in direction through maneuvers such as cutting and tacking heighten injury risks [1], particularly to lower limbs, leading to sprains and tears. This study focuses on the evolution of player movements in female soccer and how they may lead to changes in specific kinematics that are associated with non-contact lower limb injury during maneuvers. We hypothesize that maneuvers following dynamic activities (such as running) have higher accelerations than those performed after less physically demanding activities (such as walking). By analyzing the context of maneuvers, we aim to understand what factors affect the intensity of maneuvers and optimize the balance between player performance and injury risk.

METHODS

We collected kinematic data from female soccer athletes over two soccer season (2022 and 2023) to analyze the evolution of female soccer player movements. Firstly, wearable Inertial Measurement Units (IMUs) worn on the back between the shoulders are utilized to track whole-body kinematic metrics during dynamic movements. Specifically, we developed a custom high-rate IMUs with a sampling rate of 1000 Hz [2] to ensure precise measurement of dynamic activities.

IMU data are paired with time-synchronized video recordings to obtain ground-truth labels of player activities. Focusing on IMU-sensor-wearing players, the video labeling methodology categorizes five fundamental soccer movements (stationary, walk, run, shuffle, maneuver) into over 24 subcategories with 24 frame-per-second resolution classification.

The ground-truth video movements are used to label foot strikes with peak vertical accelerations exceeding $25 m/s^2$ in the IMU sensor data [2]. Foot strikes were defined over a 350ms window (100ms pre-threshold and 250ms post-threshold). We analyzed maneuver foot strikes with the highest peak accelerations in all three-axes (anterior-posterior, left-right, and superior-inferior). Peak accelerations from maneuvers following a run were compared with peak accelerations from maneuvers following a walk (Figure 1) using a Wilcoxon single-sided rank sum test.

RESULTS AND DISCUSSION

We analyzed data from a single athlete over a 90-minute entire game from the 2022 soccer season. In total, we observed 144 maneuvers, with 15 following a walk and 116 following a run. We observed that maneuvers conducted after running exhibited significantly ($p<0.05$) higher peak accelerations across all three axes compared to those following walking. Median peak accelerations increased by 66.5% in the anterior-posterior, 49.9% in the left-right, and 47.7% in the superior-inferior axes (Figure 2).
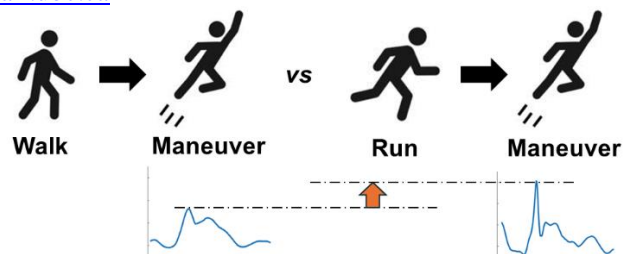

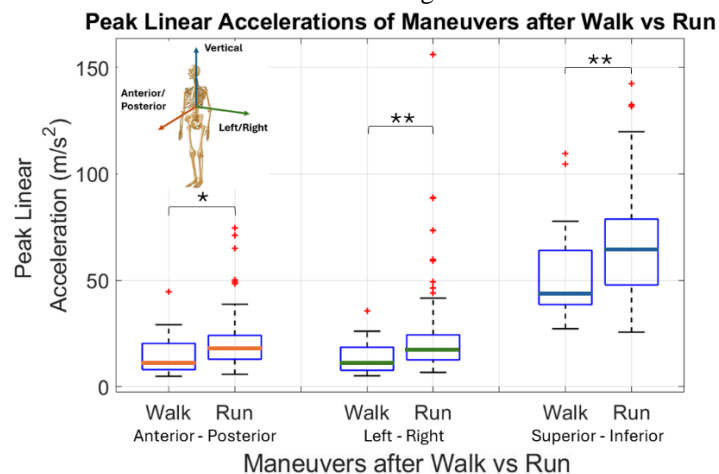**Figure 1**: Maneuvers following a run have higher peak kinematics than maneuvers following a walk.

Figure 2: Maneuvers following a run have significantly higher peak kinematics (Wilcoxon single-sided rank sum, *$p<0.05$, **$p<0.01$), particularly in the left-right direction that is commonly associated with injury.

CONCLUSIONS

The study investigates the evolution of female soccer player movements, particularly focusing on maneuvers following different activity levels. Significant increases in peak acceleration are observed for maneuvers after running compared to walking, indicating the intensity of maneuvers such as cuts depends on the context of the movement. Left-right (lateral) acceleration, which is associated with injury observed a 49.9% increase in median accelerations due to this context, highlighting the importance of understanding the time-dependent evolution of movement. This analysis is currently limited by data from a single player in one game, though our full dataset comprises over 400 games from more than 30 athletes. Nonetheless, the findings offer valuable insights into potential injury risks, emphasizing the importance of considering activity context in injury prevention strategies.

REFERENCES

1. A. Daneshjoo, et al. *PLOS ONE*, **10**(11), e0143323, 2015.
2. Kuo, C., et al. ACM TOG 38(4), 1-12, 2019.

ACKNOWLEDGEMENTS

OPPORTUNITIES FOR ULTRASOUND SHEAR WAVE ELASTOGRAPHY USE IN THE DIAGNOSIS AND MANAGEMENT OF ACHILLES TENDON INJURIES

Ozanich, NR[1], Montiel, AM[1], and Agresta, CE[2]
[1]Mechanical Engineering, University of Washington, Seattle, WA USA
[2]Rehabilitation Medicine, University of Washington, Seattle, WA USA
email: ozanich@uw.edu

INTRODUCTION
Ultrasound appears to be a useful clinical tool for diagnosing Achilles tendon injuries and monitoring their progression [1]. B-mode ultrasound, which is commonly used in clinical settings, can show morphologic changes like tendon thickening or loss of echogenicity, which are hallmark signs of pathology. Achilles tendon injuries are a result of repetitive strain, or repetitive overloading; thus, current evidence-based rehabilitation is centered around mechanical load management [2]. B-mode ultrasound can supply morphological information but not mechanical information and, therefore, has limited value in guiding the treatment of Achilles tendon injuries.

Ultrasound elastography is a technique that can estimate elastic properties of biological tissue. By deforming tissue, strain can be measured through reflected ultrasound waves and the elastic mechanical properties can be estimated. Changes in the microscopic structure of tissues, which may be indicative of pathology, can be identified by observing differences in their measured elasticity. There are two types of ultrasound elastography techniques: strain elastography, which measures deformation in response to a manual compression, and shear wave elastography (SWE), which measures the propagation of shear waves perpendicular to the transducer. SWE is typically used for clinical assessment of visceral tissue and is effective for detecting liver fibrosis [3] as well as differentiating between benign and malignant breast masses [4]. Elastography is growing in its applicability in musculoskeletal (MSK) tissues for research, but few accepted applications exist in clinical practice. Most applications have used strain elastography, which requires the operator to compress the tissue using an ultrasound transducer and assess the relative deformation. SWE, being less operator-dependent than strain elastography and capable of estimating mechanical properties unlike traditional B-mode, has potential as a valuable tool for clinical use in the management of Achilles tendon injuries.

The purpose of this study was to perform a scoping review on the current clinical use of shear wave elastography (SWE) for Achilles tendon injuries.

METHODS
We searched Google Scholar for studies using the following terms: ultrasound, elastography, shear wave, and Achilles tendon. In addition to databases, we did a hand search for relevant articles. We included only original research studies that utilized SWE on the Achilles tendon and reported stiffness values. We limited our search to those available in full-text and written in English.

RESULTS AND DISCUSSION
A total of 43 papers were included in this review. Eight studies investigated elasticity post-rupture (n=257), nine papers that investigated tendinopathy (n=354), and 26 papers that investigated healthy subjects (n=2511). All studies reported stiffness values for a specific region of interest, approximately 2cm to 6cm from tendon insertion, as either shear wave speed or elastic modulus (Figure 1).

We observed a range of methodologies, with the primary inconsistencies including differences in ankle joint position for measurement, whether to precondition the tendon with a specified load or have a rest period before measurement, and tendon location site for measurement.

Seven studies utilized SWE to longitudinally track ruptured or tendinopathic Achilles tendons. SWE was found to be diagnostically superior and correlated closer to the Victorian Institute of Sports Assessment – Achilles (VISA-A) scores than B-mode or power Doppler ultrasound for Achilles tendinopathy [5]. One study investigated the healing process of ruptured Achilles tendons for surgical (n=31) and conservative (n=24)
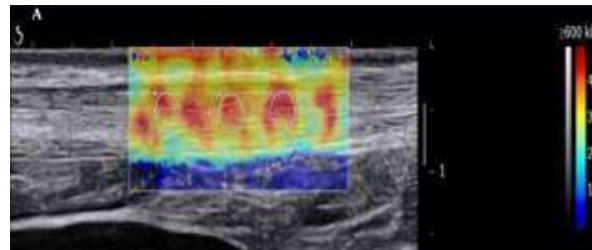

Figure 1: Scan of a normal Achille's tendon with shear wave elastography image overlayed on top [8]. Red represents stiffer tissue, while blue represents softer tissue.

intervention groups over the course of 48 weeks [6]. Both groups achieved similar elasticity values after 12 weeks, but the surgical group achieved much higher elasticity after four weeks.

Of the papers that investigated healthy Achilles tendons, six had professional or semi-professional populations. Healthy athletes' Achilles tendons were found to be 1.8 times stiffer than nonathletes' tendons using SWE [7]. However, more research is needed to document the use of SWE to gauge the risk of active and nonactive populations for developing tendinopathy.

CONCLUSIONS
SWE has potential as a clinically relevant tool for the management of Achilles injuries. Current studies suggest that SWE can differentiate between healthy and pathologic tendons. Further studies should seek to utilize SWE in assessing the effects of personalized rehabilitation loading protocols on prognosis of Achilles tendon injuries.

REFERENCES
1. T. Dirrichs, et al. *Academic Radiology* **23**, no. 10, 1204–1213, 2016.
2. K. Silbernagel, et al. *Journal of Athletic Training* **55**, no. 5, 438–447, 2020.
3. E. Herrmann, et al. *Hepatology* **67**, no. 1, 260–272, 2018.
4. J. Chang, et al. *Breast Cancer Res Treat* **129**, 89–97, 2011.
5. T. Dirrichs, et al. *Academic Radiology* **25**, no. 3, 265–272, 2018.
6. K. Yoshida, et al. *Foot Ankle Int.* **44**, no. 3, 243–250, 2023.
7. T. Dirrichs, et al. Academic Radiology **26**, no. 10, 1345–1351, 2019.
8. D. Bian, et al. *Iran J Radiol* **18**, no. 2, 2021.

OCCUPANT CHARACTERISTIC RISK FACTORS FOR WHIPLASH IN MOTOR VEHICLE COLLISIONS

Kjeryn A. Soetaert[1], JE de Lange[2], Chad E. Gooyers[2], Kayla M. Fewster[1]
[1]School of Kinesiology, University of British Columbia, Vancouver, BC, Canada
[2]Forensic Engineering, Toronto, ON and Vancouver, BC
Email: Kjeryn.soetaert@ubc.ca

INTRODUCTION

Whiplash and whiplash associated disorders (WAD) frequently result from low velocity rear-end motor vehicle collision (MVC) configurations and are one of the highest financially burdening musculoskeletal injuries due to the wide range of symptoms and variable recovery rates [1]. With up to 50% of individuals with WAD experiencing chronic symptom reporting, current research has focused on prognostic risk factors [2]. Despite substantial research on WAD injury mechanisms, definitive factors of elevated injury risk and likelihood of chronicity of symptoms remain inconclusive. Pre-existing cervical intervertebral disc (IVD) degeneration, cervical facet joint degeneration or generalized neck pain have been suggested to influence WAD symptom reporting, duration, overall prognosis, and injury risk [3,4]. Additionally, prior neck pain or injury, increased age and female biological sex have been reported to significantly increase risk of poor WAD prognosis via increased severity of present symptoms and prolonged recovery times [2,4]. Despite consensus of a few prognostic risk factors, current findings are still developing [3]. To better understand the causation of claimed WAD following MVCs, forensic engineering firms are utilized to assess the plausibility an injury was resultant from a specific collision. This provides firms with unparalleled access to collision characteristics and medical records to determine relevant pre-existing medical conditions pertaining to injury assessment. Analysis of this data provides the opportunity to associate occupant and collision characteristics with reported injury symptoms and prognostic factors while limiting reliance on individual recall. Therefore, the purpose of this investigation was to utilize medical records from individuals involved in low to moderate velocity MVCs to shift reliance from self-reported symptoms and accident recall to medical documentation and collision reconstruction. It was hypothesized that a greater proportion of occupants with evidence of cervical degeneration (facet joint osteoarthritis and/or IVD degeneration) would experience a WAD following a low to moderate velocity MVC.

METHODS

This study incorporated a secondary analysis of data provided by a Vancouver, British Columbia, Canada based forensic engineering firm (30 Forensic Engineering). Paper files were provided an associated file number entered in a searchable internal electronic database. This database, containing 23 years of cases (2000-2022), was searched by specific parameters, with only cases with a collision severity below 20km/hr being further evaluated. This list of useable cases was de-identified by the partner organization. Cases were then cataloged by specific collision and occupant characteristics including age, sex, collision severity and type, direction of collision forces, restraint use, vehicle make and model, seating position in the vehicle, prior collisions, injuries claimed, and pre-existing medical documentation. Across all cases, percentages of total cases or descriptive statistics (means and standard deviation) were calculated for seating position, collision severity, collision configuration, biological sex, presence of pre-existing cervical degeneration (degeneration grade and location) and whiplash or WAD injury claims. Within WAD injury claims, percentages of cases or descriptive statistics were calculated for biological sex, presence, severity, type of pre-existing degeneration, grade of pre-existing degeneration, collision severity, and collision configuration.

RESULTS AND DISCUSSION

In total, 161 cases met the inclusion criteria. There were more female than male claimants distributed across all claims; 39.1% were male and 60.9% were female. The mean collision severity was found to be 11.09 km/hr (SD = 5.41) across all collision types. Out of the 161 cases, 83.2% involved a claim of whiplash.
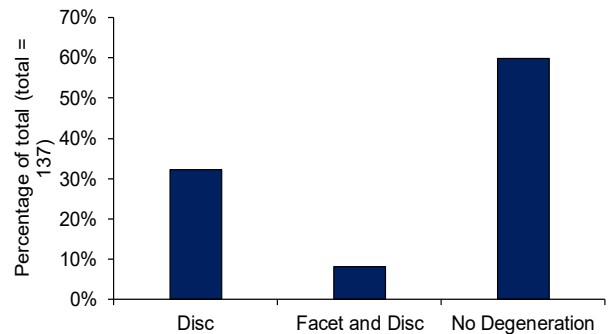

Figure 1. Percentage of Neck Injury Claims as a Function of Degeneration Type

The most common pre-existing medical condition was evidence of cervical degeneration; of which 46.3% of claimants had (Figure 1). Incidence of WAD was relatively equally distributed between biological males (82.5%) and females (83.7%). A rear-end impact was the most common collision configuration. 72% of all whiplash claims involved a rear-end collision, 84% of which had associated whiplash claims. The mean collision severity across all whiplash claims was 11.01 km/hr (SD = 5.31). There was no significant difference in rear-end mean collision severity between whiplash claimants and those without. When controlling for medical evidence of cervical spine degeneration, the average collision severity associated with a WAD was observed to decrease from 11.80 km/hr (without degeneration) to 10.10 km/hr with evidence of cervical degeneration present.

CONCLUSIONS

Results indicate that claimants with medical evidence of cervical spine degeneration have a slightly lower collision severity associated with a WAD injury claim. This was particularly evident for claimants with medical evidence of both IVD and facet degeneration. This research can be used to direct additional investigations on specific populations of whom are at potential increased risk for whiplash and WAD following a low to moderate speed MVC.

References: 1. Stemper & Corner, *J Biomech* **36**(9), 2016
2. Walton et al., *J Orthop Sports Phys Ther* **43**(2), 2013
3. Malik et al., *Int J Spine Surg* **15**(4), 2021
4. Yoganandan et al., *Semin Spine Surg* **25**(1), 2013

INVESTIGATING THE FUNCTIONAL AND PAIN-RELATED THERAPEUTIC EFFECTS OF EXERCISE THERAPY AND VISCOSUPPLEMENTATION IN A PRECLINICAL RODENT MODEL OF POST-TRAUMATIC OSTEOARTHRITIS

Sverdrup, E[1], Pancheri, NM, Kyathsandra, N, Lin, ASP, Willett, NJ, Guldberg, RE[1]
Department of Bioengineering, Knight Campus for Accelerated Scientific Impact, University of Oregon, Eugene, OR USA
email: esverdr2@uoregon.edu,

INTRODUCTION

Post-traumatic osteoarthritis (PTOA) is a subtype of osteoarthritis that occurs following joint injury and is associated with a young patient demographic and a lifetime of disease burden.[1] The gold standard treatment for PTOA is prescribed physical rehabilitation, yet outcomes are variable. Other treatments that target the joint loading environment, such as viscosupplements, are often prescribed in conjunction with exercise, but there is little mechanistic evidence to justify this course of treatment.[2] This pilot study aims to characterize the therapeutic effects of exercise and Hyalgan (HA), a common viscosupplement, following an ACL rupture in a preclinical rodent model. *We hypothesized that exercise with HA would reduce spontaneous and evoked pain related behaviors more so than exercise alone by 8-weeks post injury.*

METHODS

Procedure: Adult male Lewis rats received either a non-invasive knee injury (NIKI=6-10/group) to cause ACL rupture or a sham injury (Sham). An axial force was applied to the left hind limb to induce injury whereas the sham controls received a static preload. The HA treatment group was injected with an intra-articular dose of Hyalgan (30 μL), an FDA approved source of sodium hyaluronate, 4-weeks post injury. All studies were conducted under IACUC approved protocols.

Exercise regimen: All animals began pretraining 2 weeks prior to injury with a target running regimen of 10 m/min for 30 minutes on a custom treadmill. Exercise groups resumed daily exercise 5-weeks post injury and continued through 8-weeks.

Functional assays: Limb weight bearing (Bioseb Dynamic Weight Bearing) and evoked pain-related behavior (electronic von Frey assay) were assessed weekly from 4-weeks until euthanasia. Mixed-effect models with Tukey's post hoc test were used to compare between groups (reported for $p<0.05$).

RESULTS AND DISCUSSION

Limb Weight Bearing Function: ACL rupture significantly reduced weight bearing behavior at all timepoints regardless of treatment compared to sham controls (data not shown on graph). NIKI and NIKI+HA+Exercise groups exhibited significantly increased weight bearing by 8-weeks compared to their earlier timepoints (**Figure 1A**).

Evoked pain-related behaviors: ACL rupture resulted in increased pain sensitivity compared to both sham and baseline levels at 4-weeks after injury. NIKI+Exercise+HA had significantly increased sensitivity at all timepoints compared to baseline. All NIKI groups were significantly or trended towards significantly increased sensitivity compared to sham at 3-, 5-, and 6- weeks. NIKI+Exercise recovered to sham levels by 8-weeks (**Figure 1B**).
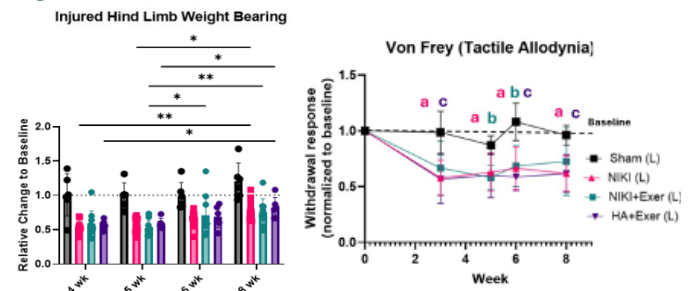

Figure 1: **A)** Bioseb assay to assess weight bearing behavior where a smaller y-value means less weight bore on the injured limb; results shown normalized to baseline (significance denoted by asterisks). **B)** Von Frey test to measure tactile allodynia where a smaller y-value means a lower sensitivity threshold; results shown normalized to baseline (significance denoted by letters).

Discussion: Results of ACL injury is consistent with data previously observed in our lab. Variability with exercise and HA is consistent with clinical data.[3] Results suggest that the applied exercise regimen should be modified to achieve greater therapeutic efficacy and conducted with a greater sample size for increased statistical power.

CONCLUSIONS

This work introduces exercise and HA for PTOA intervention in a preclinical rodent model. While clinically utilized, the efficacy of both therapies remains unclear. The analysis of injury-induced pain sensitivity and limb function allows us to quantify the therapeutic effects of these methods. Future directions include pathological assessment of tissues to compare with the reported pain and function outcomes.

REFERENCES

1. Thomas AT, Hubbard-Turner T, Wikstrom EA, Palmieri-Smith RM. Epidemiology of Posttraumatic Osteoarthritis, 491-496. J Athl Train. 2017.
2. Peck J, Slovek A, Miro P, et al.. A Comprehensive Review of Viscosupplementation of Osteoarthritis of the Knee. Orthopedic Review (Pavia). 2021.
3. Pereira TV, Jüni P, Saadat P, et al.. Viscosupplementation for knee osteoarthritis: systematic review and meta-analysis. BMJ. 2022.

ACKNOWLEDGEMENTS

SHOULDER MUSCLE ACTIVITY INCREASES AFTER ACUTE BUT NOT CHRONIC PAIN RELIEF

Taylor J Wilson[1], Motoki Sakurai[1], Phil McClure[2], Andy Karduna[1]
[1]University of Oregon, Eugene, Oregon, US, [2]Arcadia University, Glensdale, Pennsylvania, US
Email: *twilson8@uoregon.edu

INTRODUCTION
Subacromial pain syndrome (SPS; often referred to as shoulder impingement syndrome) is defined as chronic pain that arises from a broad set of pathologies localized to the subacromial space [1]. There is no consensus on how pain affects shoulder musculature. One of the leading hypotheses about muscular adaptations to pain includes the pain adaptation model (PAM). The PAM proposes that pain ridden muscles involved in movement (agonist muscles) decrease their activity, as measured by electromyography (EMG) while muscles that oppose the movement of agonists (antagonists) increase their activity, acting as a protective mechanism during movement [2].

The aim of the present study was to determine the effects of pain on muscle activity in patients with SPS, both before and after pain relief. In line with the PAM, we hypothesized that shoulder muscle activity will be higher in agonist muscles (lower in antagonist muscles) after pain relief, compared to pre-pain relief.

METHODS
Twenty-two patients were recruited from a local orthopaedic clinic. Inclusion criteria were ages $21 - 65$ years (mean $\pm$ SD; 47.9 ± 10.3 years), experienced pain during passive (assisted) provocative manoeuvres (Hawkins or Neer), active elevation, and/or isometric resisted movements and planned to receive a subacromial injection.

The subject's affected side was instrumented with wireless Delsys Trigno EMG electrodes and wireless Xsens MTi inertia measurement unit (IMU) sensors to collect muscle activity and kinematic data, respectively. Surface EMG sensors were placed on the anterior, middle, and posterior deltoid (AD, MD, and PD, respectively), and upper trapezius (UT). Two IMUs were placed on the lateral aspect of the affected arm, superior to the elbow and on the torso at the level of the xiphoid process.

The subject was then instructed to complete three bouts of humeral elevation (HE) at an angle ~30 degrees forward of the frontal plane with an externally rotated arm for block one (T1). Block two (T2) was the same, and performed on the same day, as T1 but after a subacromial injection (6 cc 0.5% Marcaine and 1 cc DepoMedrol) applied by a physician and the subject's qualitative indication of pain-relief during an arm raise. For the last block (T3), subjects completed 6-weeks of physical therapy aimed at increasing range of motion and strength on the affected side and then repeated the same HE from T1/T2.

Multiple One-Dimensional Statistical Parametric Mapping (SPM1d) two-tailed paired t-tests were used to compare the activation of each muscle under analysis (AD, MD, PD, and UT) from $40º(0\%)$ to $110º(100\%)$ of HE: T1 vs. T2 and T1 vs. T3.

RESULTS AND DISCUSSION
Partially agreeing with our hypothesis, AD, MD, and UT EMG activity increased after acute pain relief ($p<0.05$), but only for specific percentages of HE (Table 1), with a visual representation for AD (Figure 1). However, no differences in muscle activity were apparent in PD after acute pain relief (T1 vs T2) or for any muscle after chronic pain relief (T1 vs T3).

Increases in the muscle activity of the AD, MD, and UT in T2 compared to T1 are not surprising, as these muscles aid in shoulder flexion (AD,UT) and abduction (MD), while the PD aids in adduction and extension [6]. Additionally, the body may overcompensate muscle activity after acute relief of pain, whereas it returns to normal muscle activity after rehabilitation.

Table 1. Instances where muscle activity was larger in T2 compared to T1 ($p<0.05$) during movement from $40º$ (0%) to $110º$(100%) HE.

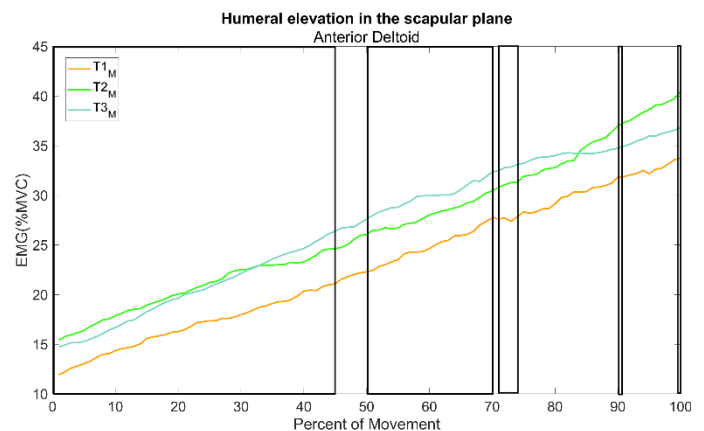| T1 EMG < T2 EMG					
Muscle	Percentage of Movement				
AD	0-44%	50-70%	72-73%	90-91%	99-100%
MD	5-8%	15-18%	27-32%	35-36%	
UT	25-27%	55-60%	63-65%	70-73%	94-100%

Figure 1. Mean anterior deltoid (AD) activity in the scapular plane before pain relief (T1), after subacromial injection (T2), and after physical therapy (T3). Muscle electromyography (EMG) activity is represented as a % of maximum voluntary contraction (%MVC). Black boxes indicate the ranges of HE where T2 EMG is significantly higher than T1 EMG ($p<0.05$).

CONCLUSIONS
Our results partially support the PAM. Impaired deltoid activity could upregulate UT activity [7], and cause further injury or denervation of the muscles. Therefore, other muscles and structures may be affected by the decreased deltoid activity due to pain, which could lead to irregular scapular and humeral movements. Future studies could look at how deltoid activity pre- and post-pain relief affects functional alternations in and around the subacromial space. Others could compare post-pain relief deltoid activity in the affected versus unaffected shoulder. If differences are found, rehab modalities may need different approaches for those after acute versus chronic pain relief.

References
[1] Mitchell et al., 2005. *BMJ*, **331**(7525), 1124-28.
[2] Hodges & Smeets, 2015. *Clin. J. Pain.*, **31**(2), 97-107.
[3] Oh et al., 2021. *Sci. Rep.*, **11**(4077), 1-10.
[4] Johansson & Sojka, 1991. *Med. Hypotheses*, **35**(3), 196-203.
[5] Robinson et al., 2015. *J. Electromyo. Kinesiol.*, **25**(1), 14-19.
[6] Moser et al., 2013. *Skeletal Radiol.*, **42**(10), 1361-75.
[7] L. Ettinger et al., 2021. *J. Sport Rehabil.*, **30**(8), 1144-50.

ACUTE FATIGUE MODIFIES ULTRASOUND-BASED PATELLAR TENDON STIFFNESS BY SEX

D. Shlesinger[1], A. W. Ricci[1], D. M. Callahan[1]
email: damienc@uoregon.edu

INTRODUCTION

Tendons transmit skeletal muscle force to produce joint torque. Insight into tendon stiffness could help better understand the limits of musculotendinous performance and may help predict the risk of soft tissue injuries [1] in response to extreme load. Clinical ultrasound (US) imaging, both traditional B-mode and more recently, shear wave elastography (SWE) have been used to assess muscle and tendon stiffness. Recent studies using SWE have illustrated that acute fatigue can decrease stiffness in skeletal muscle [3]. Others have demonstrated the effects biological sex and age on tendon stiffness using multiple US based approaches [4]. However, no studies have used SWE to assess the effect of acute fatigue on tendon stiffness, nor have any studies compared these measures with those produced using B-mode US. [2,3]. While shear wave elastography has shown promise in assessing muscle stiffness [5], we aimed to evaluate its correlation with more traditional modes of assessing tendon stiffness. The purpose of the study was to investigate the effects of fatigue and sex on tendon stiffness measured by two ultrasound-based techniques: b-mode and shear wave elastography (SWE).

METHODS

We recruited 26 young healthy males (12) and females (14) to participate. Participants performed 3 maximum voluntary isometric contractions (MVIC) of the knee extensors to evaluate maximal torque and rate of torque development (RTD) using an isokinetic dynamometer (Biodex Medical Systems, Shirley, NY). During ramped isometric contractions of 25%, 50% and 100% [3] MVIC, a linear array ultrasound transducer was used to measure elongation of the patellar tendon (PT) under load. In a subset of participants (6 older and 5 young) SWV measurements were observed during passive measurements, providing insights into the mechanical properties of the tendon under passive conditions as well as during submaximal contractions as described for B-mode measures. Participants were then instructed to fatigue their muscles by performing a bout of repeated maximum voluntary knee extensions with isotonic load set to 30% MVIC until task failure (inability to complete more than ~50% range of motion or maintain pace of contractions). Stiffness of the PT was calculated by dividing the estimated tendon force during a contraction by the measured elongation of the PT, thus quantifying the tendon's mechanical resistance to deformation during muscle contraction (stiffness). A two-way repeated measures ANOVA was used to assess differences in tendon stiffness by fatigue and sex across all contraction intensities.

RESULTS

PT active and passive stiffness was not different by sex. As measured by B-mode US, fatigue reduced active stiffness in the PT in both sexes (p<0.001), although sex by fatigue interaction effect suggest females experienced lesser reductions than males (p=0.044). Active and passive SWV was reduced by fatigue (p=0.002), but only in males.

CONCLUSION

Our data suggest that a dynamic fatiguing exercise of the knee extensors reduces patellar tendon stiffness under active and passive conditions. Males tend to experience greater reductions in stiffness than females. This sex-based variation in the fatigue response may contribute to variations in soft-tissue injury risk that are different by biological sex.

REFERENCES

1. J. Brumitt and T. Cudderford, *CURRENT CONCEPTS OF MUSCLE AND TENDON ADAPTION TO STRENGTH AND CONDITIONING.* International Journal of Sports Physical Therapy, **vol 10**, no. 6, 2015
2. P. Andonian et al., *Shear-wave Elastography Assessments of Quadriceps Stiffness Changes Prior to, during and after Prolonged Exercise: A Longitudinal Study during an Extreme Mountain Ultra-Marathon.* PLoS ONE **vol 11**, no. 8, 2016
3. E. Chalchat et al., *Changes in the Viscoelastic Properties of the Vastus Lateralis Muscle With Fatigue.* Frontiers in Physiology **vol 11,** 2020
4. E. Drakonaki. *Ultrasound Elastography for Imaging Tendons and Muscles.* Journal of Ultrasonography **vol 12**, no. 49, 2012
5. N. Šarabon et al. *Using Shear-Wave Elastography in Skeletal Muscle: A Repeatability and Reproducibility Study on Biceps Femoris Muscle.* PLoS ONE **vol 14**, no. 8, 2019
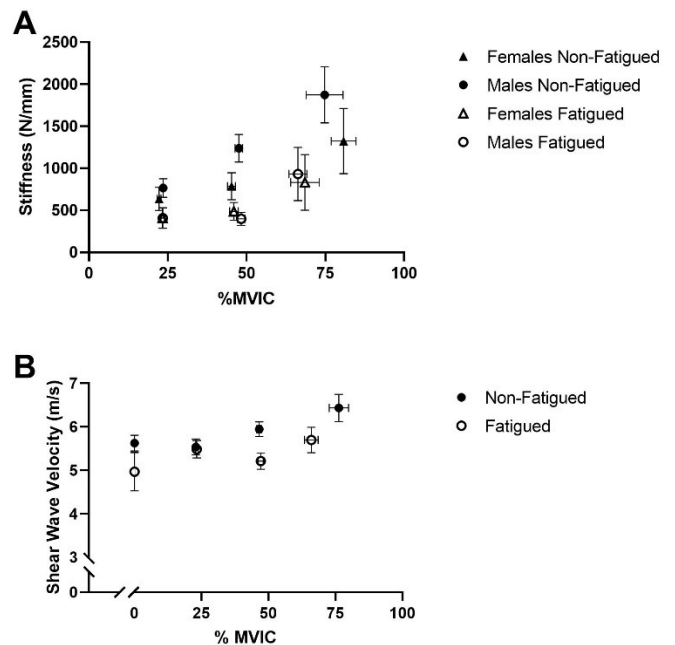
Figure 1. A) Effects of fatigue and sex on active PT stiffness measured via B-mode ultrasound. **B)** Effects of fatigue on passive and active PT shear wave velocity. Data reresented as mean ± SEM.

DESIGN OF A SINGLE-LEG EXOSKELETON WITH AUTOMATIC GAIT CONTROL FOR HEMIPLEGIC PATIENTS

Tara Zhan[1, 2], Lazar Jovanovic[2], Patrick Mayerhofer[2] and Max Donelan[2]
[1]David Thompson Secondary School, Vancouver, BC, Canada
[2]WearTech Labs, Simon Fraser University, Surrey, BC, Canada
email: tzhan0901@gmail.com

INTRODUCTION

As a student-athlete currently in high school, I have suffered several acute leg injuries that left me unable to walk for months. I understand how significantly losing the ability to walk normally affects quality of life. This, combined with my passion for engineering and medical technology, motivated me to build a solution for people who permanently experience the same struggles that I once had. Hemiplegia is a type of paralysis where one side of the body experiences a loss of motor function. Individuals with hemiplegia may be confined to walking devices or wheelchairs, which can lead to several health issues such as low bone mineral density and muscle atrophy [1]. Powered exoskeletons can help patients with severe hemiplegia regain the ability to walk and can relieve them from labour-intensive rehabilitation methods [2]. We present a proof-of-concept project showcasing an affordable single-leg exoskeleton design to aid individuals with hemiplegia. The exoskeleton offers full gait support and automatic hands-free control.

METHODS

I chose to only power the hip and knee joints to minimize the costs of the system. For the ankle joint, I used a passive orthosis. I aimed to achieve normal walking speeds ranging from 0.7 to 1.1 m/s. For the hip actuator, I used the T-Motor AK60 to produce a nominal torque of 42 Nm at 25 RPM. For the knee actuator, I used the T-Motor AK80 with a custom 2-stage roller chain gear transmission to produce a nominal torque of 38 Nm at 58 RPM. The roller chain transmission moved the motor closer to the wearer's centre of mass to reduce inertia. I built the exoskeleton on my own with limited equipment by ordering parts online and sourcing materials from local hardware stores. However, I had no way to build a suitable hip attachment to secure the exoskeleton to the body. For this, I reached out to WearTech Labs, who helped me design and 3D-print a custom form-fitted hip attachment to ensure efficient torque transmission in the hip joint. The prototype of our exoskeleton is shown in Figure 1.

I aimed to help users achieve symmetrical gait, with a high level of control and low cognitive load. This involved using gait data from the unimpaired leg to detect movement intent and use it as a signal for when to trigger the exoskeleton. I instrumented an insole using two force-sensing resistors (FSR) to measure the pressure under the heel and the ball of the foot on the unimpaired leg. I tracked the signals from the insole and an inertial measurement unit (IMU) installed on the hip to detect gait phase, and correspondingly start, keep, or stop the exoskeleton walking assistance. An example of the data for this is shown in Figure 2. The actuator rotation of the exoskeleton was modelled using the hip placed IMU as well as another IMU placed on the knee to mirror the movement of the unimpaired leg. Finally, I used a laser distance sensor to address safety. It was placed on the hip and pointed towards the ground at a 45° angle. I used the distance sensor to detect stairs, which halted the exoskeleton and allowed the user to traverse the stairs using the unimpaired leg. It does not yet provide actuated assistance for stairs. I conducted limited testing with a single able-bodied participant, who refrained from using the leg actuated by the exoskeleton. I considered the exoskeleton successful if it could 1) Correctly identify if the user wants to start, continue, or stop walking 2) Correctly identify stairs, and 3) Maintain a walking speed within 0.7-1.1 m/s.

RESULTS AND DISCUSSION

Figure 1: Front view of the built exoskeleton and the subject walking in the exoskeleton.

The total cost of the parts required to assemble the exoskeleton is around $3,000. It was successful in assisting the user in walking at a speed of 0.7 m/s. It identified the intent of the user with 100% accuracy, consisting of 30 instances over 10 trials. The exoskeleton identified stairs with 80% accuracy over 20 instances in 10 trials, where it recorded false positives 4 times due to other obstacles being falsely identified as stairs.
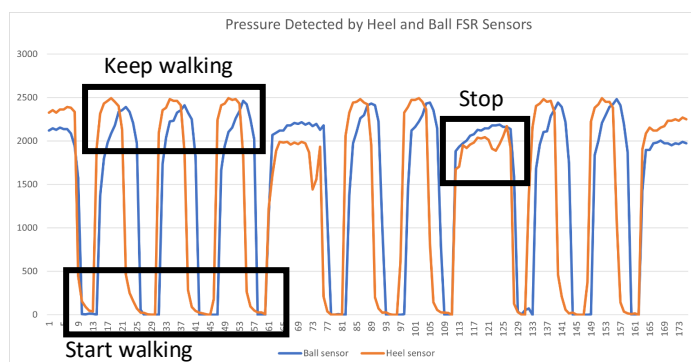

Figure 2: Graph of the pressure recorded by the FSR sensors while the user is walking and stopping periodically.

In future work, I hope to add more robust support for walking in different situations such as steep inclines and collect data from more participants. I would also like to implement fall detection so the actuated joints can provide compensation and reduce damage in a fall.

References

1. Paleg, G., et al. (2013). Systematic Review and Evidence-Based Clinical Recommendations for Dosing of Pediatric Supported Standing Programs. *Pediatric Physical Therapy*, *25*(3), 232–247.
2. Shi, D., et al. (2019). A Review on Lower Limb Rehabilitation Exoskeleton Robots. *CJME*, *32*(1).
3. Lewis, C. L., et al. (2015). Effect of posture on hip angles and moments during gait. *Manual Therapy*, *20*(1), 176–182.
4. Mentiplay, B. F., (2018). Lower limb angular velocity during walking at various speeds. *Gait & Posture*, *65*, 190–196.

AMPUTEE MOUSE FOR 2024 NORTHWEST BIOMECHANICS SYMPOSIUM

Figueroa, CA[1]; Rubio, CA[1]; Donatelli, CA[1]
[1]Robotics Lab, Fowler School of Engineering, Chapman University, Orange, CA USA
Emails: evfigueroa@chapman.edu, dirubio@chapman.edu, donatell@chapman.edu

INTRODUCTION

Upper limb amputees often face challenges in using conventional computer interfaces. Previous studies have attempted to address these challenges, but none have progressed to commercial development [1,2]. In this study, we present the design and evaluation of an enhanced mouse interface tailored specifically for upper limb amputees.

Our mouse design builds upon existing prototypes [3], addressing limitations identified in previous iterations. These limitations include a lack quick button clicking to allow for other applications such as gaming and calibration for user adjustment [1,2]. Central to our innovation is the integration of an efficient button system that facilitates intuitive and precise interaction.

This work provides a practical solution to the interface challenges faced by upper limb amputees. The enhanced mouse interface not only improves accessibility but also enhances the overall quality of interaction for this user population.

METHODS

We used existing mouse models constructed with Arduino-based components to inspire our design (**Fig. 1**), including an accelerometer and Arduino Leonardo board (Arduino, Italy), as the foundation for our enhanced mouse interface. Building upon these established frameworks [3], we focused on enhancing the clicking system to improve usability for upper limb amputees.

Central to our modification was the integration of the Adafruit Kailh Big Mechanical Key Switch (Adafruit Industries, LLC, USA), renowned for its tactile feedback and durability. We combined these tactile switches from Adafruit with 3D printed components to develop a novel "pedal system" for the clicking mechanism, enhancing the usability of the mouse interface for upper limb amputees. Additionally, we implemented a third button (**Fig. 1)** which can recalibrate the position of the mouse back to the center of the screen (**Fig. 2**). This allows the user to begin with their mouse at the center of the screen to suit any arm adjustment or fatigue.

The implementation of the tactile key switches involved careful integration into the mouse housing, ensuring optimal positioning and alignment for intuitive operation. The 3D-printed pedal system was designed to provide users with a comfortable and ergonomic interface for performing clicking actions, utilizing the tactile feedback of the key switches to enhance user experience.

RESULTS AND DISCUSSION

Overall, the results of our study indicate that the enhanced mouse interface offers a viable solution to the interface challenges faced by upper limb amputees. The combination of tactile key switches, 3D-printed pedal system, and cursor calibration functionality significantly improves usability and user satisfaction, paving the way for enhanced accessibility in computer interaction for this user population.
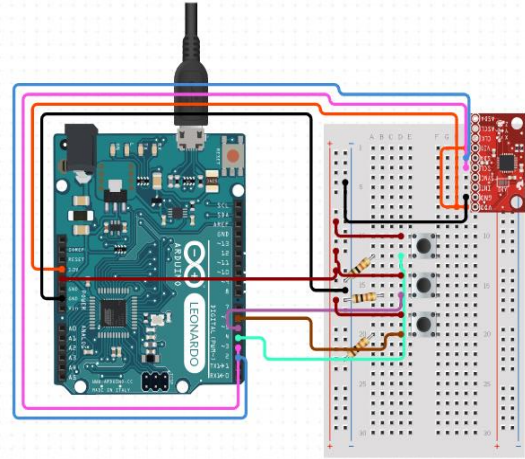

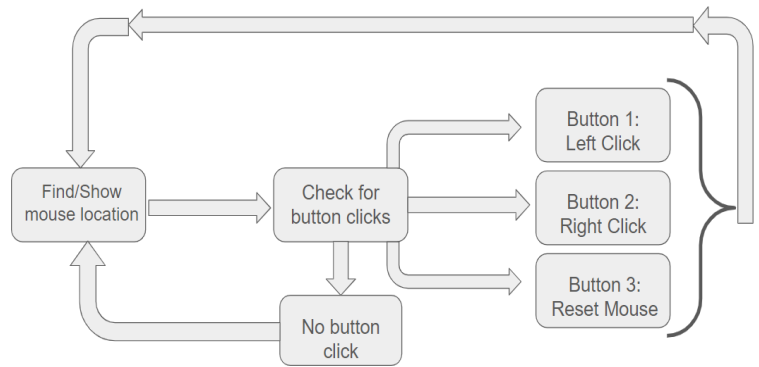**Figure 1**: Schematic of the Arduino Circuit

Figure 2: Code Diagram

CONCLUSIONS

The development of an enhanced mouse interface offers promising opportunities to enhance computer accessibility and user experience for upper limb amputees. By addressing previous limitations and incorporating efficient button systems, our device represents a significant advancement in biomechanics research with potential implications for prosthetic design and rehabilitation strategies.

REFERENCES

1. Sneiderman, P. "Upper-Limb Amputee at Johns Hopkins Builds Computer Controller Device for Feet." JH HUB, 2016, https://hub.jhu.edu/2016/06/23/gear-foot-video-game-controller/
2. Hassan, M., Shimizu, Y., Hada, Y., Suzuki, K., "Joy-Pros: A Gaming Prosthesis to Engage Para-Esports for Persons with Upper Limb Deficiencies. IEEE Access, v. 10, 2022
3. "Arduino – Accelerometer Mouse." Hobby Electronics, 13 Apr. 2017, www.mrhobbytronics.com/arduino-accelerometer-mouse/.

INFLUENCING HUMAN GAIT DYNAMICS WITH AN ADAPTIVE SPLIT-BELT TREADMILL

Jin, Z[1], Isa, JT[1], Burden, SA[1] and Ingraham, KA[1]

[1]Department of Electrical and Computer Engineering, University of Washington, Seattle, WA USA
email: zijiejin@uw.edu web: https://kim-ingraham.com/

INTRODUCTION

Walking on a split-belt treadmill, in which one belt moves faster and one belt moves slower, is a task that has commonly been used to study human locomotor adaptation and learning [1,2]. Recent studies have shown that walking on a split-belt treadmill can reduce the energy cost of walking—but only if the human learns to exploit this assistance by changing their gait pattern. The treadmill can produce net positive work to a human if they adopt a positive step length asymmetry (SLA), which is defined as the difference in step length between steps taken on the faster belt and those on the slower belt [3,4]. Previous studies have shown that humans require external guidance [3] and/or very long exposure times (> 30 minutes) to learn to adopt a positive SLA, but once they have learned this strategy, they can quickly converge to energetically efficient gaits. Previous studies have investigated how varying the split-belt ratio of the treadmill (the ratio of speeds between the faster and slower belts) might affect the SLA humans naturally choose [5], but so far these investigations have been limited to using a constant split-belt ratio. The overall goal of our work is to understand how humans adapt to walking on a split-belt treadmill with a continuously time-varying split-belt ratio. In this study, we designed an adaptive algorithm that dynamically adjusts the split-belt ratio as a function of the human's SLA, and we seek to understand how systematically varying the learning rate of the adaptive algorithm influences the human's gait.

METHODS

We completed a pilot study with three participants who had previous experience with this task. Participants walked on a split-belt treadmill at a fixed total belt speed (the sum of the belt speeds) of 2 m/s. We calculated the human's SLA in real time using the center of pressure measured from the force plates under each belt. The split-belt ratio time-varied according to the following update rule: $m_{i+1} = m_{i-1} - a * (m_i - h_i - 2)$, where m_i and h_i are the ith split-belt ratio (treadmill) and SLA (human), respectively, with a learning rate a that is empirically varied. When $a = 0$, the split-belt ratio is constant and fixed at 2 (the faster and slower belt speeds are 1.32 m/s and 0.67 m/s, respectively), which we consider the baseline condition for this experiment. Each participant performed five walking trials that lasted 200 seconds, each with a different learning rate (0, 0.1, 0.5, 0.7, and 1.0). The split-belt ratio was updated every three seconds, using the average SLA of the previous 3 steps. For each condition, we calculated the human's steady-state SLA as the average over the last 10 updates (30 seconds).

RESULTS AND DISCUSSION

Our initial observations indicate that the human's steady-state gait pattern may be changed as a result of the way the machine adapts. At the baseline fixed split-belt ratio of 2 ($a = 0$), across-participant mean (SD) steady-state SLA was 0.03 (0.08). During conditions with adaptive split-belt ratios ($a > 0$), mean steady-state SLA increased with learning rate, with a maximum of 0.09 (0.15) at $a = 0.7$. Despite overall increasing trends, participants' individual responses varied (Figure 1a). Different learning rates also resulted in differences in the steady-state split-belt ratio (Figure 1b). All participants were able to adopt a positive SLA at some learning rates, which means they were able to take advantage of the assistance from the treadmill. It is important to note that all participants had previous experience walking on a split-belt treadmill, which likely contributed to their ability to spontaneously adopt a positive SLA. As a next step, we will extend this pilot study to include more participants with a longer protocol, as well as include users without prior experience walking on split-belt treadmills.

Figure 1: Average steady-state **(a)** Human step length asymmetry (SLA) and **(b)** Split-belt ratio for three participants at different learning rates. Colored markers and error bars show mean and standard deviation over the last 10 updates (30 seconds) of each trial.

CONCLUSIONS

These pilot results demonstrate the potential of steering human SLA choices within a split-belt walking task using an adaptive split-belt ratio. These results provide further insight into human motor learning and how humans adapt to novel energy cost landscapes. This knowledge may guide the future development of control strategies and training protocols for assistive robots.

REFERENCES

[1] Malone et al. (2010), *J. Neurophysiol.* 103(4); [2] Leech et al. (2018), *Sci. Rep.* 8 (94); [3] Sánchez at al. (2019), *J. Physiol.* 597 (15); [4] Sánchez at al. (2021), *J. Neurophysiol.* 125(2); [5] Stenum et al. (2020), *J. Physiol.* 598(18)

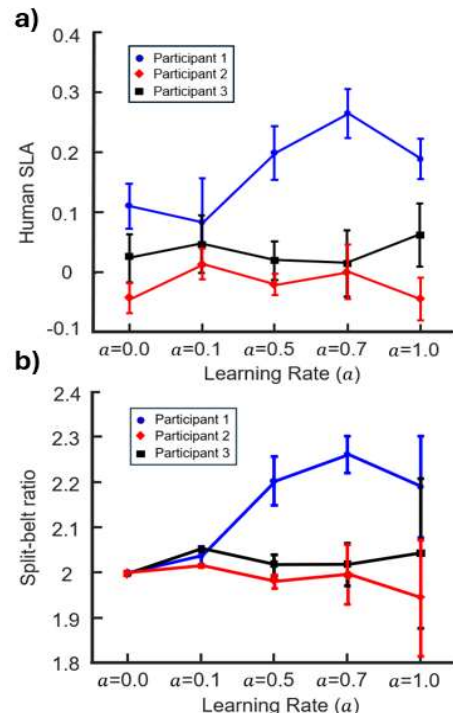# KNEE MUSCULATURE CO-ACTIVATION IS ALTERED BY PROLONGED LOAD CARRIAGE

Matthew V. Robinett[1], Samantha M. Krammer[1], Micah D. Drew[1], Tyler N. Brown[1]
[1]Boise State University, Department of Kinesiology, Boise , ID, USA
email: matthewrobinett@u.boisestate.edu

INTRODUCTION

Prolonged (> 60 minutes) walking with heavy load (> 15 kg) is common military task that contributes to a high rate of musculoskeletal injury by increasing lower limb joint moments and muscular activity, and stiffening the knee and ankle joints [1]. Yet, it is unknown if knee and ankle joint stiffness, and activity of the joint's musculature continually increase throughout prolonged load carriage. We hypothesize that knee and ankle joint stiffness, and muscle co-activation will increase with heavy load, and throughout the prolonged load carriage task.

METHODS

11 participants had lower limb neuromechanics quantified during an over-ground walk task with three body borne loads (0 kg, 15 kg, 30 kg). For the walk task, participants walked 1.3 m/s continuously for 60 minutes, and neuromechanics data (joint biomechanics and muscle activation) was recorded at minutes: 0, 15, 30, 45, and 60. At each time point, participants walked $1.3 \pm 5\%$ m/s through capture volume three times and contacted force platform with their dominant limb.

During each trial, synchronous 3D marker and force plate data were collected with 10 high-speed optical cameras (240 Hz) and single force platform (2400 Hz), while 4 surface electromyography electrodes (2400 Hz) recorded knee and ankle muscle activity. The marker and force plate data were low pass filtered (12 Hz, 4th order Butterworth) and processed in Visual 3D to calculate knee and ankle sagittal plane biomechanics. Then, knee and ankle torsional joint stiffness were calculated according to [3]. Dominant limb vastus lateralis (VL), tibialis anterior (TA), lateral hamstring (LH), and gastrocnemii (GAS) muscle activity were high-pass filtered (20 Hz; 4th order Butterworth) to remove motion artifact, and then, rectified and low pass filtered (10 Hz; 4th order Butterworth) to create a linear envelope. Filtered signal was normalized to corresponding MVICs, and then, VL:LH and TA:GAS co-activation were quantified according to [3] during pre-activity (100 ms prior to heel strike) and weight acceptance.

Knee and ankle joint stiffness, and VL:LH and TA:GAS co-activation were submitted to a repeated measures ANOVA to test the main effects and interactions between load (0, 15, and 30 kg) and time (0, 15, 30, 45, and 60 minutes). Alpha level was 0.05.

RESULTS AND DISCUSSION

Although knee and ankle joint stiffness reportedly increase up to 38% with body borne load [2], the current participants did not exhibit similar increases with load (both: p>0.05). Considering participants exhibited an insignificant 19% and 81% increase in knee and ankle joint stiffness with the addition of the heavy, 30 kg load, further work is needed to determine if

the lack of statistical significance can be attributed to insufficient sample size. Load, however, did impact VL:LH co-activation during weight acceptance (p=0.008), which increased 38% with the 30 kg compared to the 0 kg load. Interestingly, participants increased knee co-activation without a corresponding increase in knee joint stiffness during the loaded walking. Additional study is needed to determine whether participants can increase co-activation without constraining the joint flexion that would stiffen the joint.
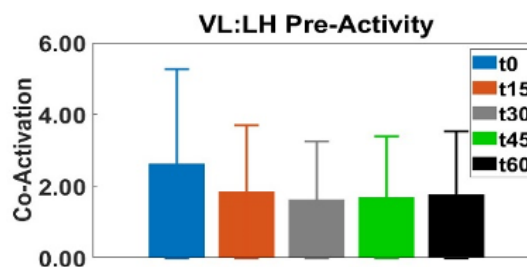

Figure 1: Depicts average VL:LH co-activation during the pre-activity phase at each time point.

Contrary to our hypothesis, time impacted VL:LH co-activation, but not joint stiffness. Both pre-activity and weight acceptance phase VL:LH co-activation decreased 41% and 55% at minute 60 compared to minute 0 (p=0.017; p=0.04, respectively; Fig. 1). The decrease in VL:LH co-activation may be attributed to reduced LH activation or shift to a quadricep-dominant strategy after prolonged walking with load. As such, the participants may be increasingly reliant on quadriceps activation throughout the task, which may elevate their injury susceptibility.

CONCLUSIONS

Individuals who perform physical activity with heavy body borne load may rely on their knee extensors to attenuate the increased impact forces and prevent limb collapse. But, prolonged physical activity with load may increase this reliance, and military practitioners may need to incorporate hamstrings training into injury prevention or training programs to reduce fatigue-related injury exacerbated by a body borne load.

REFERENCES

1. Santos T, et al. *JAB* **37**, 373-379, 2021.
2. Brown TN, et al. *JAB* **37**, 95-101, 2021.
3. Don R, et al. *Clin Biomech*, **22**, 905-916, 2007.

ACKNOWLEDGEMENTS

SEATED INFANT PRODUCTS ALTER BODY POSITION AND MUSCLE UTILIZATION

Siegel[1], Goldrod[2], Olvera[1], Bossert[2], Wilson[2], Lujan[2], Whitaker[3], Carroll[3], Mannen[1,2]
[1]Biomedical Engineering Doctoral Program, Boise State University, Boise, ID USA [2]Mechanical & Biomedical Engineering
Department, Boise State University, Boise, ID USA [3]Arkansas Children's Research Institute, Little Rock, AR USA
email: hollyolvera@u.boisestate.edu

INTRODUCTION

The musculoskeletal and motor development of infants is greatly affected by their environment [1], which varies from being held in arms, lying on a firm flat surface, to spending time in various nursery products. In the U.S., infants spend an average of 5.7 hours (range 0-16 hours) per day in seated products like car seats used outside of a motor vehicle (infant carrier), bouncers, rockers, and swings [2,3]. Excessive time in car seats has been shown to alter an infant's development and muscle utilization [4-7]. In addition, increased suffocation-related hazards exist while lying in inclined products due to the changes in body position [8,9]. While many different injuries can occur involving seated products, infants zero to six months are more likely to suffer breathing-related injuries caused by suffocation compared to older children [10]. Because of the design features present in seated products, infants may be forced into higher head-neck flexion and a slouched position, increasing their risk for a breathing-related incident. The purpose of this study was to assess how an infant's muscle activation and body position are altered while lying supine in four commercial infant products (carrier, bouncer, rocker, and swing) compared to a firm flat playmat.

METHODS

Thirteen healthy infants (4.2±1.4 mos; 7M/6F) participated in this IRB-approved study. Surface EMG electrodes (Delsys, 2000Hz) recorded muscle activity from the cervical paraspinals (CP), erector spinae (ES), abdominal muscles (AB), and quadriceps (QUAD) (**Fig. 1A**). A retroreflective marker-based motion capture system (Qualisys, 100Hz) tracked infant kinematics using custom 3-marker (6.5mm) rigid body clusters on the head, torso, and pelvis and 9.5mm markers on the shoulders and anterior superior iliac spine (ASIS) (**Fig. 1A**). Infants laid supine for three minutes on a firm flat playmat (**Fig. 1B**) and unrestrained in a commercial infant carrier, bouncer, rocker and swing (**Fig. 1C**).
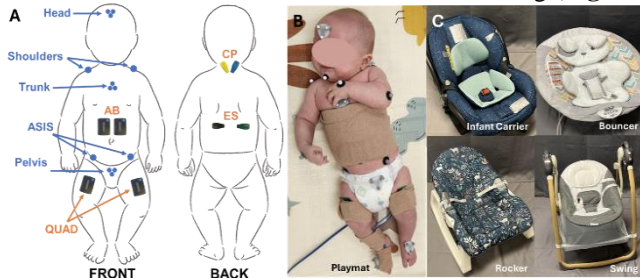

Figure 1: (A) EMG and motion capture marker placement, (B) experimental setup on playmat, and (C) four seated products.

The EMG signal was filtered, and the mean was taken over 60 seconds for each condition and muscle group, then normalized as a percent of the playmat. The head-neck and torso-pelvis flexion was calculated using the angular orientation between adjacent body segments from the local coordinate systems defined by rigid body clusters on each segment when the head, torso, and pelvis were visually aligned in the sagittal plane. Trunk flexion was determined using the law of cosines between the shoulder and ASIS markers. All angles were normalized to the playmat condition to account for each infant's anatomical differences. All calculations were completed in MATLAB. Paired t-tests ($p < 0.05$) compared the four products to the playmat in SPSS.

RESULTS AND DISCUSSION

In all products tested, infants exhibited increased head-neck and torso flexion of up to 21° and 27° above the playmat, respectively (**Fig. 2**). Previous research determined that head-neck flexion angles of just 15° to 30° can alter infant breathing patterns significantly [11]. Trunk flexion was significantly higher for all products (between 23° and 27° on average) compared to the playmat which relates to the conformity and/or concavity of the product longitudinally. For most products, infants exhibited higher abdominal muscle activity, which may indicate that infants use their diaphragmatic muscles at a higher level to overcome breathing challenges related to the flexed posture [12,13].
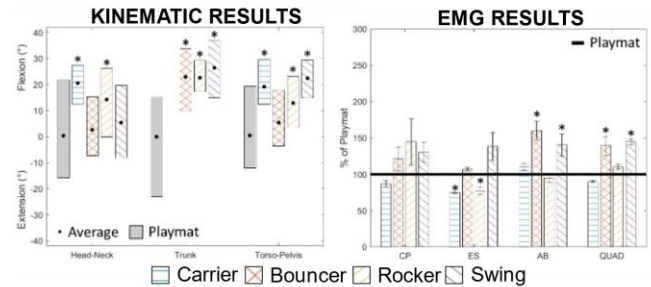

Figure 2: Kinematic results (left-mean, min, and max) and EMG results (right-mean± stdev). *$p < 0.05$ compared to the playmat.

CONCLUSIONS

This research quantified body posture and muscle activity of infants lying in a variety of seated products, suggesting that to prevent respiratory-related hazards and musculoskeletal or motor developmental delays, prolonged use should be avoided.

REFERENCES

1. Hadders-Algra 2018, *Neuro & Bio Revs* 2. Little 2019, *Inf Beh & Dev* 3. Callahan 1997, *Arc Peds & Ado Med* 4. Littlefield 2003, *JOP J Prosth & Orthot* 5. Pin 2007, *Dev Med & Child Neuro* 6. Jiang 2016, *Ped Phys Ther* 7. Siddicky 2020, *J Biomech* 8. Mannen 2019, *U.S. CPSC Report* 9. Wang 2020, *J Biomech* 10. Gaw 2017, *Peds* 11. Wilson 1980, *J Appl Physio* 12. Lee 2010, *Resp Phys & Neurobio* 13. Lin 2006, *Arch Phys Med & Rehab*.

ACKNOWLEDGEMENTS

COMPARISON OF SEX-BASED BIOMECHANICAL MODELS TO A DEFAULT MODEL

Abigail R. Brittain[1] and Tyler N. Brown[2]
[1]Biomedical Engineering PhD Program, [2]Boise State University, Boise, Idaho
email: abbybrittain@boisestate.edu

INTRODUCTION

Joint kinetic analysis is dependent on the accuracy of link-segment models, which, rely upon segment anthropometric parameters, including segment center of mass, moments of inertia, and geometry. Visual 3D is a biomechanics software commonly used for kinetic analysis that uses segment anthropometric parameters that do not account for sex variation in their link-segment model, potentially producing inaccurate kinetic analyses. It is unknown if using models that include sex-specific segment properties alters joint kinetic output. We hypothesized that a sex-based biomechanical model would produce significant alterations in knee joint kinetics compared to a default Visual 3D model for both male and females, but larger alterations would be observed for females.

METHODS

14 female and 17 male had 3D lower-limb biomechanics quantified while running (4 m/s ± 5%) with 4 body borne loads (20, 25, 30, and 35 kg). Three (default, male, and female) lower limb link-segment models consisting of 7 segments and 24 DOFs were created in Visual 3D. The default model was built as described in [1]. Each sex-specific model had segment mass, mass moment of inertia, center of mass, and geometry modified using male and female anthropometrics published in [2]. Kinematic and GRF data recorded during each run trial were filtered (fourthorder, low-pass Butterworth filter at 12 Hz), and processed in Visual 3D using standard inverse dynamics analysis to obtain dominant limb stance phase (heel strike to toe off) knee joint kinetics with each model. Knee joint kinetics were normalized to participant mass. Peak knee flexion, abduction, and internal rotation joint moments, and anterior knee joint reaction force were submitted to a two-way (load*model) repeated measures ANOVA, and the corresponding waveforms were submitted to a statistical parametric mapping (SPM) two-way repeated measures ANOVA. Males and females were analyzed separately, and alpha was $p < 0.05$.

RESULTS AND DISCUSSION

In agreement with our hypothesis, both male and female sex-based models produced significant alterations in peak and waveform knee joint kinetics compared to the default Visual 3D model. For females, there were significant load by model interaction for peak anterior (p=0.038) knee joint reaction force.

Significant main effects of model were only seen for females. The current default model may underestimate female knee joint kinetics, as both peak knee flexion (p<0.001) and abduction (p<0.001) moments were greater for the female-based model than the default model. Unexpectedly, adding body borne load only increased peak knee abduction moment (males: p=0.016, females: p=0.01) and anterior knee joint reaction force (both: p=0.003). Females exhibited greater peak knee abduction moment with 25kg and 30kg than 20kg load (p=0.002; p=0.011), while males exhibited greater knee abduction moment with the 35kg compared to 30kg (p=0.009) and 20kg (p=0.006) loads. Both sexes exhibited greater anterior knee joint reaction force with the 35kg than the 20kg (p=0.015; p=0.003) and 25kg (p=0.007; p=0.002) loads, but the males also exhibited greater reaction force with the 30kg than the 20kg (p=0.003) load. Both the male and female-based model impacted each knee joint kinetic waveform (Fig. 1). For knee flexion moment, the female-based model significantly differed from default between 0-7%, 26-53%, and 70-100% of stance (p<0.033), and the male-based model differed between 0-8% and 93-100% of stance (p<0.029). For knee abduction moment, the female-based model significantly differed from default between 0-15%, 20-29%, and 34-96% of stance (p<0.024), while the male-based model differed between 84-94% (p=0.015) of stance. For knee internal rotation moments, the female-based model significantly differed from default between 5-15%, 20-32%, 53-59%, and 68-100% (p<0.034), of stance, and the male-based model differed between 13-15% and 81-92% (p<0.048) of stance.

CONCLUSIONS

The current findings support the need for sex-based biomechanical models in research. Updating the link-segment model with sex-specific anthropometric measures led to significant alterations in knee joint kinetics.

REFERENCES

[1] Brown et al. (2018), *J Biomech* 69; [2] Dumas et al., (2007), *J Biomech* 40; [3] https://spm1d.org/
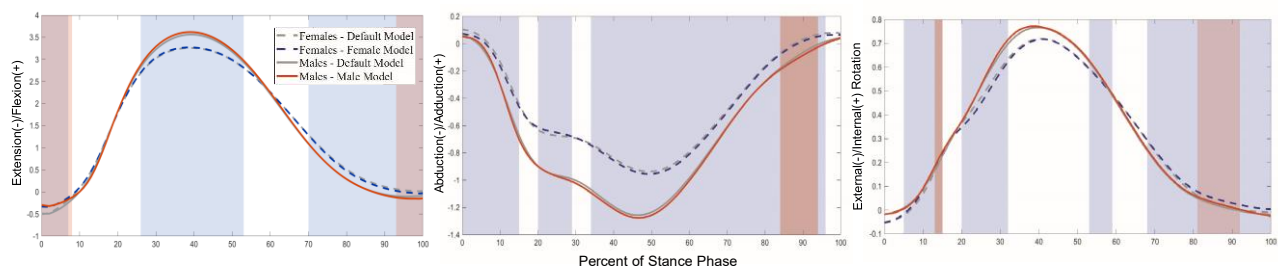
ACKNOWLEDGEMENTS

Figure 1: Knee Joint Moments Compared Between Models. Means are represented with a dashed-line (females) and a solid line (males), and shaded regions refer to significant differences found with SPM analysis, blue (females) and orange (males).

USING OPENCAP TO ASSESS SINGLE- AND DUAL-TASK SINGLE LEG VERTICAL JUMP PERFORMANCE

Fatemeh Aflatounian[1], Kaylan Wait[1], Brendan Silvia[1], Alexandra C. Lynch[1], James N. Becker[1], Keith A. Hutchison[1], Janet E. Simon[2], Dustin R. Grooms[2], and Scott M. Monfort[1]
[1]Montana State University, Bozeman, Montana, USA, [2]Ohio University, Athens, Ohio, USA
email: fatemehaflatounian@montana.edu, web: https://www.montana.edu/biomechanics/index.html

INTRODUCTION

Single-leg vertical jump (SLVJ) assesses upward jumping ability, emphasizing knee extensor power, particularly relevant to identifying altered function following an anterior cruciate ligament (ACL) reconstruction [1]. ACL injuries often happen during sports when visual attention is externally focused; however, common clinical assessments often neglect cognitive-motor deficits that lead to riskier movements [2]. Dual-task screening simultaneously tests cognitive and motor skills, aiding in identifying such deficits [3]. However, traditional motion analysis is costly and time consuming for data collection and processing [4]. OpenCap enhances clinical accessibility to full-body kinematics by using iOS devices and automated cloud processing, reducing both cost and time burden [4]. The purpose of this study was to demonstrate the ability of a clinically-feasible approach (i.e., OpenCap) to reflect similar kinematics obtained by standard marker-based motion capture during single- and dual-task SLVJ. Given OpenCap's success in capturing sagittal plane kinematics in other jumping movements, we hypothesized strong correlations between OpenCap and marker-based outcomes.
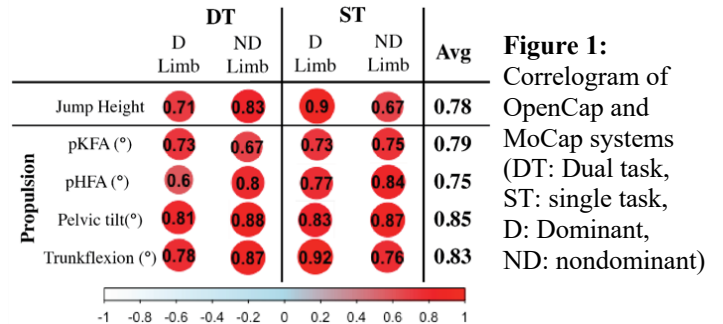
METHODS

10 healthy athletes (5F/5M, 19.8±2.3 yrs; 1.66±0.18 m; 67.8±11.0 kg; Tegner: 7.5±1.3; Marx: 10.6±3.6) completed the SLVJ task. Participants performed the SLVJ under both single-task (ST) and dual-task (DT) conditions on both limbs, with three trials each. DT involved two peripheral lights (FITLIGHT Sports Corp) for Go/No-Go cues and one overhead light for a memory task, adapted from a visual-cognitive triple hop [5]. Participants awaited a pre-defined 'Go' color on one of the peripheral lights before performing the SLVJ, focusing on the overhead light to recall three rapidly displayed colors. Full-body kinematics were simultaneously captured using both a marker-based motion capture system (MoCap) (10 cameras, Motion Analysis Corp; 5 AMTI force plates) and OpenCap with two iOS devices. MoCap data were processed in Visual3D using an inverse kinematics model [6], while OpenCap data were processed using the automated cloud processing within the OpenCap workflow. Kinematic trajectories from both methods were analysed in MATLAB to extract jump height and peak trunk, hip (pHFA), and knee flexion angle (pKFA), and pelvis tilt during the propulsive phase (from 0.4 sec before leaving the force plate until toe off) [1]. Toe-off was defined using force plate data for MoCap and when the pelvis vertical position exceeded a 5% increase from the standing position for the OpenCap data. Pearson correlations (or Spearman if data were not normally distributed) were used to compare outcomes between two approaches, with $p < 0.05$ indicating statistical significance.

RESULTS AND DISCUSSION

There were strong correlations between MoCap and OpenCap values for both ST and DT variables jump height and joint kinematics during the propulsion phase of SLVJ (r = 0.6 to 0.92,

$p = 0.05$ to <0.001, Figure 1). These results demonstrate a strong ability for OpenCap to capture trends in SLVJ outcomes (e.g., the individuals with higher jump height or joint flexion measured via MoCap were also identified with OpenCap). It is worth noting that these strong correlations were obtained after omitting OpenCap trials with unrealistic pose estimation from the automated OpenCap cloud processing. Out of the 120 good (i.e., hands remained on hips, clean landing, reacting to correct color for DT) trials collected, 10 were later omitted due to unrealistic OpenCap pose estimations. Opportunities to further enhance the ability to leverage OpenCap to assess SLVJ performance and minimize dropped trials include optimizing the number and position of the cameras for this movement as well as improving the color contrast between participants and their environment. Additional opportunities to refine the analyses pipeline to more robustly extract the variables with minimal manual effort also exists. In general, OpenCap captured essential variables related to ACL injuries during SLVJ, which has potential as a useful tool for clinicians. However, there is a still need for future studies with larger cohorts, including individuals with ACL reconstruction, and to streamline the workflow to optimize clinical feasibility.

	DT		ST			
	D Limb	ND Limb	D Limb	ND Limb	Avg	
Jump Height	0.71	0.83	0.9	0.67	0.78	
pKFA (°)	0.73	0.67	0.73	0.75	0.79	
pHFA (°)	0.6	0.8	0.77	0.84	0.75	
Pelvic tilt(°)	0.81	0.88	0.83	0.87	0.85	
Trunkflexion (°)	0.78	0.87	0.92	0.76	0.83	

−1 −0.8 −0.6 −0.4 −0.2 0 0.2 0.4 0.6 0.8 1

Figure 1: Correlogram of OpenCap and MoCap systems (DT: Dual task, ST: single task, D: Dominant, ND: nondominant)

CONCLUSIONS

Improving clinicians' access to high resolution, joint-level kinematics during return-to-sport tasks may provide a more comprehensive approach for clinicians to evaluate the readiness of their patients to return to sport. In this study, OpenCap strongly correlated with key kinematic outcomes across multiple joints during single- and dual-task SLVJ. Future efforts using this clinically-feasible approach to collect these data and relate to patient outcomes are needed to demonstrate the clinical relevance of these data.

REFERENCES

1. Kotsifaki et. al. (2022) *Br J Sports Med* 56(9): 490-498
2. Vargas et. al. (2023) *IJSPT* 18(1): 122-131
3. Monfort et. al. (2019) *Am J Sports Med* 47(6):1488–1495
4. Uhlrich et. al. (2023) *PLoS Comput Biol* 19(10): e1011462
5. Farraye et. al. (2023) *J Sport Rehabil* 32(7): 802-809
6. Fischer et al. (2021) *J Applied Biomech* 37(4)

ACKNOWLEDGEMENTS

A COMPARISON OF MUSCLE RECRUITMENT PATTERNS
BETWEEN RECREATIONAL DANCERS AND NON-DANCERS IN DROP JUMP LANDINGS

Burr, B[1,3], Pollard, CD[2,3], Hannigan, JJ[2,3] and Phillips, D[1,3]
Program in [1]Kinesiology and [2]Physical Therapy, Oregon State University-Cascades, Bend, OR USA
[3]School of Exercise, Sport, and Health Sciences, Oregon State University, Corvallis, Oregon, USA
email: burrbe@oregonstate.edu

INTRODUCTION

Lower extremity injuries are common across a range of athletic activities. For example, anterior cruciate ligament (ACL) tears, a commonly occurring knee injury, impact over 200,000 people each year in the United States [1]. Understanding the muscle recruitment patterns leading to lower-risk jump landings could allow us to adapt and modify training protocols in a way that may alleviate risk-related techniques among athletes, such as those impacted by ACL injury.

Jumping is a common mechanism used in dance. Past research has shown that experienced dancers have lower incidences of ACL injury than athletes in other jump-landing sports, and they also demonstrate safer landing techniques during single-leg drop jump landings, including increased gluteus maximus activation, decreased knee valgus, decreased ankle eversion, and increased ankle dorsiflexion [2, 3]. In this study, we looked at whether there is a difference among the lower extremity muscle recruitment patterns of recreational dancers compared to non-dancers, as a variation in muscle activation patterns and timing could underly some of the differences we see in overall landing kinematics.

METHODS

Twenty healthy females (age 30.1 ± 8.2 years, height 167.7 ± 6.8 cm, mass 68.8 ± 9.1 kg), including 10 recreational dancers and 10 non-dancers were included in this study. Recreational dancers were recruited from a pool of members and instructors at a local dance fitness studio, and for the purposes of this study, are defined as those participating in dance as a regular part of their exercise routine.

10 drop jump trials for each participant were used for analysis. Kinetic and kinematic data was collected using a Qualysis 10-camera, 3D motion capture system (Qualysis AB. Göteborg, Sweden). Muscle activation data was collected synchronously using nine wireless surface electromyography (EMG) sensors on the lower extremity at 2,000 Hz (Trigno Sensor System, Delsys Inc., Natick, MA, USA). EMG sensors were placed over the following muscles: gluteus medius, gluteus maximus, semitendinosus, biceps femoris, rectus femoris, vastus medialis, medial and lateral gastrocnemius, and the tibialis anterior.

EMG signals were normalized as a percentage of peak muscle activation. A 2x5 mixed effects analysis of variance (ANOVA) was used for analysis, with time points evenly distributed between contact and 200 milliseconds prior to landing ($\alpha = 0.05$).

RESULTS AND DISCUSSION

No significant differences were found between measures in eight of the EMG sensors, although a trend was demonstrated in the medial gastrocnemius ($p = 0.081$).

In the biceps femoris, a significant interaction effect was found between the dancer and non-dancer groups for pre-activation signals ($p = 0.05$), with significant differences at 100 ms and 50 ms prior to initial contact ($p < 0.05$, Figure 1).
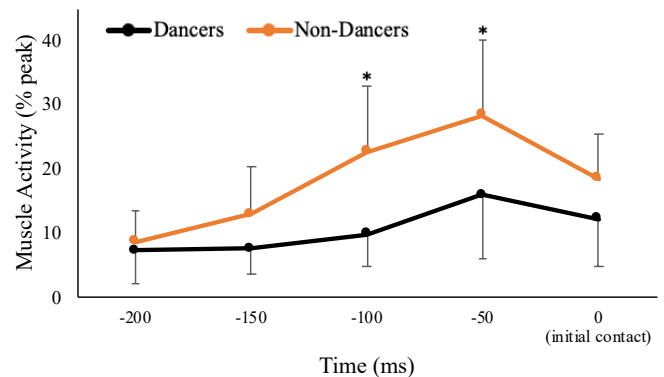

Figure 1: Pre-activation of the biceps femoris.
 * indicates significant difference ($p < 0.05$)

CONCLUSIONS

Although other muscle recruitment patterns in the lower extremity were similar, there was a significant difference in the pre-activation muscle recruitment of the biceps femoris between dancers and non-dancers, indicating that the biceps femoris may play a part in the safer landing techniques used by dancers.

Hamstring activation has been shown to be a protective mechanism at the knee, particularly in terms of the biceps femoris reducing load at the ACL [4]. While overall muscle activation was lower in the dancer group, a visual analysis of the data shows a steeper decline in the non-dancer group just prior to contact. As this study looked particularly at pre-activation, further research into muscle coordination post-contact may provide a clearer picture as to how these differences in muscle activity impact the mechanics at contact and throughout the loading phase.

While the exact link between the recruitment patterns of the biceps femoris muscle in connection with safer landing patterns has yet to be determined, these notable findings open up an avenue for further study surrounding the potential ability to use dance techniques – such as repetitive jumping, training neuromuscular control, or improving balance – in order to develop muscle coordination patterns that may reduce risk of injury.

REFERENCES

1. Musahl, V & Karlsson, J. *N Engl J Med* **380**, 2341–48, 2019.
2. Hansberger, BL, et al. *J Athl Train* **53,** 379-85**,** 2018.
3. Turner, C, et al. *Phys Ther Sport*, **31**, 1-8, 2018.
4. Biscarini A, et al. *Eur J Appl Physiol*, **113,** 2263-2273, 2013.

DIFFERENCES IN MECHANICAL EFFICIENCY BETWEEN PIN AND FREERIDE BINDINGS

Westling, G., Burgess, I., Samuels, S., Seifert, J., Becker, J.
Department of Human Food Systems, Nutrition, and Kinesiology, Montana State University, Bozeman MT
email: garrett.westling88@gmail.com web: montana.edu/biomechanics

INTRODUCTION

Backcountry ski touring is one of the fastest growing segments of the skiing industry. Participants generally have the choice of two types of bindings, pin (P) or freeride (FR) bindings. While P bindings are lighter, they lack safety features like DIN settings or forefoot release incorporated in FR bindings. The weight difference may be particularly important as backcountry ski equipment should increase uphill travel efficiency through decreasing mechanical work required to maintain high outputs of metabolic work in the presence of fatigue. While previous studies have examined the physiological response to mass added at the ankle during uphill skinning, no studies have evaluated the physiological response to specific equipment [1]. Therefore, the purpose of this study was to compare mechanical efficiency (ME) between P and FR bindings while skinning uphill at different grades.

METHODS

Ten healthy participants (age:21 ± 1.49, height:$1.8m\pm1.49$, mass:$76kg\pm7.25$) participated in this study. A VO2 max protocol specifically designed for uphill walking was used to determine the relationship between heart rate VO2 and RER with increasing workload [2]. This relationship was used to determine the relative VO2 while skinning uphill on a ski treadmill at two grades (8 and 15%), speeds (0.62 and 1.12 m/s), and using either P or FR bindings. The two speeds were chosen so results could be compared based on matched speeds, as has been done previously [3] or matched relative intensities (i.e. slower speeds up a steeper grade should have the same metabolic cost). For all conditions metabolic work (MW) was calculated based on the VO2 and RER. Vertical work (VW) was calculated as the product of mass, gravity, sine of the slope, and treadmill velocity. Finally, ME was determined as the ratio of mechanical work to metabolic work. Differences in VW, MW, and ME across bindings and grades were evaluated using 2x2 repeated measures ANOVAs.

RESULTS AND DISCUSSION

Mean and standard deviations for VW, MW, and ME under all conditions are shown in Table 1. VW showed a main effect of grade for both matched speeds ($p < .001$) and matched relative intensities ($p < .001$). This difference at matched relative intensities was unexpected and was likely due to the inability to perfectly set the velocity on the treadmill given the resolution of available speed increments.

At matched speeds MW showed main effects of grade ($p < .009$) with more MW at 15% and a trend toward a main effect of binding ($p = .089$) with greater MW in the FR binding. Similar results were observed at matched intensities, with MW being greater at 15% ($p = .003$) and trending towards being greater in the FR binding ($p = .07$). Finally, at matched speeds participants showed greater ME at higher grades ($p < .001$). However, at matched relative intensities participants had greater ME both at higher grades ($p = .005$) and with P bindings ($p = .036$).

These differences in ME between bindings are consistent with previous studies which added mass to the ankle [1]. These results should be replicated in on-snow conditions to further clarify how binding design influences ME in real world environments.

CONCLUSIONS

When evaluated at similar relative intensities, ME in P binding is greater than FR bindings.

REFERENCES

1. Tosi, P. et al. *J Sports Med Phys Fitness.* **49**, 25-29, 2009.
2. Aadland, E. et al. *Scand J Med Sci Sports.* **27**, 1248-1257, 2017.
3. Lasshofer, M. et al. *Front Sports Act Living.* **4**, 886025, 202

Table 1. Mean and standard deviations for matched speeds and intensities at 8% and 15% grade.

	8% – 1.11m/s			15% – 1.11m/s			15%– 0.62m/s	
	Pin	Freeride		Pin	Freeride		Pin	Freeride
Vertical work (J)	74.1 ± 5.7	74.5 ± 5.6		138.0 ± 10.7	138.7 ± 10.4		77.2 ± 6.0	77.7 ± 5.9
Metabolic work (W)	1098.4 ± 196.9	1158.6 ± 177.0		1345.9 ± 250.1	1362.4 ± 216.6		871.0 ± 216.9	979.0 ± 131.2
Mechanical efficiency (%)	7.0 ± 1.3	6.5 ± 1.1		10.5 ± 1.9	10.4 ± 1.8		9.4 ± 2.7	8.7 ± 1.9

GROUND REACTION FORCE DIFFERENCES BETWEEN INDOOR AND OUTDOOR SURFACES DURING INCLINE AND DECLINE RUNNING

Anand, A[1], Robinson, R[1], Hahn, M[1]

[1]Neuromechanics Laboratory, Department of Human Physiology, University of Oregon

Email: aanand@uoregon.edu

INTRODUCTION

Previous studies have evaluated the effects of graded running on ground reaction force (GRF) using an instrumented treadmill [1]. While differences in running biomechanics have been observed between treadmill and outdoor running on level ground, it is unknown whether graded treadmill running is representative of outdoor graded running [2]. Force-sensing insoles measuring normal forces between the foot and shoe are reliable sensors that allow for the measurement of GRF parameters outside of the lab [3]. Using these sensors, a biomechanical comparison can be made between laboratory and real-world outdoor running settings. Evaluating the differences between settings could inform future data collection methodologies and application of clinical gait analyses. Therefore, the purpose of this study was to determine whether GRF variables measured during graded treadmill running are representative of graded outdoor running. It was hypothesized that the surfaces would yield similar GRF data.

METHODS

Institutional Review Board approval was obtained prior to data collection and all participants provided informed consent. Seven healthy recreational runners (age: 21, height: 172 cm, mass: 64 kg) completed a 5-mile outdoor run which included a paved 7.5° uphill and downhill section. Each runner was equipped with a GPS watch (Garmin, Olathe, KS, USA) and force-sensing insoles (Novel, St. Paul, MN, USA). GPS data were collected at 1 Hz, and force-sensing insole data were collected at 100 Hz. All runs were performed at a self-selected pace. The same participants performed 30s running trials on a 7.5° inclined and declined treadmill at three different speeds (0:30 min/mile, 1:00/mile, and 1:30/mile slower than their self-reported 5k pace).

Custom MATLAB programs were used for analysis. GPS data were utilized to identify sections of the course where participants ran up and down a 7.5° grade. While speeds varied between participants, the indoor and outdoor speeds differed by <0.2 m/s within each participant. The peak normal GRF (pGRF), average normal GRF, normal impulse (IMP), and normal average loading rate (ALR) were calculated for each right footstep. The IMP was calculated as the time integral of GRF. The ALR was calculated as the average slope of the middle 60% of GRF from initial contact to impact peak. The mean and standard deviation of pGRF, ALR, average force, and IMP were calculated for 10 steps of inclined and declined running for indoor and outdoor conditions. Paired t-tests were used to determine whether GRF variables differed between surfaces ($p < 0.05$).

RESULTS AND DISCUSSION

For incline running, the average outdoor speed was 3.33 ± 0.45 m/s, and the average indoor speed was 3.61 ± 0.34 m/s ($p > 0.05$). For decline running, the average outdoor speed was 3.52 ± 0.52 m/s, and the average indoor speed was 3.44 ± 0.43 m/s ($p > 0.05$). Average GRF, IMP, and ALR during incline and decline running were not significantly different between indoor and outdoor conditions ($p > 0.05$, Table 1). While pGRF was not different between conditions for incline running, pGRF was significantly higher in the outdoor condition for decline running ($p = 0.03$). These results suggest that biomechanics of graded running are similar between overground and treadmill surfaces, consistent with previous lab-based studies [4]. Because speed was not controlled for in the outdoor run, some participants' indoor and outdoor running speeds did not match exactly. While indoor and outdoor speeds were not significantly different, the slightly faster outdoor decline running speed may explain the higher pGRF compared to indoor running. To identify further differences in indoor and outdoor running mechanics, future studies should evaluate differences between these two settings using loading parameters derived from inertial measurement units.

CONCLUSIONS

The only GRF variable that differed between indoor and outdoor running during this investigation was downhill peak GRF. While other biomechanical variables may change in response to the running setting, these findings indicate that GRF variables stay relatively consistent. From these findings, it appears that graded treadmill running is comparable to outdoor graded running, as the two settings yield relatively similar GRF data, with some caution recommended in the interpretation of downhill running data.

REFERENCES

[1] Honert et al., *Sensors*, 2022, 22(9)
[2] Lafferty et al., *Sports Health*, 2022, 14(5)
[3] Renner et al., *Sensors*, 2019, 19(2)
[4] Firminger et al., *Gait Posture*, 2018, 63(109-113)

ACKNOWLEDGEMENTS

Table 1: GRF variables for indoor and outdoor graded running. *significantly different from indoor ($p < 0.05$)

Grade Direction	Running Surface	Average Speed (m/s)	Peak Vertical GRF (BW)	Average Loading Rate (BW/s)	Average Vertical GRF (BW)	Vertical Impulse (BW*s)
Incline	Indoor	3.61 ± 0.34	2.14 ± 0.30	28.48 ± 6.19	1.23 ± 0.14	0.36 ± 0.05
	Outdoor	3.33 ± 0.45	2.26 ± 0.10	30.45 ± 4.03	1.29 ± 0.09	0.33 ± 0.04
Decline	Indoor	3.44 ± 0.43	2.35 ± 0.23	63.23 ± 16.96	1.39 ± 0.11	0.36 ± 0.04
	Outdoor	3.52 ± 0.52	2.54 ± 0.24*	66.47 ± 14.30	1.40 ± 0.12	0.36 ± 0.02

ASYMMETRY CHANGES DURING DISTANCE RUNNING IN RECREATIONAL RUNNERS

Smith, K[1], Denton, AN[1,2], Robinson, RM[1] and Hahn, ME[1]
[1]Bowerman Sports Science Center, Department of Human Physiology, University of Oregon, Eugene, OR USA
[2]Knight Campus for Accelerating Scientific Impact, University of Oregon, Eugene, Oregon, USA
email: ksmith32@uoregon.edu

INTRODUCTION

Despite widespread participation in running worldwide, it is not well-known how the symmetry of running mechanics change with the onset of fatigue as a run progresses. Symmetry in athletics is when there is the same shape, size, and form on both sides of a given axis, whereas bilateral asymmetry indicates a difference between the two sides of the axis [1]. As fatigue increases, running mechanics change and result in an elevated metabolic energy cost, which in turn causes a decrease in mechanical efficiency [2]. Since symmetry is thought to contribute to mechanical efficiency [3], it follows that a decrease in mechanical efficiency would be associated with an increase in asymmetry. A majority of running studies have been completed indoors despite known differences between outdoor and indoor running [4]. Understanding changes in running mechanics throughout the duration of a run in the natural running environment can provide useful insight into running technique and injury prevention. The purpose of this study was to determine how asymmetry changes between the right and left foot peak accelerations and at the sacrum, throughout an outdoor long run.

METHODS

A total of 24 training runs from 8 participants (3M/5F) were analyzed. All participants were recreationally trained, running a minimum of 10 miles/week, and participating in a half marathon or marathon training program. Participants ran a self-selected route and distance (13.7±4.5 miles) at a self-selected pace (9:24±0.05 min/mile). Data were collected using inertial measurement units (IMU) (Casio, Tokyo, JPN) on the dorsum of both shoes and at the sacrum. Participants were also equipped with a GPS watch (Garmin, Olathe, KS) during free training runs. A custom MATLAB (Mathworks, Natick, MA) script was used to find the peak resultant acceleration for each left and right foot strike, and at the sacrum following a left or right foot strike. Asymmetry was calculated using symmetry angle (SA) expressed as a percentage [5],

$$(SA = \frac{45° - arcTan(X_{Left} - X_{Right})}{90°} \times 100).$$

Zero percent is perfect symmetry, while 100% is completely asymmetric in equal and opposite magnitudes [5]. Runs were grouped into lower mileage (<13.5 miles) or higher mileage (>13.5 miles) and asymmetry percentages were averaged over quarters of the run. A one-way ANOVA was used to test for the effect of mileage on asymmetry (α=0.05).

RESULTS AND DISCUSSION

Symmetry angles were not significantly different throughout the quarters of the lower or higher mileage runs (p>0.05). Additionally, symmetry angles were not significantly different between the overall lower and higher mileage runs (p>0.05). Though not significant, average SA at the feet tended to increase throughout each quarter in both lower and higher mileage runs (Figures 1 & 2). However, average sacral SA tended to increase from the first to second quarter, decrease during the third quarter, and again increase during the fourth quarter in the lower mileage group (Figure 1). Average sacral SA in the higher mileage group tended to decrease from the first quarter to the second quarter, then increase during the third quarter, and finally decrease again in the fourth quarter (Figure 2). Average SA tended to be greater at the sacrum than at the feet during lower mileage runs, but the opposite trend was observed in higher mileage runs. Overall changes in average SA between quarters tended to be larger in the higher milage group (7.05-9.17 at the feet and 5.16-5.6 at the sacrum) than the lower mileage group (5.18-5.47 at the feet and 5.29-5.75 at the sacrum).
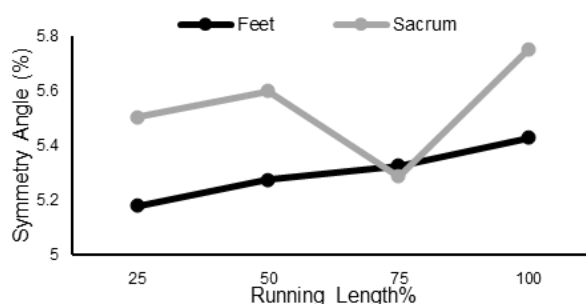

Figure 1: Average asymmetry percentage over each quarter of the run in the feet and the sacrum for lower mileage runs.
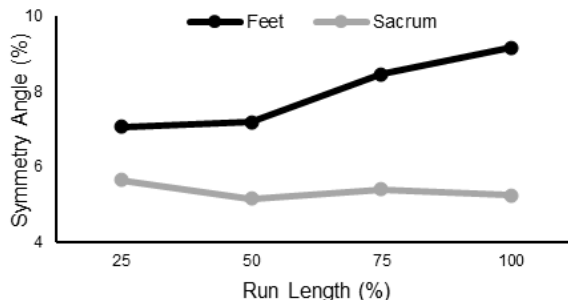

Figure 2: Average asymmetry percentage over each quarter of the run in the feet and the sacrum for higher mileage runs.

CONCLUSIONS

While there are notable changes in asymmetry throughout the progression of a run, they are not statistically significant at the group level. However, the SA varied greatly between participants. It is possible individual participants experienced significant changes in asymmetry. Future studies should focus on within-runner differences throughout the duration of a long run.

REFERENCES

1. Maloney et al., *JSCR*, 2019
2. Mizrahi et al., *Hum Mov Sci*, 2000
3. Melo et al., *J Biomech*, 2020
4. Lafferty et al., *AOSSM*, 2021
5. Zifchock, et al., *Gait & Posture*, 2008

INVESTIGATE MUSCLE FATIGUE ON LOWER BODY KINEMATICS DURING LAY–UP AND LANDING IN RECREATIONAL BASKETBALL PLAYERS

Brandon Yang and Li Jin
Departments of Kinesiology, San José State University, San José, CA USA
email: chengyin.yang@sjsu.edu

INTRODUCTION

Understanding how muscle fatigue contributes to musculoskeletal injuries in sports is crucial. Dynamic physical activities commonly induce muscle fatigue, which has been linked to an increased risk of injuries among athletes [1]. Muscle fatigue not only affects maximum force production, reaction time, and exercise capacity but also alters biomechanical parameters such as joint angles during landing and lay–up activities [2]. Previous research has shown that fatigue can lead to decreased hip and knee flexion angles during landing, increased hip and knee extension angles, and decreased ankle range of motion during both landing and lay–up [3]. While there is considerable research on knee joint movements under fatigued conditions, there is a notable gap in studies focusing on ankle and hip joint movements under similar circumstances. Therefore, the purpose of this study was to investigate the effects of fatigue on ankle, knee and hip joint kinematic patterns during lay–up and landing activities. We hypothesized that fatigue would increase peak ankle plantar flexion angle, peak knee extension and hip extension angle in both landing and lay–up activities.

METHODS

Six healthy individuals (age: 24.00 ± 1.10 years, height: 1.77 ± 0.08 m, mass: 78.67 ± 12.59 kg) participated in this study. At the beginning, participants performed a lay–up using a three–step approach, utilizing their dominant leg and taking off from the force plate. Afterward, participants executed drop–jumps from a 0.3 m box, landing on the force plate with their dominant leg. Next, participants underwent the fatigue protocol [4]. Upon completing the fatigue protocol, they repeated the same lay–up and landing tasks. Bilateral attachment of 36 retroreflective markers to anatomical landmarks on the lower body was conducted [5]. Kinematic data were then collected using an 8–camera motion capture system (Vicon, Oxford, UK) at a frequency of 100 Hz. Ground reaction force (GRF) data were collected using two force plates (AMTI, Watertown, MA, USA) at a frequency of 1000 Hz. Outcome measurements comprised peak vertical GRF, peak ankle plantar flexion moment, and peak knee and hip extension moment. All variables underwent processing using an inverse dynamics model in Visual 3D software (C–Motion, Germantown, MD, USA). A paired t–test was performed to analyze the biomechanical differences ($\alpha = 0.05$) between pre– and post–fatigue outcome measures using SPSS software (V26.0, IBM, Armonk, NY, USA).

RESULTS AND DISCUSSION

No statistically significant differences were found for the outcome measures between pre–fatigue and post–fatigue conditions. While participants exhibited a 17.11% in peak knee extension angle and a 5.95% decrease in peak hip extension angle after fatigue during landing (Table 1). Additionally, there was a slight decrease (4.78%) in peak ankle plantar flexion angle and a 15.74% increase in peak hip extension angle in lay–up activity after fatigue (Figure 1).
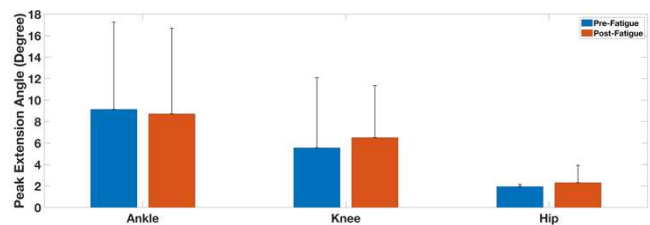

Figure 1: Peak ankle, knee and hip extension angle in lay–up between pre– and post–fatigue conditions.

CONCLUSIONS

Our research revealed that fatigue led to an increase in peak knee and hip extension angles during both landing and lay–up activities, confirming our hypothesis. Moreover, fatigue tended to decrease the peak ankle plantar flexion angle during landing and lay–up movements. These results indicate that acute muscle fatigue disrupts lower extremity joint kinematic patterns in both landing and lay–up activities. These insights hold significant value for the development of injury prevention programs aimed at athletic trainers and clinical professionals. Future studies should delve into the effects of fatigue protocols on joint and limb power and mechanical work patterns during lay–up and landing activities.

REFERENCES

1. Pappas et al. *J of Sport Sci & Med*, **6(1):** 77–84, 2007
2. Kim et al. *The Knee*, **24(6)**, 1342–1349, 2017.
3. Byungjo et al. *BMJ Open Sport & Exerc Med*, **6(1)**, 2020.
4. Liederbach et al. *Am J Sport Med*, **42(5)**, 1089–95, 2014.
5. Horst et al. *Plos One*, **12(6)**, 201

Table 1: Peak joint extension angle during landing in pre–fatigue and post–fatigue condition.

Peak Joint Angle (Deg)	Fatigue Condition, Mean $\pm$ SD, Percentage Change, P–Value			
	Pre–Fatigue	Post–Fatigue	Percentage Difference	P–Value
Ankle Plantar Flexion	12.67 ± 3.07	12.55 ± 1.04	0.94	0.935
Knee Extension	5.37 ± 3.66	6.38 ± 4.51	17.11	0.323
Hip Extension	12.04 ± 7.71	11.34 ± 6.29	5.95	0.723

VOLUME RECONSTRUCTION ACCURACY OF A 3D FREEHAND ULTRASOUND APPROACH

Hayashi, H[1] and Hahn, ME[1]
[1]Neuromechanics Lab, Department of Human Physiology, University of Oregon, Eugene, OR USA
email: hhayash7@uoregon.edu

INTRODUCTION
While the Achilles tendon is the largest and strongest tendon in the body, it is susceptible to developing tendinopathy due to its relatively long and compliant nature, and that it is subject to loads as high as 10 times bodyweight during running. Structurally, Achilles tendinopathy is accompanied by an increase in cross-sectional area as well as decreased elastic modulus [1]. Previously, it has been demonstrated that a "sweet spot" of about 5-6% strain of the Achilles tendon promotes positive adaptations such as increased stiffness and increased expression of type 1 collagen fibers [2]. Yet, common approaches to quantify Achilles tendon strain often include the proximal aponeurosis-like portion of the tendon, which underestimates free Achilles tendon strain. Thus, the quantification of the free Achilles tendon strain is important to better inform rehabilitation practices.

One approach to quantify free Achilles tendon strain is 3D freehand ultrasound (3DfUS). This technique involves obtaining a stack of ultrasound images whilst simultaneously tracking the position and orientation of the ultrasound probe. The images are then mapped into 3D space, and the structure of interest segmented to obtain a 3D reconstructed volume. To obtain accurate reconstructions, the precision and accuracy of spatial calibration and volume reconstruction is crucial. Therefore, the purpose of this study was to assess the accuracy and precision of spatial calibration using the crosswire phantom, as well as the error of volume reconstruction using an acrylic phantom of known volume.

METHODS
A crosswire phantom composing a pair of intersecting wires within an acrylic box submersed with water was constructed. A cluster of 4 retroreflective markers attached rigidly to the probe were used to define the probe coordinate system and were tracked using a 5-camera motion capture system at 120 Hz. (Motion Analysis Corp., USA). The 3DfUS system was spatially calibrated by imaging the crosswire at several different angles and positions of the ultrasound probe (fig. 1) [3]. After spatial calibration, an acrylic cylinder submersed in water was scanned in the transverse cross-section with ultrasound along its length. This was performed 3 times on separate days.

The quality of spatial calibration was assessed by reconstruction precision and accuracy, and the quality of volume reconstruction was assessed by the percent error from the known volume. To test calibration precision, 14-20 ultrasound images of the crosswire were obtained, and the position coordinates of the crosswire in the ultrasound images were mapped into the 3D global coordinate space. This created a cloud of points in 3D space, and the average distance between each pair of points was calculated. To assess calibration accuracy, the average distance between the known location of the crosswire in 3D space and the reconstructed position of the crosswire from the ultrasound images were

calculated. Finally, to assess the accuracy of volume reconstruction, a voxel array containing the stack of ultrasound images of the cylinder phantom was reconstructed. The reconstructed voxel array was imported into 3D slicer, and the cylinder was manually segmented to calculate the volume.
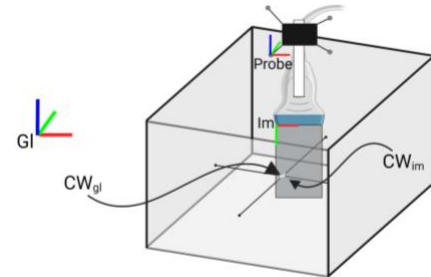

Figure 1: Illustration of the crosswire phantom imaged with the ultrasound probe, and the coordinate systems involved. Made with biorender.com

RESULTS AND DISCUSSION
Across the three trials, the average calibration precision was 1.30 ± 0.20 mm, the average calibration accuracy was 0.89 ± 0.09 mm, and the average volume reconstruction error was 1.39 ± 0.39 %.

To obtain accurate reconstructions, the precision and accuracy of spatial calibration and volume reconstruction is crucial. Our results suggest that a 3DfUS system calibrated with a crosswire phantom produces high quality calibrations and allows for accurate volume reconstructions.

CONCLUSIONS
The high precision and accuracy of 3DfUS calibration and volume reconstruction indicates that 3DfUS offers an alternative to obtain 3D reconstructed volumes of the free Achilles tendon that is more cost effective compared to other imaging modalities. Given that 3DfUS can measure subject specific tendon morphology and quantify tendon deformation under load, this method may help to inform individualized rehabilitation protocols to promote tendon healing in patients with Achilles tendinopathy.

REFERENCES
1. Arya & Kulig (2010) *J App Physiol* 108(3)
2. Pizzolato et al. (2019), *Br J Sports Med* 53(1)
3. Weide et al. (2017) *J Vis Exp* 129

ACKNOWLEDGEMENTS

FUNCTIONAL RECOVERY TIMECOURSE IN A PRECLINICAL MODEL OF ACHILLES TENDON INJURY

Forer, JM[1,2*], Link, K[1], Yannello, B[1], Pacheco, YC[1], Hahn, ME[2], Willett, NJ[1]
[1]Department of Bioengineering, Knight Campus for Accelerating Scientific Impact, University of Oregon, Eugene, OR USA
[2]Neuromechanics Lab, Department of Human Physiology, University of Oregon, Eugene, OR USA
email: jforer@uoregon.edu

INTRODUCTION

Tendons are integral components of the musculoskeletal system, transmitting forces from the muscles to the skeleton to create movement. Additionally, tendons are minimally vascularized compared to other peripheral tissues, resulting in poor healing outcomes [1]. Considering tendon injuries make up 45% of the more than 60 million musculoskeletal injuries that occur annually in the United States, an obvious need exists to investigate and improve functional recovery [2]. A plethora of preclinical models on tendon injury exist in the literature; most studies implementing these models have investigated the effects of different treatments on healing. However, many do not study the effects of injury to the point of full recovery, and fewer still measure functional outcomes to quantify recovery. von Frey (VF), a method of testing tactile allodynia, is used broadly in the field of orthopedic research, but has not been used in a model of complete tendon rupture and repair or measured more than two weeks after tendon injury. We used electronic VF (Bioseb) and Dynamic Weight Bearing (DWB, Bioseb) (an assessment of spontaneous limb function) to quantify full functional recovery from a surgically induced Achilles tendon rupture over a period of two months. Structural outcomes including tendon cross-sectional area, mass, and fluid content, as well as tracer clearance were measured at a timepoint before full recovery to further describe the consequences of this injury model. We hypothesized that full Achilles tendon rupture and suture repair would lead to increased sensitivity and offloading of the injured limb as shown by VF and DWB, and that both metrics would recover to baseline levels over a period of two months.

METHODS

All procedures were conducted in accordance with IACUC protocol. Female Sprague-Dawley rats received a unilateral complete transection of the Achilles tendon followed immediately by suture repair. In a cohort of 12 animals, VF and DWB tests were conducted one day before injury, and 4-, 7-, 14-, 28-, and 56-days post injury. A second cohort of 6 animals was euthanized at 14 days to collect data about tendon morphology. Images of the tendon were taken in situ following removal of surrounding tissue and analyzed with ImageJ (FIJI) to determine cross-sectional area. Mass was measured immediately post-excision, and fluid content was calculated from the ratio of mass after and before 72 hours of lyophilization. Prior to euthanasia, 5 µL injections of near-infrared tracer dye were delivered to injured and contralateral tendons of three animals 1-week post injury. Tracer clearance analyses were conducted via an IVIS Spectrum (Revvity). VF and DWB data were analyzed with two-way ANOVA (Tukey's posthoc) and structural and clearance data were analyzed with paired t-test in Prism (Graphpad), with an alpha level of 0.05.

RESULTS AND DISCUSSION

VF measurements showed an initial increase in sensitivity (decrease in withdrawal force) of the injured leg that returns to baseline four weeks after injury (Fig 1a). At four weeks post-injury, there was still a significant difference between the injured and contralateral limbs, which was not present at eight weeks. DWB measurements showed significant offloading of the injured limb after injury that fully recovered at four weeks post injury (Fig 1b). Two weeks post-injury tendon cross sectional area (p=0.0002), fluid content (p=0.0052), and mass (p=0.0223) were all significantly increased in the injured limbs compared to the contralateral limbs. Tracer clearance curves of injured limbs had significantly lower time constants than contralateral limbs (p=0.0258).

Both VF and DWB demonstrated loss of function followed by functional recovery from a full Achilles tendon transection over a two-month period. The results between the two differed however, with DWB showing full recovery by 4 weeks while VF still showed differences between contralateral and injured legs at that timepoint. The incorporation of multiple functional tests represents a holistic picture of the healing response. The
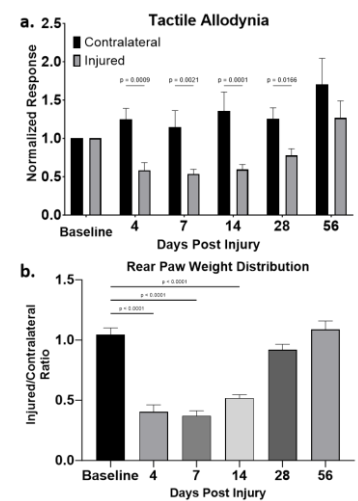

Figure 1: a) VF and b) DWB normalized to baseline. n=12 for all timepoints other than 56 days post injury, where n=6. Data shown as mean ± SEM.

structural changes shown two weeks after injury are consistent with the lack of full functional recovery at that time. Measurement of functional tracer clearance from the injury site implies that this injury leads to accelerated clearance when compared to contralateral limbs. Limitations of this study include a lack of multiple timepoints for the structural measurements and functional clearance parameters, and the lack of a sham control group for the functional testing cohort. These findings motivate investigation into how these structural changes and functional clearance parameters differ with time since injury. Clarifying this relationship between structural and functional recovery of preclinical tendon injury will aid in the development of treatments by better detailing the standard healing process of the tissue.

REFERENCES

1. Chen, T. M. et al. *Clin. Anat.* 22: 377-385, 2009.
2. Smallcomb, M., et al. *Am. J. Phys. Med. & Rehab.* 101: 801, 2022.

ACKNOWLEDGEMENTS

COMPARING MOTOR VEHICLE COLLISION (MVC) INJURY INCIDENCE BETWEEN PREGNANT AND NON-PREGNANT INDIVIDUALS: A CASE CONTROL STUDY

Jade Levine[1,2], Vivian Chung[1], Sarka Lisonkova[3], Peter Cripton[1,2,4]
[1]Orthopaedic and Injury Biomechanics Group, [2]Department of Mechanical Engineering, [3]Department of Obstetrics and Gynecology, [4]School of Biomedical Engineering, University of British Columbia, Canada.
email: levine.jade@gmail.com

INTRODUCTION

In industrialized nations such as Canada and the United States, injuries sustained from motor vehicle collisions (MVCs) are the leading cause of trauma during pregnancy and fetal mortality not related to the pregnancy itself [1-3]. While seat belts have been proven to reduce injury risk in the event of an MVC, studies have shown that even when the pregnant vehicle occupant is properly restrained, the risk of adverse fetal outcomes exceeds 60% at crash speeds greater than 50 km/h [4]. During the later stages of pregnancy, 50-80% of the uterus lies below the midline of the lap belt, resulting in the belt resting on abdominal soft tissue rather than the preferred bony landmarks of the pelvis [5]. If the belt was loaded in this position during an MVC, the resultant forces could cause direct uterine loading, a mechanism that results in adverse fetal and maternal outcomes.

Because the anthropometry of pregnant motor vehicle occupants differs both throughout pregnancy and from the non-pregnant population, it was necessary to understand how those differences influence injury risk in the case of an MVC. Therefore, the goal of this study was to identify if pregnant occupants were at a greater risk of moderate injury than non-pregnant female occupants during an MVC. Furthermore, the study also compared the risk of injury within the pregnant occupant group between the three trimesters. We hypothesized that, for the same conditions, pregnant vehicle occupants are more likely to be injured than their non-pregnant counterparts and that the risk of injury for pregnant occupants would increase with increasing gestational age.

METHODS

All data sets included in this study are from the Crash Investigation Sampling System (CISS) from the National Highway Traffic Safety Administration (NHTSA) database. All cases between 2017 and 2022 were downloaded as .sas files and analyzed using SAS® Studio software [6]. To generate the complete dataset for analysis, first the general vehicle, occupant, and injury files for each year were horizontally joined using SAS's recommended merging protocols. Next, each year of files was vertically joined to its subsequent year through matching of column names. The study population included all women between the ages of 15 and 45 in the USA that were involved in an MVC that had been reported in the CISS between 2017 and 2022. From the dataset, we compared the risk of injury for women who were pregnant with those who were not pregnant at the time of the MVC. The primary outcomes were based on the Maximum Abbreviated Injury Scale (MAIS) and defined as moderate to critical injury (MAIS 2-5) and mild to no injury (MAIS 0-1).

Potential confounding factors such as vehicle model year, age, seat belt positioning, and position within the car were accounted for in the study design. The risk of each primary outcome was calculated by dividing the risk of that outcome in each group by the total population of that group. The risk ratio of pregnant versus non-pregnant occupants was calculated in SAS software using the PROC FREQ Chi squared relative risk comparisons. Finally, we used multivariate regression analysis to identify the significance and proportion of potential confounders.

RESULTS AND DISCUSSION

A total of 9679 non-pregnant females and 210 pregnant females (62 in the first trimester, 77 in the second trimester, 61 in the third trimester and 10 of an unknown trimester) were included in this study. For the non-pregnant group, 4207 had at least one injury with an abbreviated injury score (AIS) of two or more. For the pregnant group, 30 individuals in the first trimester, 45 individuals in the second trimester, and 24 individuals in the third trimester had injuries with an AIS of two or more. There was a total of 113 cases of occupant mortality in the non-pregnant group and two cases in the pregnant group. Additionally, there were four cases of fetal mortality, one in the first trimester, two in the second trimester, and one in the third trimester.

CONCLUSIONS

The results of this study will add important data to a growing field of injury biomechanics. While there have been previous studies comparing injury rates between pregnant and non-pregnant female occupants [7], to our knowledge, no other studies have compared injury rates between trimesters of pregnancy. Understanding how the risk of injury during pregnancy changes could influence research in the automotive injury by forcing researchers to not only include pregnant occupants but to also include a diverse population of pregnant individuals in their studies.

REFERENCES

1. Weinberg L, et al. *Anaesth. Intensive Care* **33**, 167-180, 2005.
2. Brown H L, *Obstet. Gynecol* **114**, 147-160, 2009.
3. Weiss H B, et al, *JAMA* **286**, 1863-1868, 2001.
4. Klinich K D, et al, *Am. J. Obstet. Gynecol* **198**, 450.e1-450.e9, 2008.
5. Klinich K D, et al, *International Congress & Exposition*, SAE International, 1999.
6. Copyright, SAS Institute Inc. SAS and all other SAS Institute Inc. product or service names are registered trademarks or trademarks of SAS Institute Inc., Cary, NC, USA
7. Koh S, et al, *Healthcare* **9**, 1414, 2021.

High-Density Surface Electromyographic Signal Composites for Lower Limb Prosthetic Control

Joseph R. Redmond, Fred W. Christensen, Corey A. Pew*
Department of Mechanical and Industrial Engineering, Montana State University, Bozeman, MT
*corey.pew@montana.edu

Introduction

Surface electromyography (sEMG) is utilized as a control interface for active, robotic protheses, resulting in higher quality of life for individuals with lower limb amputation [1]. sEMG reads myoelectric signals from a residual limb, providing a natural control interface for the user. However, signal noise from skin impedance, motion of the skin relative to the muscle, and sensor displacement are common for sEMG, reducing robustness [1]. Lower limb prostheses (LLP) require reliable control signals, as errors risk falls and subsequent injury to the user [2]. High-Density surface electromyography (HDsEMG) shows potential in improving signal quality, allowing for more reliable and integrated control. We hypothesize that **(1)** signal-to-noise ratio (SNR), a quantification of signal quality [3], is better with HDsEMG relative to Standard sEMG (SsEMG), **(2)** individual HDsEMG signals have a lower root-mean-square (RMS) power due to smaller electrodes, **(3)** composite signals can compensate for the decrease in individual signal power.
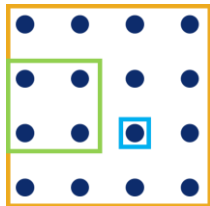

Figure 1: 16 Ch. Sensor composites Best-1 (blue), Comp-16 (gold), Comp4 (green).

Methods

11 Participants (3 individuals with lower limb amputation and 9 non-amputees) were recruited for the Montana State IRB approved protocol. Data was collected using bipolar SsEMG sensors and 16 channel HDsEMG sensors. Four superficial muscles, two knee flexors, the Semitendinosus (ST) and Bicep Femoris (BF), and two extensors, the Vastus Laterallus (VL) and Rectus Femoris (RF) were measured. Sensors were placed optimally and displaced distally 1 cm to simulate sensor displacement during prosthesis pistoning. Participants performed activities of daily living, walking straight, turning left/right, stair and ramp ascent and descent, sit to stand, and squats. An analysis using straight walking data of 1 participant was conducted to initially evaluate signal compositing methods. SNR was calculated for the SsEMG signals, and the individual channels of HDsEMG sensors. RMS values were computed in a previous study of this data [4]. The single HDsEMG channel with the best SNR was selected (Best-1). Composite HDsEMG signals were computed, including a combination of all 16 channels (Comp-16) and a cluster of 4 channels (Comp-4) (Fig. 1). Comp-4 was created by evaluating the mean SNR in the 9 possible 2x2 square clusters. The 4-node cluster with the highest mean SNR was then combined.

Results & Discussion

SNR was found to be over 200% better for Best-1 compared to the Standard signal (Fig. 2). Previous work indicated sEMG data to be clean from noise artifacts with an SNR over 10dB [5]. This 10dB SNR threshold provides an initial benchmark for signal viability prior to control system implementation. The standard signals fail to meet this threshold for both optimal and displaced positions with an SNR under 5dB. In optimal placement, Best-1 exceeded this mark at over 18dB, a product of selectivity based on signal
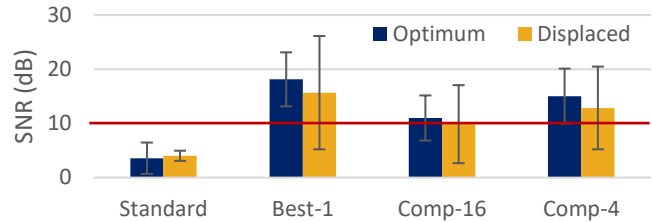

Figure 2: Average SNR +/- Standard Deviation computed of VL, SL, and BF, 8 straight walking trials of 1 participant for SsEMG and 3 HDsEMG configurations.

quality. Standard signals had a higher RMS compared to Best-1 by a factor of 150-300%, depending on the muscle evaluated (Fig. 3). The smaller size of the HDsEMG nodes reduces voltage pickup by a function of unit area, driving the need for composite analysis. Comp-16 has an SNR near the 10dB threshold, while Comp-4 is slightly better around 15dB. A higher SNR is indicative of a cleaner and more reliable signal, which can be trusted more when integrated into the control of LLP. Composites are of lower quality than Best-1, as signal combination will combine the best signal with lower quality signals. Within the size of the HDsEMG sensor field, some signals had lower SNR, lowering the overall SNR of Comp-16. Comp-4 maintained selectivity in the combination method, improving SNR. The standard signal saw minimal change in SNR with displacement, which has been attributed to low overall signal quality. In displacement, HDsEMG signals have the highest SNR along a single row/column, and the geometry of the composite configurations evaluated incorporate nodes of poor signal quality. Composite schemes that do not include fixed geometric configurations and are adaptive to sensor behavior over time need to be explored to maintain signal quality over a greater range of operating conditions. Future data analysis will evaluate signal composites for both SNR and RMS in all participants and activities.
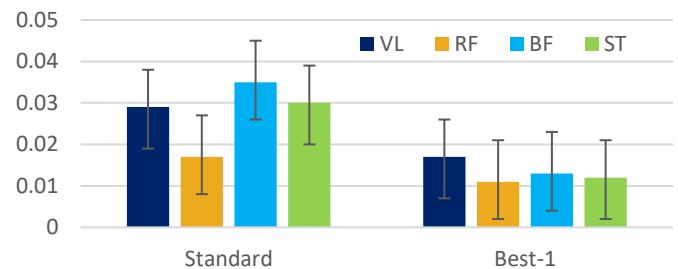

Figure 3: Previous analysis of normalized RMS in all participant trials for Standard and Best-1 Configurations, with standard error [4]

References

1. Gehlhar et al. *Annual Reviews in Control* **55**, 2023.
2. Ahkami et al. *IEEE TMRB* **5** 2022.
3. Sinderby et al. *J Applied Physiology* **79**, 1995.
4. Christensen, *Theses at Montana State*, 2022.
5. Fraser et al. *IEEE TIM* **63**, 2014.

Acknowledgements

BALANCE PLATFORM AND INVERTED PENDULUM FOR ROBOTIC VESTIBULAR CONTROL

Bolen, BP[1]; McNeal, JS[1]; and Hunt, AJ[1]

[1]Agile and Adaptive Robotics Lab, Department of Mechanical and Materials Engineering, Portland State University, Portland, OR
USA
email: bbolen83@gmail.com

INTRODUCTION

In our lab we are working on biomimetic robots, in part, to gain insight into biological processes. Our robots are actuated with Festo brand Braided Pneumatic Actuators (BPAs) that serve as artificial muscles. When designing to be truly biomimetic, these BPAs are controlled with a Synthetic Nervous System[1], although that is outside the scope of this abstract.

The work presented here is the creation of an inverted pendulum actuated by BPAs that serves an analogous function to a human tibia and foot. This inverted pendulum is to incorporate pseudo-vestibular feedback via an Inertial Measurement Unit (IMU). It had the further requirement of 150 degrees range of motion (RoM). The inverted pendulum was to be placed on a balance platform and maintain balance while the platform oscillated.

METHODS

The balance platform is designed with an 80/20 brand extruded aluminum frame, a 1 DoF aluminum plate for the inverted pendulum to sit on, and motor and power screw to rotate the plate, a potentiometer for plate angle feedback, a 24V power supply, and an Arduino microcontroller to control the movement of the plate (Figure 1).

The inverted pendulum had a base ("foot") and body ("tibia") connected with a single DoF Joint. All constructed with 3D printed Onyx material, save for some extruded aluminum at the bottom of the foot. A 9-axis L3GD20 + LSM303D IMU was attached to the top of the tibia. Proportional pressure control was used to control the BPAs. A novel reverse pulley system was used reach our desired high RoM. The BPAs were mounted to the base and connected the tibia via high strength string acting as artificial tendon (Figure 1).

A second inverted pendulum was created that was more biomimetic than the first version. It had a ball and socket ankle joint actuated with three BPAs, one for plantarflexion and two for dorsiflexion (one inverting and the other everting). The BPAs were mounted to the tibia and controlled with a bang-bang controller sending signals to the valve manifold (Figure 2).

RESULTS AND DISCUSSION

The balance platform was able to oscillate as desired. The inverted pendulum was able to maintain upright balance on the oscillating balance platform. It could achieve the desired RoM.
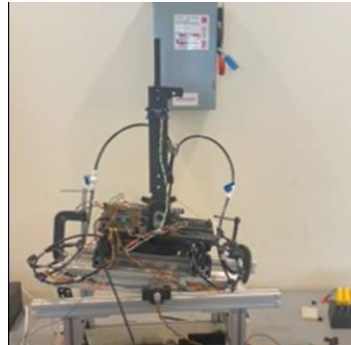

Figure 1: Inverted pendulum balancing on oscillating platform.

The biomimetic inverted pendulum was not tested on the platform, but was able to maintain upright balance with no assistance.

Figure 2: Biomimetic inverted pendulum.

CONCLUSIONS

Further testing can be done with both inverted pendulums and modifying the controllers to use a Synthetic Nervous System.

REFERENCES

1. Hilts WW, et al. *Conference on Biomimetic and Biohybrid Systems*, LCNS **10384**, 2017.

ACKNOWLEDGEMENTS

CUSTOM MATERIALS INSPIRED BY BIOLOGICAL ARMOR

Tapia, E[1], Marshall[1], T, Chier, E[1], Donatelli, CM[1]
[1]Fowler School of Engineering, Chapman University, Orange, CA USA
[2]Wilkinson College of Arts, Humanities, and Social Sciences, Chapman University, Orange, CA USA
email: cassandra.donatelli@gmail.com

INTRODUCTION

A recurring issue in the design of assistive devices is the expense of custom designs [1], [2]. Even injuries sustained by NASA astronauts are due to ill-fitting extravehicular activity (EVA) suits [3]. These devices are designed to protect the user from injury, but they also restrict movement, causing long term joint pain and tissue damage. Extensive research has gone into the design of assistive devices, with one of the main challenges being designing systems that work differently for people with different anatomies [4]. As a result of the complexity of this problem, most designs forgo customizability in favor of using traditional "Small, Medium, Large" sizes.

The goal of this research is to design a lightweight and low-cost system that protects from acute injury while allowing a natural range of motion. My lab proposes to use armored fishes as a model for the design of bioinspired materials for protective systems. Fish evolved biological armor to serve functions from protection to energy storage to hydrodynamics. The critical aspect of this armor is it must be both protective and flexible so as not to restrict the movement of the animal. Engineers have looked to fish armor as inspiration before (i.e. [5]) to take advantage of its protective yet flexible nature. Like patients undergoing physical therapy and astronauts moving between earth and orbit, armored fishes evolved to seamlessly move between different habitat types and changes in force regimes.

METHODS

We first collected and analyzed micro computed tomography (uCT) scans of armored fishes (Figure 1C) and analyzed them using Slicer3D to measure armor shape, density, and overlap. We then use the models to create a series of idealized designs and created composite material by 3D printing PLA directly onto a flexible mesh fabric. We tested these models on a 3-point bending rig attached to an Instron as well as a custom rig with a camera setup to measure elasticity.

RESULTS AND DISCUSSION

Shape, orientation, and overlap both play significant roles in the material properties of a armored system (Fig 1A, 1B). Interestingly, circular, and triangular scales result in a somewhat equally flexible material, while diamonds and hexagons require much mor work to deform (Fig 1B). Orientation also plays a large role, with orientations resulting in sharper joints between armor rows increasing load (Fig 1B).

CONCLUSIONS

Our results show a promising step in the direction of bioinspired materials that can be used in the biomedical field. The relationships between parameters such as shape, overlap, and orientation is not 1:1, so more work is needed to develop a series of principles that will make the design of custom materials a quicker and more iterative process.

REFERENCES

1. S. P. Chappell et.al., "Evidence Report: Risk of Adverse Health Outcomes & Decrements in Performance due to In-Flight Medical Conditions," NASA Hum. Res. Progr., 2017.
2. V. Jaggard, "Astronauts' Fingernails Falling Off Due to Glove Design," Nat Geographic News, 14-Sep-2010.
3. S. Strauss et.al., "Extravehicular mobility unit training and astronaut injuries," Aviat. Sp. Environ. Med., 76.5, 2005.
4. R. A. Opperman et.al., "Probability of Spacesuit-Induced Fingernail Trauma Associated with Hand Circumference," Aviat. Space. Environ. Med., 81.10, 2010.
5. J. Duro-Royo et al., "MetaMesh: A hierarchical computational model for design and fabrication of biomimetic armored surfaces," CAD. Computer Aided Des., 2015.
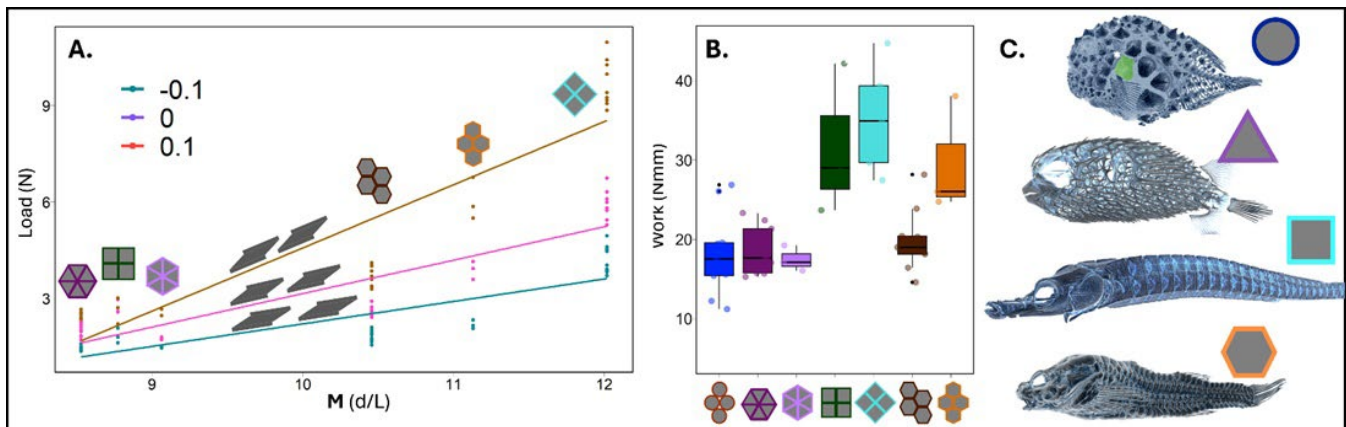
ACKNOWLEDGEMENTS

Figure 1. **A**. Material testing data fit to an equation representing the bending moment of different designs. Lines represent different scale overlap percentages. **B**. Work required to deform models of different shapes and orientations. **C**. Armored fishes that inspired different shapes: from top to bottom: Pacific Spiny Lumpsucker, Pufferfish, Gar, Rockhead Poacher.

THE SWITCH KIT: BRIDGING THE GAP IN THERAPEUTIC TOYS FOR CHILDREN WITH MEDICAL COMPLEXITIES

Kate Bokowy[1,2], Mia E. Hoffman[1,2], Alisha Bose[3], Tiffany Li[4], Heather A. Feldner[2,4], Katherine M. Steele[1,2]
[1]Department of Mechanical Engineering, [2]Center for Research and Education on Accessible Technology and Experiences,
[3]Department of Human Centered Design and Engineering, [4]Department of Rehabilitation Medicine, University of Washington,
Seattle, WA USA

INTRODUCTION

Assistive technology can support children with complex medical needs through communication, self-initiated movement, and play. However, there are not enough devices available to support the wide range of play for young children receiving early intervention[1]. To fill this gap, families, clinicians, and community makers have fabricated switch-adapted toys and other custom play supports. However, these DIY creations are often too time consuming, untested, and unavailable to those who need them[2].

In conjunction with families of children receiving early intervention and their clinicians, we have designed an affordable switch kit used to make personalized therapeutic toys. The goal of this switch kit is to support the creation of personalized therapeutic toys and motivate children while they are engaging in therapy. This kit includes an input device that connects switches to a computer or tablet. It also includes premade switches and materials to adapt them or create their own switches.

METHODS

During the design phase, 35 papers were reviewed to define the specific needs of a therapeutic device. From these needs, we developed five initial switches, considering the activation movement, materials, ease of construction, and adaptability. All initial designs were evaluated for durability and reliability. The switch designs were then evaluated by clinicians and families, as part of the larger switch kit. Four clinicians and four families were each given a switch kit and shown how to use it during a two-hour long session. Interviews were conducted about their current play methods, then we would demonstrate and play with the switch kit, while asking design-related questions. The design of the initial switch concepts was modified to fit each child's needs during the sessions. At the end, the participant completed the Quebec User Evaluation of Satisfaction with Assistive Technology (QUEST 2.1: Children's Version)[3] a Likert scale quantifying their perceptions of the switch kit (Figure 1).

RESULTS AND DISCUSSION

All five switch designs were evaluated until passing design specifications. All switches passed 1-meter drop tests and tug tests on wiring. Each switch design was pressed 200 times and passed if the error was <10%. All switches can be activated by a 45g weight, as that is close to a young child's hand weight, or a 15° tilt. Passing this test shows that the switches' designs were ready for use. Each visit with clinicians or families was crucial in learning how the switch kit will function as a practical therapeutic tool. After visiting with the families, we designed a new switch or adapted a current one that would work even better to suit their needs. This could be anywhere from making a switch more entertaining to adding stability. For example, the tilt switch was redesigned to be lighter on the user's body (Figure 2). The tap switch was adapted to provide feedback when the switch was pressed with crinkly aluminum foil (Figure 3). The switch kit was successful in adapting to each child's needs and each clinician's desired movement goal. The switch kit's evaluation shows that it's feasible for the parents to set up, for the children to use, and met both the families' and clinician's needs (Figure 1). It also shows that there is still room for improvement, especially in reliability.
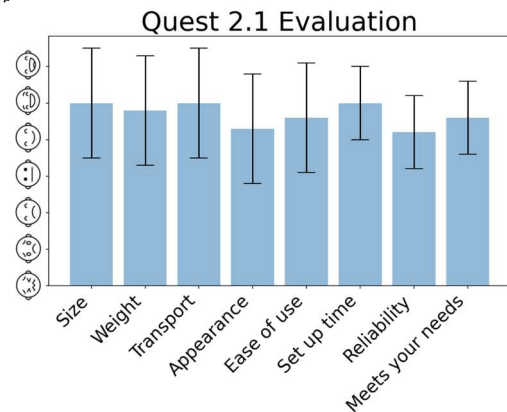

Figure 1: QUEST 2.1 scores after participant's initial interaction with the switch kit.

CONCLUSIONS

We were able to create a kit used to make custom therapeutic devices. The children, families, and clinicians used it effectively and adapted along the way. Continued research and development will be key to maximize its therapeutic potential and establish it as a vital tool in early intervention.

REFERENCES

1. Fikar, et al., DIS, 2018
2. Alharbi, et al., CHI, 2020
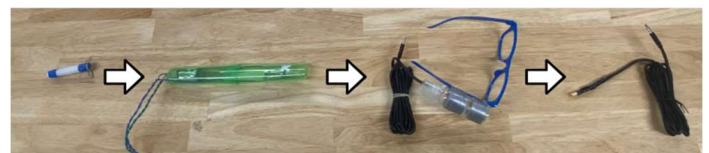3. Demers, et al., Assistive Technology, 1996

Figure 2: The design change of the tilt switch
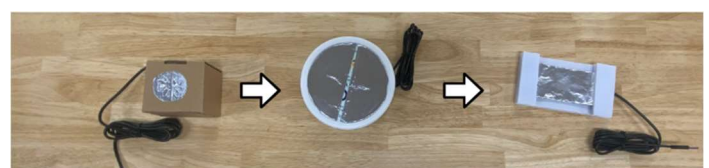

Figure 3: The design change of the tap switch

A TELEHEALTH TOOL TO AUTOMATE MOBILITY TESTING FOR LOWER LIMB AMPUTEES

Mojtaba Mohasel, Corey A. Pew*
Montana State University, Mechanical and Industrial Engineering, Bozeman, Montana
*Corey.Pew@montana.edu

INTRODUCTION: Clinical mobility testing critically evaluates health, functionality, and prosthesis fit in individuals with lower limb amputation (LLA). The 2-Minute Walk Test (2MWT) [1] and Timed Up and Go (TUG) [2] tests are simple assessments used to measure mobility [3]. Currently, mobility testing is performed in-clinic, during regular visits; however, in many states, the closest clinic is hours away from the patient's location. Lack of access to medical care can result in poor prosthesis fit limiting mobility and damaging long-term health outcomes. Remote healthcare options, such as mobile assessment devices can surmount some of these challenges. Yet, current mobile assessment devices (StepWatch and MoveMonitor) are prohibitively expensive and must be returned to the clinician with a time delay between measurement and assessment. Therefore, no live telehealth tool enables individuals with LLA to conduct mobility testing at home with low-cost, real-time assessment. Our purpose is to create this telehealth tool.

METHODS: Hardware/software development utilized data from 16 non-amputee participants and 2 individuals with LLA. Hardware development selected Inertial Measurements Unit (IMU) [4] sensors for data collection. Eleven IMUs were placed on the lower limb segments with 2 on each thigh and shank, one on each foot, and one on the lower back of participants. Each participant performed 5 trials of the 2MWT and TUG tests in a randomized order. Two experimenters measured the distance for 2MWT jointly and had individual measurements for the TUG times. The resultant IMU acceleration was mean corrected to zero [5] and used as the primary signal for calculation. We developed 3 methods for 2MWT and 1 for TUG assessment. 2MWT methods: *1) Integration:* Employs double integration to derive velocity from acceleration and displacement from velocity on non-zero intervals [5]. *2) Step Count:* Determines steps taken by identifying peaks in the signal, then multiplying by average step length obtained by integration. *3) Machine Learning (ML):* Divides the 2-minute duration into 120 one-second windows. Each window is labeled with the overall distance divided by 120. *ML* extracts features [6] for windows and uses a Random Forest regressor [7] to estimate the distance for each window. *ML* model training employs hold-out method, utilizing data from all participants except the test participant. TUG method: *1) Threshold:* Identifies a specific value (e.g., $10 \frac{m}{s^2}$) as an indicator for the start and stop of the TUG task through manual observation of signals from several participants. Acceptable error for 2MWT methods was set at +/- 6 m to the human measurement [5]. Success for TUG calculation should be within the two experimenters' 95% confidence intervals. We randomly selected three participants for an initial evaluation of the 2MWT to demonstrate the effectiveness of each developed method. However, for the TUG test, we only reported results for one randomly selected participant, as the code is still in the early stages of development.

RESULTS AND DISCUSSION: For the 2MWT, *Integration* outperformed other methods (Fig. 1), closely predicting participant 1 within a meter in all trials. *Step Count* was the weakest distance estimator due to averaging step lengths and missing peaks. The *ML* model overestimated participant two and underestimated participant three. The utilization of uniform approximations for one-second windows by the *ML* limited exposure to diverse data, hindering effective regression fitting. *Integration* was positioned at the center of the shaded area for all test participants. This demonstrates that our *Integration* method closely resembles the previous automated distance estimator, achieving a similar error rate (15 meters in the worst case) [5]. *ML* exhibits the lowest standard deviation error across all participants,

Figure 1: 2MWT Error (Mean+/-SD)

Figure 2: Threshold TUG Compare

indicating its potential for further development as our final distance estimator. Our current results fall within the minimal detectable change range for LLAs (34.3 meters) [8], indicating clinical relevance.

For the TUG test (Fig. 2), *Threshold* was successful in 3 out of 5 trials for Experimenter 1 and in 2 out of 5 trials for Experimenter 2. However, it inaccurately predicted trial 2 due to signal quality issues, resulting in a time difference of 3.3 seconds from the average of experimenters. To address this issue, we plan to implement a signal quality validation stage before start and stop identification. Our current results fall within the minimal detectable change range for LLAs (3.6 seconds) [8]. Future work will move in two directions: 1) Improving *Integration* and *ML* by incorporating a validation stage for selected intervals and including deep learning. 2) Evaluating varying sensor placement.

CONCLUSIONS: A potentially low-cost software and hardware system that can improve access to healthcare for LLA is in development. It is built with open-source code that utilizes a single sensor. It reliably calculates clinical mobility measures automatically. The availability of our open-source code will facilitate researchers in developing their own methods or enhancing our approach. This endeavor aims to provide clinicians with a reliable assessment tool, highlighting the potential of IMU sensors in telehealth solutions.

REFERENCES 1) N. A. Capela et al, IEEE EMBS 36 2014; 2) E. Barry et al, BMC Geriatr, 14 (1), 2014; 3) S. C. White, ASHA, 32, 1990; 4) N. Ahmad et al, Int. J. Signal Process. Syst, 1(2), 2013; 5) K. Trentzsch et al, Brain Sci, 11(11), 2021; 6) M. Christ et al, Neurocomputing, 307, 2018; 7) S. M. Moghadam et al, IEEE Sens J, 2023. 8) Resnik et al, Physical therapy, 91(4), 2011
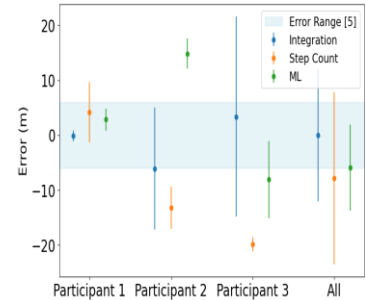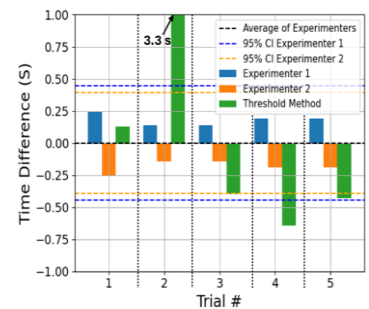
UPPER BODY EXOSKELETON IN ANIMAL CARE TECHNICIANS

Conway, EJ[1], Overduin, A[2] and Fewster, KM[1]
[1]Fewster Spine Lab, School of Kinesiology, University of British Columbia, Vancouver, BC Canada
[2]Workplace Health Services, University of British Columbia, Vancouver, BC Canada
email: ejconway@student.ubc.ca

INTRODUCTION

Musculoskeletal disorders (MSD) in the upper extremities are prevalent in the workplace, particularly in occupations that require repeated overhead work and/or manual lifting and carrying tasks [1], [2] Exoskeletons have emerged as an innovative solution to the complicated and taxing actions of overhead work [3], [4], [5], [6]; however, there have been few studies of their use in complex, non-manufacturing work environments. Animal care technicians at the University of British Columbia (UBC) are a relevant population due to the demands of their job (i.e. frequent cage changing which involves forward reaching and lifting cages within floor to above shoulder level) and reports of upper extremity MSDs. This suggests that an exoskeleton may be an effective intervention for this population, however, very few intervention investigations exist in non-manufacturing work environments. The purpose of this study was to assess the effectiveness of the Levitate AIRFRAME® upper extremity passive exoskeleton among animal care technicians as a potential intervention strategy to reduce MSDs within this population.

METHODS

Volunteer participants consisted of animal care technicians actively employed at UBC. Following consent, several questionnaires were distributed to participating technicians. These pre-training, post-training, and post-use questionnaires addressed various aspects of the exoskeleton and its perceived effectiveness in the workplace. Questions addressed previous work-related pain/discomfort, exoskeleton fit and ease of adjustment as well as it's utility for their specific work tasks. Participants were also filmed completing cage changes with and without the exoskeleton to assess any potential postural and temporal changes during their work. Immediately following filming, participants also reported perceived full body discomfort (RPD) and perceived exertion (RPE).

RESULTS AND DISCUSSION

Collectively, RPD scores were lower and reported in fewer body areas without exoskeleton use, in comparison to with exoskeleton use. Similarly, RPE scores were the same or lower without exoskeleton use (Figure 1). The average cage change time with the exoskeleton was 65.4 seconds, while without the exoskeleton the average cage change was completed in 69.0 seconds. Participants also spent 56% of the average cage change in a neutral posture (<60° shoulder angle) while wearing the exoskeleton compared to 47% without the exoskeleton. After wearing the exoskeleton to complete cage changes, 75% rated the exoskeleton as somewhat to very uncomfortable and indicated they would not consider wearing it due to challenges faced while working in a variety of postures. Likewise, 60% reported the exoskeleton unhelpful while working (Figure 2).

Results from the current investigation present similar results to previous literature with regards to perceived effectiveness and comfort being a primary factor in the adherence to wearing an exoskeleton. Despite improved performance with exoskeleton use, none of the participants wanted to continue using the exoskeleton past the intervention investigation.
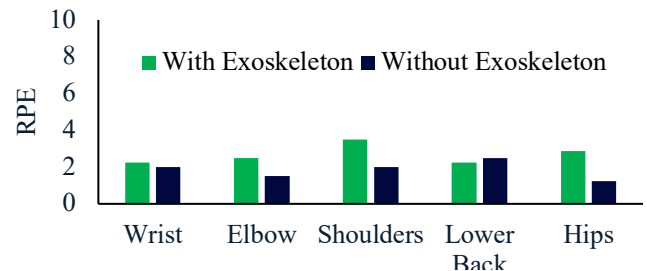

Figure 1: Average RPE of participants during a cage change

CONCLUSIONS

This research displays some nuances of exoskeleton use that should be considered by practitioners and professionals before implementing exoskeletons in a non-manufacturing work environment. Using an exoskeleton for tasks requiring a dynamic use of a full range of motion may result in more complications than benefits. We will be continuing to explore its use in other non-manufacturing environments.
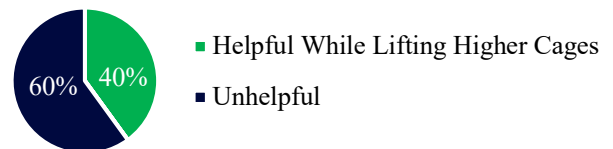

Figure 2: Technician feedback: How helpful was the exoskeleton?

REFERENCES

[1] McFarland and Fischer, *IISE Trans Occup Ergon Hum Factors*, **7**, no. 3–4, pp. 322–347, Oct. 2019.
[2] Theurel et al., *Appl Ergon*, **67**, pp. 211–217, Feb. 2018.
[3] McFarland et al., *Appl Ergon*, **98**, Jan. 2022.
[4] Smets, *IISE Trans Occup Ergon Hum Factors*, **7**, no. 3–4, pp. 192–198, Oct. 2019.
[5] Yin et al., *Journal of Electromyography and Kinesiology*, **55**, Dec. 2020.
[6] Kim et al., *Appl Ergon*, **70**, pp. 315–322, Jul. 2018.

UNDERSTANDING THE PREGNANT WADDLE: IMPAIRED BALANCE OR PROTECTIVE MECHANISM?

Abedzadehzavareh, Z* and Catena, RD
Gait and Posture Biomechanics Laboratory, Washington State University, Pullman, WA, USA.
*Corresponding author's email: z.abedzadehzavareh@wsu.edu

INTRODUCTION
Pregnancy can cause many alternations to balance and gait patterns due to various biomechanical and physiological changes. One of these alterations is the waddling gait pattern. The defining features of waddling gait during pregnancy include amplified trunk lateral movement, expanded step width, increased thorax extension, and increased anterior pelvic tilt [1]. Although waddling is typical during pregnancy, there is a lack of information regarding its exact purpose - its relationship to other spatiotemporal variables, balance, and energetics during walking in pregnant women. To what extent is waddling good as a protective mechanism for balance or bad as a sign of poor balance or because of increased energetic cost? This study addresses the current knowledge gap by examining how waddling (step width) during pregnancy correlates with balance and mechanical energy. Knowing the purpose of waddling and the link to balance control will provide a basis for clinical management of waddling gait in typical healthy pregnant women. However, our primary future purpose is for pregnant women that use a lower-limb protthesis - as a population where increased step width is common [5] until corrected through training and prosthetic adjustments.

METHODS
Twenty-three pregnant women were assessed longitudinally in 4-week intervals between 18 and 34 weeks of gestation. Participants were asked to complete a 10s trial of quiet comfortable standing and 60s of walking at the preferred speed on a treadmill. Motion capture was used to measure spatiotemporal variables and body centre of mass (COM) motion, from which we derived measures of balance and gait energetics. Multiple linear regression analyses were used to explore the correlation between the variables.

RESULTS AND DISCUSSION
We found no significant relationship between step width and BMI (p=0.259). Additionally, our analyses indicate no correlation of step width to other spatiotemporal measures (p>0.059). We hypothesized a natural inverse relationship between step width and length [2]. However, the results of the study rejected this hypothesis. Perhaps there is a local advantage at the hip and ankle to maintaining step length or a systems advantage through cost of transport. This should be explored further in future research.

We found a positive correlation between step width average and increased lateral motion of the center of mass (ML-COMv) (R^2=0.624, p<0.001), as expected, but ML-COMv is also typically used as a measure of reduced balance control [3]. So we explored balance further and identified a positive correlation between step width variance and lateral margin of stability (R^2=0.339, p=0.004). Since there was a lack of correlation between margin of stability and step width average, we are led to believe that the wider steps are used to protect against loss of balance, but may not always be needed to do so, indicating either

a lack of body awareness or a protective mechanism for unexpected perturbations. However, since we previously found no change in body awareness during pregnancy [4], we are led to believe our findings to indicate waddling as a protective mechanism. Interestingly, our analysis found no significant relationship between step width and recovery of energy during walking (p=0.714) or total mechanical work done in the sagittal plane (p=0.530). Combined, these findings indicate widening steps (characteristics of waddling gait) is not an inefficient movement pattern. Future research should examine this further through direct measure of metabolic energy consumption.

Our analysis between step width and standing balance measures indicates a moderate negative correlation (R^2=0.315, p=0.005), meaning as step width increases, standing balance improves. We conducted this analysis with standing balance to verify a correlation between waddling and balance control independent of walking. Combined with walking findings, we are led to believe that waddling is not a sign of poor balance and is a positive gait pattern for pregnant women to increase safety with no apparent (as of yet) consequences. This should be verified through a controlled waddling experimental design in future studies.

CONCLUSIONS
This study found that waddling is a protective mechanism for balance during pregnancy. This finding will be helpful for clinicians or prosthetists who work with pregnant women. Clinicians can use this information to train pregnant individuals to use waddling gait for safety. Since the goal of training waddling gait would be to only promote advantageous aspects, our future studies will expand from our definition of waddling (step width) to an all-encompassing definition mentioned in the introduction and focus on differentiating the beneficial aspects of waddling from the costly aspects through machine learning. Using that information can be helpful for both typical and lower-limb amputee pregnant women. Based on our current findings, prostheses for pregnant amputees should not be adjusted merely to eliminate waddling gait during pregnancy. This is the opposite of the typical goal of adjusting prosthetics to promote a more natural gait pattern for non-pregnant amputees. Perhaps instead, the prosthetics team can find methods to strategically enhance controlled waddling with a prosthesis during pregnancy.

REFERENCES
1. McCrory et al. *J Biomech*, **47**, 2014.
2. Kurz et al. *J Theoretical Biology,* **252**, 2007
3. Lee & Chou. *APMR*, **87**, 2006.
4. Jamali et al. *Exp Brain Research,* **242**, 2024
5. Su et al. *J Rehab Research and Development*, **44**, 2007

COMMON INFANT PRODUCT MATERIALS NEGATIVELY IMPACT BREATHING PATTERNS IN ADULTS

Olvera, HL[1], Bossert, A[2] Mannen, EM[1,2]
[1]Biomedical Engineering Doctoral Program, Boise State University, Boise, ID USA
[2]Mechanical & Biomedical Engineering Department, Boise State University, Boise, ID USA
email: HollyOlvera@u.BoiseState.edu

INTRODUCTION

In the U.S., infants spend an average of 5.7 hours (range 0-16 hours) per day in seated products like infant carriers, bouncers, rockers, and swings [1,2]. In products, infants are constantly surrounded by fabrics and plush materials which may come in contact with their nose and mouth. Infants <6 months are more likely to suffer breathing-related injuries caused by suffocation compared to older children, so plush soft goods are a concern [3]. Previous research has established the safe sleep guidelines: alone, on their back, and in a crib [4]. Even with these guidelines, infants nap or sleep in commercial products which may be hazardous. Pillows, blankets, or soft goods on products are commonly found near infants when they are in commercial infant gear, yet there is a lack of understanding how material composition of these various surroundings impact airflow. No previous research has examined how different materials in common infant products may affect breathing patterns. Our lab currently has a biomechanical respiration model that could be used to evaluate safety of materials, but the model has not been validated with human respiration data. Therefore, the purpose of this study is to characterize how common infant soft good materials influence respiration, and to validate a biomechanical model of respiration.

METHODS

Ten healthy young adults (age: 22.5 ± 3.0 years; 4M, 6F; height: 66.9 ± 4.6 inches; weight: 137.9 ± 23.3 pounds) participated in this IRB approved study. Each participant was fitted with a Capnostream 35 respiratory monitor nose and mouthpiece (collecting breathing rate and end-tidal carbon dioxide ($EtCO_2$)) and finger clamp (to collect heart rate and oxygen saturation (SPO_2)) for each trial. Once fit with the capnoline and finger clamp, participants laid prone on a table (Figure 1).
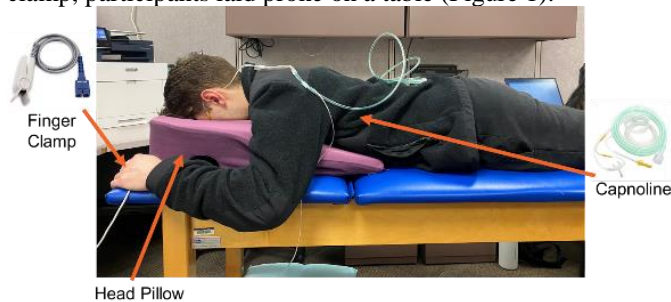

Figure 1: Experimental setup with a participant.

Participants were asked to breathe normally under seven conditions, ten minutes per condition. Three trials measured baseline respiration at the start, middle, and end of the session. The other four trials were randomized for each participant, placing a material in the pillow hole such that the participant was breathing through the material. The four materials selected for this study were chosen based on the common material composition of infant products like bouncers, swings, rockers, and car seats: 100% cotton (cotton), 100% polyester (polyester), 50% cotton 50% polyester (50/50 blend), and 10% spandex 90% polyester (spandex) [5]. After each ten-minute trial, participants sat upright for 2.5 minutes and breathed normally before beginning the next trial. The mean values for $EtCO_2$ and SPO_2 were calculated for each participant across all four materials, and were normalized to the mean of the three baseline trials. The mean and standard deviation of the change was then calculated for all participants under each material condition, and t-tests compared values of each condition to the baseline ($p<0.05$).

RESULTS AND DISCUSSION

Participants baseline $EtCO_2$ and SPO_2 levels were 5.3% and 95% respectively, and there were no significant differences between the three baseline trials. For each material, participants had an increase in $EtCO_2$ output and a decrease in SPO_2 levels from their baselines (Fig2A). The 50/50 blend had the largest changes from baseline for both $EtCO_2$ (12.9%) and SPO_2 (-3.2%). Using the same materials tested in this study, we can now validate our biomechanical respiration model (Fig 2B).
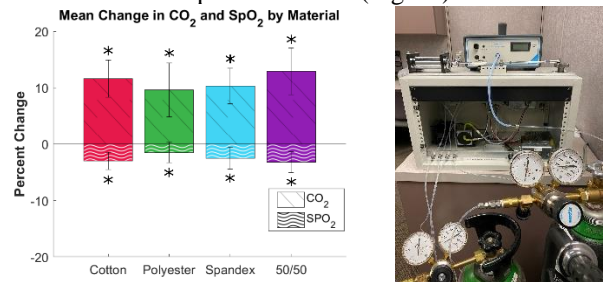

Figure 2: The mean percent change in CO_2 and SPO_2 by material (A). All were significantly different vs. baseline ($p<0.05$); Rebreathing machine to model respiration (B).

CONCLUSIONS

Our research indicates that materials commonly used in infant products can negatively influence breathing for adults. Considering their use in infant products, manufacturers should consider how the design of products and use of these materials may introduce suffocation-related hazards to the vulnerable infant population. A benchtop biomechanical model of respiration would allow for manufacturers to easily evaluate the safety of their products, and this study provides data to enable the future validation of our model. Finally, this human data indicates that common materials influence respiration patterns, and facial contact with these soft goods should be prevented.

REFERENCES

1. Little, et al. *Infant Beh & Dev*, 2019 2. Callahan, et al. *Arc Peds & Ado Med*, 1997 3. Gaw, et al. *Peds*, 2017 4. Moon RY, et al. *American Academy of Ped*, 2022 5. Mannen, et al. *CPSC*, 2023

ACKNOWLEDGEMENTS

ASSESSING CO₂ LEVELS EXHIBITED THROUGHOUT BREATHING DURING NOSE DEFORMATION

Brandes, ID[1], Olvera[2], CA, and Mannen, EM[1,2], ID

[1] Dept of Mechanical and Biomedical Engineering, [2]Biomedical Engineering Doctoral Program, Boise State University, Boise, ID
email: giadabrandes@u.boisestate.edu

INTRODUCTION

The nose is a primary system for respiration, acting as airway filtration and thermal regulation. Obstructed breathing during sleep creates a challenge for nasal respiration during the night, affecting nearly 24% of the population between ages 30 to 60 years old. Obstructed breathing derives from infectious, genetic, and physiological factors affecting an individual's nasal resistance. Nasal resistance is affected by the radius of the nose's entrance near the nasal valve, which is the narrowest part of the nose and divides the nasal cavities with a thin cartilage. Physiological features such as soft, deformable cartilage or even abnormal tissue such as cysts, can alter breathing patterns [1]. Neonates and infants have underdeveloped nasal cavities which cause higher nasal resistance because of their radially smaller middle cavity and the lack of an inferior meatus, resulting in less airflow [2]. Furthermore, infant respiration is underdeveloped, and suffocation risk is increased for this population, especially during sleep. Understanding how nose deformation influences breathing can inform design of test methods to reduce suffocation risk in infant products. The long-term goal of this work is to apply the mechanics of adult breathing and nose deformation to infant breathing and test design.
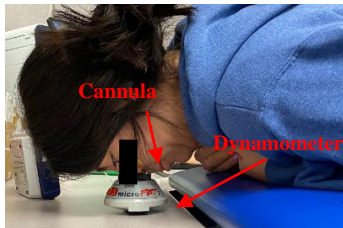
METHODS

Figure 1: Participant performing "tip-down" nasal orientation on the dynamometer with a nasal cannula.

Six young, healthy adults (21.3±1.7, 3M/3F) each laid prone on a bench and rested their nose on a MicroFet dynamometer where the peak force was recorded. Participants' noses were in contact with the plate with inserted nasal cannulas that were connected to a Capnostream 35 Portable Respiratory Monitor. These cannulas measured the end-tidal carbon dioxide (EtCO₂) levels which was used to indicate changes in inhaled carbon dioxide. To simulate face-down positioning, four distinct nose deformations were defined as right ala closed, left ala closed, the tip of the nose pushed upwards, and the tip of the nose pressed downwards. Participants completed five trials for each nose deformation in a random order, including a control trial of nasal respiration with no deformation. According to Medtronic, the respiratory monitor takes 2.95 to 5.0 seconds to register. It was determined that 8 seconds would be a sufficient duration for each trial. After the allotted time, participants slowly lifted their head from the plate while the dynamometer read the maximum force that was exerted during the trial.

RESULTS AND DISCUSSION

Percentages were derived from calculating the difference between participants' baseline trials and their average CO₂ level for that specific trial. Overall CO₂ levels decreased from the
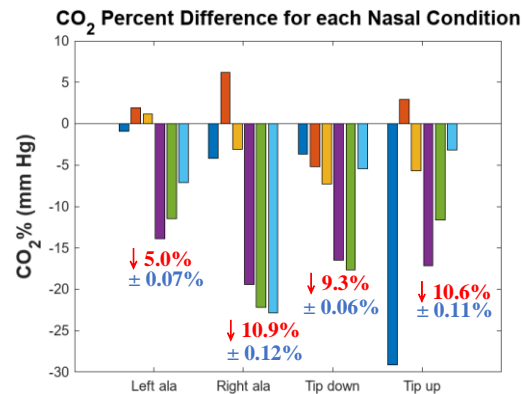

Figure 2: Graph of CO₂ percent differences for each nasal condition. Each color represents a participant (n = 6).

baseline trials as shown in Figure 2, averaging 38±3.3 mm Hg across all participants. The average percent decrease for each condition is marked in red and the standard deviation is marked in blue. Tip-down orientation was found to have significant correlation to breathing patterns (p = 0.01) as all participants experienced lower CO₂ levels during this stage. Because over-breathing causes excessive loss of carbon dioxide from the blood, leading to reduced tissue oxygenation [3], this indicates that less air is being exhaled from the body. Tip-down orientation also had the largest average force reading (22.2 N). The average weight of a human head is 5 kg (49.1 N), denoting that approximately 45% of the head weight is being exerted on the nose in this position. The remaining stages did not have significant correlation to respiratory breathing.

CONCLUSIONS

Tip-down deformation contributes to obstructed breathing as weight is distributed across the nose in this position. It is noted that a control force was not taken in this experiment. An average head weight was used as a reference which may have altered data, resulting in over-estimating, or under-estimating the significance of the force readings. Future work should include analysis of nasal characteristics and their effect on deformation. This study also demonstrates the basis of future research and development of synthetic nasal breathing devices and infant nasal respiration

REFERENCES

1. Mirza, N, et al.,. *The Nasal Airway and Obstructed Breathing during Sleep*, 1999.
2. Corda, J, et al., *Nasal airflow comparison in neonates, infant and adult nasal cavities using computational fluid dynamics, 2022.*
3. Ruth, A, *The health benefits of nose breathing,* 2015.

ACKNOWLEDGEMENTS